MATERIAL CHARACTERIZATION OF ALASKAN ASPHALT MIXTURES CONTAINING RECLAIMED ASPHALT PAVEMENT (RAP)

By

Beaux M. Kemp

A Thesis Submitted in Partial Fulfilment of the Requirements

for the Degree of

Master of Science

in

Civil Engineering

University of Alaska Fairbanks

December 2016

APPROVED:

Dr. Jenny Liu, Committee Chair
Dr. Steve Saboundjian, Committee Member
Dr. William Schnabel, Committee Member
Dr. Leroy Hulsey, Chair
Department of Environmental and Civil Engineering
Dr. Douglas Goering, Dean
College of Engineering and Mines
Dr. Michael Castellini, *Dean of the Graduate School*

ABSTRACT

Recycled asphalt pavement (RAP) material has been combined with hot-mix asphalt (HMA) paving for several decades to reduce construction costs and environmental impacts. In Alaska, the HMA specification allows up to 15% RAP for Type-II A mixes (typically used in wearing courses) and 25% for Type II-B mixes (used in wearing or base courses). Highway construction projects statewide are expected to see an increase in the use of RAP in future mix designs. Pavement engineers use mechanistic procedures (e.g. Alaska Flexible Pavement Design software and Mechanistic-Empirical Pavement Design Guide) to develop flexible pavement design alternatives. These procedures require material engineering properties as an input source. Consequently, it is essential to properly establish the engineering properties of HMA mixtures containing RAP.

In order to characterize Alaskan HMA materials containing RAP, this study evaluated 11 HMA mixtures comprised of three typical Alaskan asphalt binders (PG 52-28, PG 58-34 and PG 52-40) containing 0%, 25% and 35% RAP that were either produced in the lab or a hot-plant (i.e. collected from actual paving projects in Alaska). Various binder and mix properties were determined including; true high binder grades, complex shear modulus (G*) and phase angle (δ) at high performance temperatures, as well as asphalt mixture performance tests (AMPT); dynamic modulus (|E*|) and flow number (FN). The original (η-based) and the modified (G*-based) Witczak |E*| predictive models were evaluated for these mixtures based on job mix formulae availability for use in mechanistic design procedures. It was found that the incorporation of RAP into Alaskan HMA increased |E*| and FN of the mixtures, which indicates that the addition of RAP increased the stiffness and rutting resistance of the mixtures tested. A local calibration of the Witczak predictive models may be required for increased accuracy of |E*| predictions. For Alaskan conditions, a savings of $13.60/ton of mix was estimated for a 25% RAP mix. For an 18-feet wide one lane-mile of HMA mat, it is estimated to have a 21% savings in the 25% RAP mix compared to the conventional virgin (no RAP) mix.

TABLE OF CONTENTS

LIST OF FIGURES

Page

LIST OF TABLES

Page

LIST OF APPENDICES

Page

For my mom

ACKNOWLEDGEMENTS

I would like to express my special appreciation and thanks to my advisor Dr. Juanyu Liu. I would like to thank you for your continued encouragement and support from my undergraduate studies through graduate school at UAF. Your advice on both academics as well as on my career have been priceless.

I would like to thank Dr. Stephan Saboundjian for lending me his technical expertise and support as well as being part of my advisory committee.

I would like to thank Dr. William Schnabel for serving on my advisory committee and for being there when I needed it most.

I would like to thank the researchers at the Center for Sustainable Transportation in Cold Climates; Dr. Sheng Zhao, Gabriel Fulton and Kannon Lee, for their contributions to this research.

Special thanks go to my family. Words cannot express how grateful I am to my mother-in-law, Susan, and father-in-law, Charles, for all the help and guidance they have provided me. Your encouragement and council were invaluable to the writing of this thesis. At the end, I would like to express my appreciation to my beloved wife Melissa and our wonderful boys, Cruz and Brody for providing me with unfailing support and continuous encouragement. Thank you for always being there.

CHAPTER 1 INTRODUCTION

1.1 Background

The design of infrastructure construction projects, such as roads, is driven by their economic and environmental impacts. With a decline in quality aggregate, growing concern over waste disposal and the rising cost of asphalt binder, the use of recycled asphalt pavement (RAP) has seen a substantial increase in recent hot-mix asphalt (HMA) paving projects. In Alaska, the cost of liquid asphalt is currently over $600/ton. This substantial cost has driven pavement engineers to consider substitutions for virgin asphalt. The use of recycled materials such as RAP, can be used in road construction to reduce the dependence on virgin asphalt binder and aggregate.

RAP has been used in HMA paving projects for many years. It has been estimated that the use of RAP in HMA pavements provides a savings of 14% to 34% for RAP contents between 20% and 50% (Kandhal and Mallick, 1997). Other studies have shown cost savings of 26% (Brock and Richmond, 2007) and 35% (Willis et al., 2012) with the use of 50% RAP. Most agencies limit the amount of RAP utilized in HMA mixtures due to unknown and/or undetermined mechanistic and performance properties associated with such pavements. Washington State DOT allows 20% RAP in HMA mixtures. Oregon and New Hampshire DOTs currently allow up to 30% RAP. Nebraska DOT allows up to 50% RAP for primary uses of asphalt mixtures. A study conducted by the FHWA (1993) showed an acceptable level of performance for HMA mixtures containing 80% RAP. Although the maximum use of RAP has been desired, there are significant drawbacks to its use at high percentages. The undesirable inherent characteristics of RAP include aged (stiff) binder and inconsistent aggregate properties. These undesirable properties of RAP can have negative consequences to a pavements performance and service life. A recently completed project, NCHRP 09-46 (West et al., 2013), proposed changes to existing specifications to account for HMA containing high RAP content. This study aimed at developing a mix design and analysis procedure for HMA containing high RAP content that provides satisfactory long-term performance.

Numerous studies have been reported in the literature concerning performance of HMA mixtures containing RAP (Kennedy et al., 1998; McDaniel and Anderson, 2001; Al-Qadi et al.,

2007; Huang et al., 2011). There is a general consensus regarding RAP use; when RAP was used in HMA at low or medium levels, equivalent or better performance was observed when compared to virgin HMA. However, the degree of improvement is a function of the material source, quantity and quality or the utilized RAP.

In Alaska, the evaluation of HMA containing RAP has been very limited. A preliminary study by Teclemariam and Saboundjian (2010) was undertaken to investigate how three RAP contents affect the Superpave performance grade (PG) of the blended binder. Another project (Connor and Li, 2009) evaluated the performance of HMA with the inclusion of 15% RAP for the Fairbanks International Airport Runway 1L/19R Reconstruction. The results showed that the addition of 15% RAP did not adversely impact the quality of HMA. The new highway specification allows up to 15% RAP materials in the wearing course (Type II-A mix) and 25% in the Type II-B mix and base layer(s). However, the performance data for HMA containing RAP for surface course applications is limited. Because of this, it is essential to properly characterize (i.e. establish engineering properties for) typical Alaskan HMA mixes containing RAP material.

To produce more durable and higher performance pavements in a cost-effective manner, pavement design is trending toward more mechanistic based design methodologies. Following this direction, the Mechanistic-Empirical Pavement Design Guide (MEPDG) was developed by the National Cooperative Highway Research Program (NCHRP) in 2002 in an effort to improve current design methods. The MEPDG uses mechanical principles to evaluate pavement responses such as stress, strain and deflection. Empirical models are used to predict pavement performance based on pavement responses. One of the most important mechanistic properties of HMA, with regard to pavement response, is the dynamic modulus ($|E^*|$). $|E^*|$ is a measure of the stiffness of viscoelastic materials. It is proposed by MEPDG that $|E^*|$ is a key input parameter which correlates material properties to field fatigue cracking and rutting performance (2002 Design Guide, 2004).

The MEPDG has three hierarchical input levels with Level 1 being the most laboratory intensive. Level 1 analysis requires the direct laboratory testing of dynamic modulus. According to NCHRP Project 9-19 (Witczak, 2007) and Project 629 (Bonaquist, 2008), a series of tests, known as simple performance tests (SPTs), are currently available to evaluate the resistance of

asphalt mixtures to permanent deformation and fatigue cracking. Tests are performed using the asphalt mixture performance tester (AMPT). These SPTs detail the procedures for laboratory evaluation of mixture dynamic modulus. In Level 2 and 3, |E*| is estimated using the Witczak model. The Witczak model is an empirically derived model based on conventional multivariate regression analysis. It was originally developed by Matthew W. Witczak in 1972 with revisions made in 1995, 1999 and 2006. The model uses aggregate gradation, mixture volumetric properties and binder rheology to describe the relationship between dynamic modulus and loading rate.

As part of the SPTs, flow number (FN) has been found to correlate with field rut depths. This correlation has been supported throughout the literature (Li and Liu, 2014; Shen and Yu, 2012; Witczak, 2007). The FN test has been recommended to evaluate rutting potential of HMA and to compliment the pavement design to ensure reliable mixture performance over a wide range traffic and loading conditions. The NCHRP Report 673 recommends testing the flow number as part of a local materials characterization plan to develop a material-performance relationship and improve the overall quality of the pavement design (Advanced Asphalt Technologies, LLC, 2011).

Many state agencies have been using SPTs to evaluate HMA mixtures and to determine if the performance tests and the MEPDG are suitable for implementation into their pavement design programs (Pellinen, 2001; Kim et al., 2004; Bhasin et al., 2005; Mohammad et al., 2005; Obulareddy, 2006; Williams et al., 2007). These studies have been conducted to develop a catalog of local |E*| inputs in the MEPDG and to provide state DOTs a familiarity with the |E*| parameter. A material database consisting of modulus properties can be used to develop a locally calibrated dynamic modulus prediction model and provide more accurate inputs to the MEPDG. According to Shen and Yu (2012) an |E*| database and locally calibrated |E*| prediction model has many benefits to pavement design:

- greater understanding of local materials for the selection of cost-effective material combinations for different design purposes;
- assist with performance prediction through accurate modulus prediction based on local materials;
- more accurate material input properties based on representative local materials;

- develop |E*| predictive models with locally calibrated model coefficients;
- develop Level 2 and 3 designs with greater accuracy.

Li and Liu (2014) conducted a comprehensive study to characterize Alaskan HMA mixtures using SPTs and an asphalt pavement analyzer (APA). The SPTs included: |E*|, FN, and flow time (FT). The APA was used to evaluate rutting resistance and to correlate results with FN measurements. Loose asphalt mixtures were collected from 21 projects in three regions of the Alaska Department of Transportation and Public Facilities (ADOT&PF), including 10 from Northern region, nine from Central region, and two from the South Coast region. The collected mixes covered a wide range of HMA used in Alaska, however, no mixtures contained RAP. Due to the increased use of RAP in pavement construction, it is necessary to evaluate the dynamic modulus properties of mixtures with RAP so they may be included in the local material database.

1.2 Problem Statement

With the current trend of developing mechanistic flexible pavement design and more reliable design procedures, accurate characterization of HMA properties is needed. Highway construction projects are relizing the economic and environmental benefits to incorporating recycled materials into their mix designs and as a result, are expected to increase the use of these sustainable materials. Pavement engineers develop pavement design alternatives using mechanistic analysis procedures and then use life cycle cost analysis (LCCA) to select the most cost-effective solution. Mechanistic pavement design requires material properties as inputs for analysis. Consequently, it is essential to properly characterize the physical properties of HMA containing RAP material.

As mentioned previously, one important physical property of asphalt concrete is the dynamic modulus or |E*|. This property is an indicator of material stiffness and is used to evaluate the stress/strain relationship of asphalt pavements under traffic loading. The primary pavement distresses evaluated by |E*| are fatigue cracking and permanent deformation. Laboratory |E*| testing is expensive and time consuming due to the necessary specialized equipment and specimen preparation process. Because of this, |E*| predictive models have been developed using routinely collected data contained in the mixes' job mix formula. These models were developed using data collected from several different types of asphalt mixtures, however,

the influence of recycled materials, such as RAP, were not addressed. The addition of RAP in asphalt mixtures produces changes to the pavement's physical characteristics. Failure to account for these changes may result in unknown error in the predictive models' accuracies. Therefore, it is essential to evaluate the |E*| predictive capabilities of these models with asphalt pavement containing RAP.

1.3 Objective

The research presented in this thesis was conducted as part of a project titled "Characterization of Alaskan Hot-Mix Asphalt Containing Reclaimed Asphalt Pavement" funded by the Center for Environmentally Sustainable Transportation in Cold Climates (CESTiCC) and ADOT&PF (Liu et al., 2016). The objectives of this thesis were intended to support that modeling activity through a set of laboratory measurements and model analyses. The specific objectives of this thesis include:

- establish a catalog of |E*| test results for typical Alaskan HMA mixtures containing RAP;
- evaluate the rutting performance for typical Alaskan HMA mixtures, and
- assess the ability of the original Witczak and modified Witczak models in |E*| prediction for Alaskan asphalt mixtures containing RAP.

1.4 Research Methodology

The following major tasks were accomplished to achieve the objectives of this study:

- Task 1: Literature Review
- Task 2: Development of a Materials Collection Plan
- Task 3: Specimen Fabrication, Asphalt Binder and Mixture Performance Tests
- Task 4: Data Processing and Analysis
- Task 5: Evaluation of Witczak |E*| Models
- Task 6: Conclusions and Recommendations

Task 1: Literature Review

The purpose of this task is to review the existing and current efforts in characterization of HMA mixtures containing RAP. The standard characterization methods and a summary of the economic benefit of RAP use in HMA mixtures is provided. This task is presented in Chapter 2.

Task 2: Development of a Materials Collection Plan

The materials for this study included the following: RAP collected from Northern region contractor stockpiles, two RAP contents (25% RAP for Type II-A and Type II-B mixes, and 35% RAP for Type II-B), and three asphalt binders (PG 52-28, PG 58-34, PG 52-40). The matrix of HMA mixtures used in this study is summarized in Chapter 3. HMA mixtures were collected from various paving projects in both the Central and Northern regions of ADOT&PF. Virgin aggregates and asphalt binders were collected to laboratory-produce mixtures that were not available directly from active paving projects. Details of material information and job mix formulas are provided. This task is presented in Chapter 3.

Task 3: Specimen Fabrication, Asphalt Binder and Mixture Performance Tests

The dynamic shear rheometer (DSR) was used to measure the viscoelastic behavior of the rolling thin film aged (RTFO)-aged binder in terms of complex modulus (G*) and phase angle (δ) following AASHTO T315.

Following AASHTO T27 and T308, ignition and sieving analysis tests were performed to verify binder content and gradation for each RAP source. Laboratory-mixed specimens were prepared according to standard procedures. Volumetric properties of mixtures were verified before performing performance tests. The project examined how properties changed as different amounts of RAP were added. Adhering to AASHTO TP-79, this study evaluated the performance of HMA containing RAP by measuring dynamic modulus (|E*|) and flow number (FN). This task is presented in Chapter 3.

Task 4: Data Processing and Analysis

Laboratory data from Task 3 was processed and analyzed. A database of dynamic moduli and flow number for typical Alaskan HMA mixtures containing RAP was developed. A preliminary cost comparison of paving jobs with varying RAP contents was conducted. This task is presented in Chapter 4.

Task 5: Evaluation of Witczak |E| Models*

The original (1996) Witczak model and the modified (2006) Witczak model were evaluated at both MEPDG Level 2 and 3 for |E*| prediction accuracy. Seven of the eleven mixes evaluated in this study were provided with job mix formulae, and were therefore selected for

analysis by the Witczak models. The binder rheological properties were determined using the viscosity-temperature susceptibility (A-VTS) method. Dynamic shear rheometer (DSR) data was provided by researchers at the University of Tennessee, Knoxville. This task is presented in Chapter 4.

Task 6: Conclusions and Recommendations

Upon completion of the aforementioned tasks, findings from this study and suggestions for further research are summarized. This task is presented in Chapter 5.

CHAPTER 2 LITERATURE REVIEW

2.1 Background of RAP

Utilization of RAP in HMA became popular in the US in the 1970's. The rising price of asphalt binder drove the industry to look for cost saving strategies. Because RAP contains binder as well as quality aggregate, its re-use quickly became very popular. These days, there is an increasing demand for green technologies. The use of RAP in new HMA fits this ideology well. By re-using the old road to build the new, we take a great stride in the direction of sustainability.

Current road construction practice has shown that the use of recycled asphalt pavement in the production of new roads has many advantages. The main advantages fall under two broad categories; economic and environmental. The more RAP a project can utilize, the less high quality virgin aggregates and binder are necessary. Thus, the benefit is immediate to the cost and sustainability of the project in that new materials need not be purchased and the natural resource is preserved. Also, the apprehension over waste transport and disposal is reduced since the material will be reused near its original location. This can greatly cut the amount of fuel needed to haul the old material. The use of RAP also benefits the environment by reducing the amount of fossil fuels required to produce fresh hot mix asphalt. Aurangzeb and Al-Qadi (2014), using a life-cycle cost analysis (LCCA), showed a reduction in cost of up to $94,000 per mile for HMA mixes with up to 50% RAP. Their research also concluded that the environmental impact of construction can be reduced up to 28% with higher RAP use when compared with virgin asphalt mixes.

Laboratory research is also identifying the benefits of RAP while addressing the sources of resistance to its use. Most agencies currently use small amounts (up to 25% by weight of total mix) of RAP in their HMA mix designs and the average national usage rate was estimated to be 12% in 2007 (Copeland, 2011). The greatest cause of concern for higher RAP use is the pavements performance. Many researchers have studied the performance of HMA with RAP generally concluding that increasing the RAP content increases the stiffness and rutting resistance while decreasing the fatigue resistance. Fatigue resistance is of special concern in regions with cold climates because decreased fatigue resistance means decreased thermal resistance and potentially increased thermal cracking. Because of this, it is essential to properly characterize Alaskan HMA containing RAP.

2.2 Characterization of Hot-Mix Asphalt with RAP

The response of hot-mix asphalt to load, deformation and environmental conditions is considered as the basis for HMA characterization (Brown et al., 2009). HMA characterization allows for the design of asphalt pavement structures, evaluating material performance, and provides construction quality assurance.

Previous HMA characterization tests where empirically derived based on correlations between testing results and material performance. The most prominent of these tests include the Marshall stability test, the Hveem stabilometer and the various loaded wheel tests. The Marshall stability test is part of the Marshal mix design method and is an indicator of HMA strength. It was developed in the 1940's and is currently in use by ADOT&PF. The test is performed on a cylindrical specimen 2.5" thick and 4" in diameter. The specimen is subjected to a compressive load along the longitudinal axis through a semicircular testing head. To simulate the most critical field condition, the test is performed at 60 °C. The maximum load carried by the specimen is defined as the Marshal Stability. The flow index, defined as maximum deformation at maximum load, is also obtained in this test. The major influencing factors to Marshall stability are binder viscosity and aggregate internal friction.

The Hveem stability test was empirically developed to measure the internal friction within a HMA specimen. The test is performed on a cylindrical specimen 2.5" thick and 4" in diameter. The specimen is subjected to a compressive load with confining pressure at 60 °C. Hveem stability is calculated following Equation 2..

$$S = \frac{22.2}{\left[\frac{P_h \times D}{P_v - P_h}\right] + 0.222}$$

Equation 2.2

where,

S = Hveem stability (0-100)

P_h = horizontal pressure for corresponding Pv (psi)

D = displacement of specimen

P_v = vertical pressure (typically 400 psi when the vertical load is 5000 lbf.)

The Marshal and Hveem stabilities determined from these tests are used during the HMA mix design to determine optimum asphalt content. The stabilities are not based on mechanical properties of the HMA and do not correlate well with field performance parameters such as rutting (Brown et al., 2004) and potential fatigue cracking (Kandhal and Parker, 1998).

Permanent deformation of HMA along the wheel path, commonly referred to as *rutting*, has been identified as a primary pavement distress. The loaded wheel test is currently the most widely practiced standardized laboratory test to evaluate a pavements rutting resistance. The loaded wheel test measures the rutting potential of HMA by rolling a loaded wheel across the surface of an asphalt sample. There are many variations of the loaded wheel test; the Asphalt Pavement Analyzer (APA), the Georgia Loaded Wheel Tester (GLWT), the Superfos Construction Rut Tester, the Hamburg Wheel Tracking Device (HWTD), the Purdue University Laboratory Wheel Tracking Device (PURWheel), and the French Pavement Rutting Tester (FPRT). Among these variations, the APA is the most prominent and most widely used in the literature. Performance of the test specimens has been accurately correlated to the actual in-service pavement performance. The APA induces rutting by mechanically tracking a loaded aluminum wheel back and forth along a pressurized linear hose over a HMA sample. The wheel is moved across the HMA for 8,000 cycles using a load of 100 lb and a hose pressure of 100psi (see Figure 2.1). The APA has been adopted by many DOTs and transportation agencies following AASHTO test specification T340. A very good correlation has been shown between binder property $G^*/\sin\delta$ and rutting susceptibility (Stuart and Izzo, 1995).

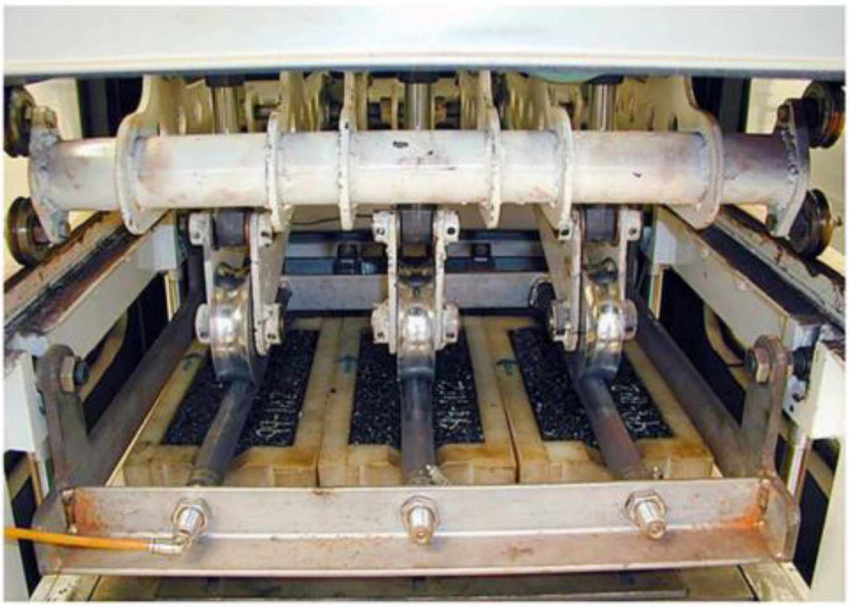

Figure 2.1 Asphalt Pavement Analyzer (courtesy of *http://www.virginiadot.org*)

Historically speaking, these tests have worked well for the design of pavement structures, however, they incorporate fundamental limitations to the new design standards and lack the flexibility to incorporate other materials such as RAP. Because they are empirical tests, their results do not yield true mechanical properties. Modern HMA characterization techniques are moving toward mechanistic based tests for the purpose of producing more durable and higher performance pavements in a cost-effective manner. These new tests are replacing the historic empirical-based tests. Among these mechanistic-based testing methods, dynamic modulus (|E*|) and flow number (FN) have been adopted as asphalt material performance tests (AMPT) in the NCHRP 9-19 project (Witczak, 2007). |E*| is an indicator of the resistance of an asphalt mixture to pavement distress including rutting and fatigue cracking. FN tests have shown significant correlation with field rut depth of HMA structures. The dynamic modulus of HMA has been recognized as an important input to current Mechanistic-Empirical Design Guide (MEPDG) pavement design procedures and flow number has been recommended to compliment this procedure for evaluating rutting potential of the mix (NCHRP report 673, 2011).

The MEPDG was adopted by AASHTO in April, 2011 to replace the previous pavement design criteria known as, 1993 AASHTO Pavement Design Guide. MEPDG is a significant improvement in pavement performance prediction methodology. The benefits allow for achieving cost effective and reliable pavement design. The MEPDG uses an integrated analysis

approach to predict pavement behavior over time by means of a user-friendly software interface. As its name implies, this approach incorporates both mechanistic and empirical data to optimize the design process. MEPDG is mechanistic in that it utilizes stress, strain and deformation data collected from real-world pavement response models. It is empirical because it inputs pavement performance data from lab developed models which have been adjusted according to observed field performance. MEPDG uses a limited national database to develop performance models. Because of this, it is essential for the models to be locally calibrated to account for variations in materials, traffic and environmental conditions (Muthadi and Kim., 2007). The authors define calibration as a means to reduce the total error between the measured and predicted distresses by varying the appropriate model coefficients. There are three major steps involved in calibrating MEPDG to local materials and conditions; verification, adjust model coefficients, and validation. In the verification step, models are developed using the data from the national calibration effort of the NCHRP 1-37A project. The second step involves adjusting the model coefficients to eliminate bias and reduce standard error to within an acceptable level. The third step evaluates the model predictions by testing several pavement sections not used in the calibration effort. A thorough characterization of asphalt materials is necessary in obtaining the appropriate material property inputs.

The MEPDG includes three hierarchical analysis levels. Level 1 requires the most accurate material property inputs and is used for the design of high priority pavements where early failure is of great concern. At this level, laboratory measurement of indirect tensile strength, creep compliance and dynamic modulus are required. Level 3 designs are based on default properties contained in the national database. This level of design is generally used for low priority roads where the consequences of early failure is minimal. Level 2 design provides an intermediate level of accuracy and confidence. At this level, the dynamic modulus of HMA is determined using the Witczak predictive model (Witczak and Fonseca, 1996) based on aggregate gradation, loading frequency, HMA volumetrics, and viscosity of asphalt binder. A summary for the required inputs are provided in Table 2.1.

Table 2.1 Summary of required inputs for MEPDG (from 2002 Design Guide, 2004)

Input Level	Description
1	• Conduct E* (dynamic modulus) laboratory tests at loading frequencies and temperatures of interests for the given mixture. • Conduct binder complex shear modulus (G*) and phase angle (δ) testing on the proposed asphalt binder (AASHTO T315, 2013) at ω=1.59 Hz (10 rad/s) over a range of temperatures. • From binder test data estimate Ai-VTSi for mix-compaction temperature. • Develop master curve for the asphalt mixture that accurately defines the time-temperature dependency including aging.
2	• No E* laboratory test required. • Use E* predictive equation. • Conduct G* δ on the proposed asphalt binder (AASHTO T315, 2013). The binder viscosity can also be estimated using conventional asphalt data such as Ring and Ball Softening Point, absolute and kinematic viscosities, or using the Brookfield viscometer. • Develop Ai-VTSi for mix-compaction temperature. • Develop master curve for the asphalt mixture that accurately defines the time-temperature dependency including aging.
3	• No E* laboratory test required. • Use E* predictive equation. • Use typical Ai-VTS values provided in the Design Guide software based on PG, viscosity or penetration grade of the binder. • Develop master curve for the asphalt mixture that accurately defines the time-temperature dependency including aging.

2.3 Dynamic Modulus

The MEPDG uses dynamic modulus (|E*|), also known as HMA stiffness, as an indicator of the resilient properties of an HMA mixture to pavement distresses such as rutting and fatigue cracking. |E*| is used in structural analysis to calculate the stresses, strains and displacements of flexible pavement under various loading conditions.

HMA is a viscoelastic material. Viscous materials are characterized by their tendency to flow and deform under their own weight while elastic materials rebound. When a material is subjected to vibratory conditions, a purely viscous material will exhibit a phase difference

between stress and strain where strain lags stress by 90 degrees. A purely elastic material experiences no lag, the stress and strain are in phase, and occur simultaneously. The behavior of HMA is between these two extremes (see Figure 2.2).

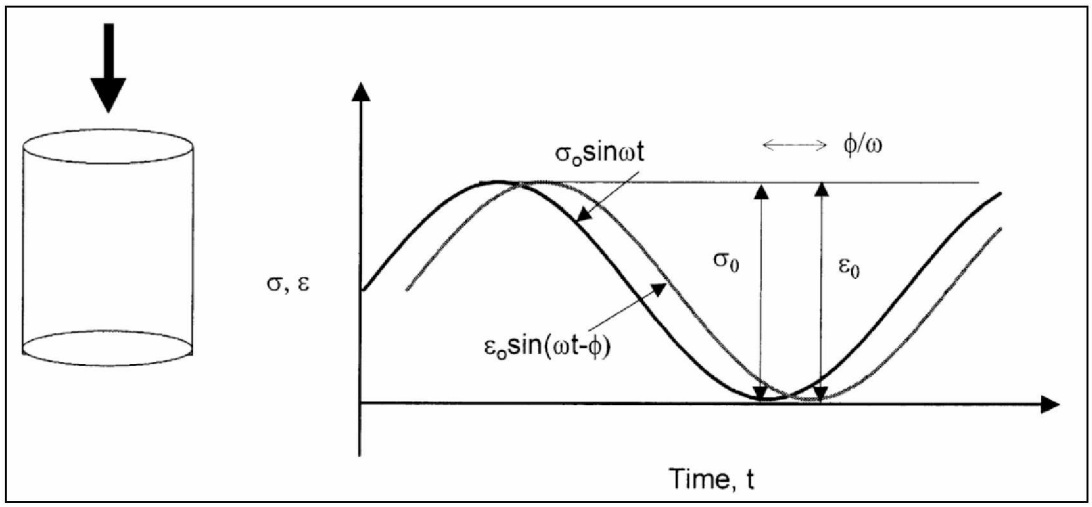

Figure 2.2 Loading pattern for the dynamic modulus test (from Witczak et al., 2002)

The ratio of stress to strain experienced by an HMA sample while under continuous sinusoidal uniaxial loading results in a complex number, (E*). By definition, a complex number is a combination of a real number and an imaginary number. The real number part of (E*) is representative of the elastic stiffness and the imaginary part defines the internal dampening of the material. The absolute value of (E*) is commonly referred to as the dynamic modulus, |E*|. The dynamic modulus is defined as the ratio of peak stress to peak strain:

$$E^* = \frac{\sigma}{\varepsilon} = \frac{\sigma_0 e^{i\omega t}}{\varepsilon_0 e^{i(\omega t - \phi)}} = \frac{\sigma_0 \sin(\omega t)}{\varepsilon_0 \sin(\omega t - \phi)}$$

and,

$$|E^*| = \frac{\sigma_0}{\epsilon_0}$$

Equation 2.1

where,

σ_0 = peak stress

ϵ_0 = peak strain

ϕ = phase angle (degree)

ω = angular velocity

t = time (seconds)

For viscoelastic materials, such as HMA, the modulus measured at low temperature and high frequency is equal to the modulus measured at high temperature and low frequency. Because of this association, the time-temperature superposition principle can be implemented to characterize |E*| over a wide range of loading frequency. At a given reference temperature (usually 20°C), the |E*| values collected over a range of temperatures and frequencies can be shifted with respect to the independent variable axis (frequency/time) to form a smooth S-shaped curve. This curve is commonly referred to as the "master curve" of |E*|. The master curve is used to analyze the temperature and frequency effects on asphalt as well as an input for the MEPDG.

To determine the amount of horizontal shift, a shift factor is determined using Equation 2.2. The shift factor is a function of temperature as illustrated by Equation 2.3. The coefficients a, b and c are obtained through a regression analysis after the shift factors at the prescribed temperatures are determined. The sigmoidal function, Equation 2.4, can be used to describe the master curve as described by Pellinen and Witczak (2002).

$$a(T) = \frac{f}{f_R}$$

Equation 2.2

$$a(T) = 10^{aT^2+bT+c}$$

Equation 2.3

$$log_{10}|E^*| = \delta + \frac{\alpha}{1 + e^{\beta+\gamma\cdot\log(f_R)}}$$

Equation 2.4

where,

a(T) = shift factor as a function of temperature

f = loading frequency, Hz

f_R = reduced loading frequency at reference temperature 20°C, Hz

T = temperature, °C

$|E^*|$ = dynamic modulus, MPa

$\delta, \alpha, \beta, \gamma, a, b, c$ = regression constants

The least-squares method is used to determine the regression constants δ, α, β, γ and the shift factors are fit using Equation 2.4. The seven coefficients (δ, α, β, γ, a, b, c) are the same as used in the MEPDG and are also used to construct the master curve.

2.3.1 Dynamic Modulus Testing

The first dynamic modulus evaluation protocol was developed by Coffman and Pagen at Ohio State University in the 1960's (Witczak, 2002). It was defined by ASTM in 1979 as ASTM D3496 and was withdrawn in 2010 with no replacement. Currently, the most widely used standard is AASHTO T342, *Determining Dynamic Modulus of Hot Mix Asphalt (HMA),* (previously TP62). The current standard determining $|E^*|$ using the AMPT is AASHTO TP79, *Determining the Dynamic Modulus and Flow Number for Asphalt Mixtures Using the Asphalt Mixture Performance Tester (AMPT).* Test specimens, 100 mm in diameter and 150 mm in height, are prepared using a gyratory compactor following AASHTO PP60, 2013, *Preparation of Cylindrical Performance Test Specimens Using the Gyratory Compactor (SGC).* During the test, a uniaxial sinusoidal compressive load is applied to the test specimen with a continuous haversine waveform under strain controlled conditions. The test is preformed over a range of loading frequencies (0.1, 0.5, 1, 2, 5, 10, 20 and 25 Hz) and four temperatures (4.4, 21.1, 37.8 and 54 °C). The axial strain is measured by three linear variable transducers (LVDT) placed radially at 120°. The dynamic modulus of the sample is determined using Equation 2.1. The testing results are presented as HMA master curves and then used in the MEPDG for pavement performance prediction accounting for the effects of temperature and traffic variations.

2.3.2 Influencing Factors

Li et al. (2008) studied the effect of RAP percentages and sources on the stiffness ($|E^*|$), of asphalt mixtures. Ten asphalt mixtures, with two different binder grades (PG 58-28, PG 58-34), from two different sources, with three RAP content percentages (0%, 20%, 40%) were evaluated. Experiential results indicated that asphalt mixtures containing RAP have higher dynamic modulus values than control mixes containing no RAP. The stiffer asphalt binder results in higher dynamic modulus values for both the control and the RAP-modified mixtures.

Experiential data reveal that RAP source is not a significant factor for the dynamic modulus at low temperatures, although it significantly affects dynamic modulus at high temperatures. No significant statistical relationship between dynamic modulus and fracture energy was observed. Li et al. (2004) also did a similar study with analogous results. The 2004 study consisted of ten asphalt mixtures with three percentages of RAP (0%, 20%, 40%), two binder grades (PG 58-28, PG 58-34) and RAP from two different sources. The study concluded that as RAP content in the mixture increased, the dynamic modulus also increased.

One common method currently under investigation of compensating for the stiff binder of RAP is the addition of virgin binder to the HMA mixture. This technique helps to soften the mix and increase fatigue and rutting resistance as well as workability. (Boriack et al., 2014) studied the effect of added virgin binder on performance of asphalt mixtures containing 0, 20, 40 and 100 percent RAP. The evaluation of performance was based on laboratory experimentation and included the following criteria: stiffness (dynamic modulus), fatigue resistance and rutting resistance (flow number (FN) and asphalt pavement analyzer). Their study concluded that increasing the binder content of the 0% and 20% RAP mixtures by 0.5% resulted in a 200% increase in fatigue and rutting resistance with only a 1% decrease in dynamic modulus. For the 40% RAP mixture, the addition of 0.5% and 1.0% binder resulted in a 60% and 80% decrease in FN, respectively. Little to no change was observed in the fatigue resistance and there was a decrease in rutting resistance. The dynamic modulus was decreased by 21% with the addition of 1% binder in the 40% RAP mix. For the 100% RAP mixtures, both stiffness and rutting resistance were considerably higher than all other mixes, however, the fatigue resistance was significantly lower until 1.5% binder was added. The authors recognize at this binder level, the mix would not be stable in the field having the following properties: only 0.2% VTM, a VFA of 98.5% and a density at $N_{initial}$ of 95.7%.

Several researchers (Mohammad et al., 2005; Mohammad et al., 2006; Obulareddy, 2006), have reported that nominal aggregate size, air void content, and traffic level are significant influencing factors to |E*|. As traffic volumes increase, air voids decrease, lending to an increase in dynamic modulus of HMA. Binder content has been shown to have a greater influence on |E*| than aggregate angularity. As little as 0.3% increase in binder content has a statistically significant increase in |E*| at intermediate and high temperatures. Kim and King

(2005), found that binder variables including; source, performance grade, and content, had a more significant effect on |E*| than aggregate variables. The overall density of HMA was also found to have a significant effect on dynamic modulus (Blankenship and Anderson, 2010). A 15% increase in |E*| was attributed to a 1.5% increase in density.

2.3.3 Dynamic Modulus Prediction Models

1. Witczak |E| predictive model (Witczak and Fonseca, 1996)*

The original Witczak model (Equation 2.5) is based on a nonlinear regression analysis. It is currently being used to predict the dynamic modulus of asphalt mixes in level 2 of the MEPDG. The model was originally developed using 1430 data points from 149 HMA mixtures containing conventional binders (Witczak and Fonseca, 1996). It was later refined using an additional 1320 data points of 56 new mixes including 34 mixes with modified binders, however, no RAP mixtures were included (Andrei et al., 1999). These mixtures were obtained over a 30-year period at the laboratories of the Asphalt Institute, the University of Maryland and the Federal Highway Administration (2002 Design Guide, 2004). The input parameters for this model are volumetric properties, gradation, binder viscosity and loading frequency. The overall coefficient of determination (R^2) for this model is 0.96.

$$\log_{10}|E^*| = -1.249937 + 0.02923p_{200} - 0.001767(p_{200})^2 - 0.002841p_4 - 0.05809V_a - 0.802208\frac{V_{beff}}{V_{beff} + V_a} + \frac{3.871977 - 0.0021p_4 + 0.003958p_{3/8} - 0.000017(p_{3/8})^2 + 0.00547p_{3/4}}{1 + exp(-0.603313 - 0.31335\log_{10} f - 0.393532\log_{10} \eta)}$$

Equation 2.5

where,

$|E^*|$ = dynamic modulus (10^5 psi)

p_{200} = percentage of aggregate passing the #200 sieve

p_4 = percentage of aggregate retained on the #4 sieve

$p_{3/8}$ = percentage of aggregate retained on the 3/8" sieve

$p_{3/4}$ = percentage of aggregate retained on the ¾" sieve

V_a = percentage of air voids (by volume of mix)

V_{beff} = percentage of effective asphalt content (by volume of mix)

f = loading frequency (Hz)

η = binder viscosity at temperature of interest (10^6 Poise)

For this model, binder viscosity (η) at the temperature of interest is a critical input parameter. The ASTM viscosity temperature relationship can be used to determine the viscosity of asphalt binders.

$$\log\log \eta = A + VTS\ \log T_R$$

Equation 2.6

where,

η = binder viscosity (cP)

T_R = temperature, Rankine

A = regression intercept

VTS = regression slope of Viscosity Temperature Susceptibility

Currently, some traditional binder tests (viscosity, softening point and penetration) have been made obsolete by the SuperPave mix design and are not routinely conducted. To account for this, another model has been developed to determine binder viscosity using the DSR (Bari and Witczak, 2006) following AASHTO T315:

$$\eta = \frac{|G^*|}{10}\left(\frac{1}{sin\delta}\right)^{4.8628}$$

Equation 2.7

where,

η = binder viscosity (Poise)

$|G^*|$ = binder shear modulus (Pa)

δ = binder phase angle (degree)

Using equation 2.7 and 2.8, the regression constants (A and VTS) can be determined. Once determined, the asphalt binder viscosity can be calculated at any temperature. It is noted in

the literature (2002 Design Guide, 2004) there is a limit to this extrapolation. Because asphalt binders reach a maximum viscosity of $2.7x10^{10}$ Poise at low temperatures and high loading rates, the lesser of the calculated viscosity and $2.7x10^{10}$ Poise is used.

Using the dynamic shear rheometer test (DSR), A and VTS can be determined for Level 1 and Level 2 MEPDG design procedure. A and VTS may also be estimated at Level 3 using the provided default values based on binder PG grade.

An issue has been identified with the 1996 version of the Witczak model. As shown in Equation 2.5, loading frequency (f) and binder viscosity (η) are considered as independent variables, when in reality, the viscous properties of binder are frequency dependent. Changes in loading frequency create changes to the viscosity of the binder. This is due to the viscoelasticity of the asphalt binder. As discussed earlier, asphalt binder is characterized as a viscoelastic material, meaning, at high temperatures and long loading rates the modulus will approach that of an unbound granular material. At cold temperatures and short loading rates the material will react in an elastic mode (2002 Design Guide, 2004). This model suggests the possibility of changing frequencies with constant viscosity, however, this scenario can never be realized. This discrepancy has been addressed in the 2006 modified Witczak model. The modified Witczak model uses the dynamic shear modulus ($|G^*|$) and corresponding phase angle (δ) obtained from DSR tests. The G^* and δ values at the temperatures of interest are estimated from the asphalt binder master curves or from the A-VTS method described earlier.

2. Modified Witczak $|E^*|$ predictive model (Bari and Witczak, 2006)

The modified Witczak model uses binder dynamic shear modulus $|G^*|$ instead of binder viscosity as used in the original model. A database of 7400 data points from 346 mixtures was used in the development of this model. The mixes used to develop this model did not adequately represent RAP mixtures. The modified Witczak model is shown here in Equation 2.8.

$$\log_{10}|E^*| = -0.349$$
$$+ 0.754|G^*|_b^{-0.0052}\left(\begin{matrix}6.65 - 0.032p_{200} + 0.0027(p_{200})^2 + 0.011p_4 - 0.0001(p_4)^2 \\ +0.0006p_{3/8} - 0.00014\left(p_{3/8}\right)^2 - 0.08V_a - 1.06\dfrac{V_{beff}}{V_{beff}+V_a}\end{matrix}\right)$$
$$+\frac{2.558 + 0.032V_a + 0.713\dfrac{V_{beff}}{V_{veff}+V_a} + 0.0124p_{3/8} - 0.0001\left(p_{3/8}\right)^2 + 0.0098p_{3/4}}{1 + exp(-0.7814 - 0.5785\log_{10}|G^*|_b - 0.8834\log_{10}\delta_b)}$$

Equation 2.8

where,

$|G^*|_b$ = dynamic shear modulus of rolling thin film oven (RTFO)-aged asphalt binder (psi)

δ_b = binder phase angle associated with $|G^*|_b$ (degree)

Other variables as defined previously.

Using the Witczak models, Mohammad et al. (2005), showed that |E*| can be predicted with reasonable reliability. According to Azari et al. (2007) and Gedafa et al. (2009), these models produce predicted |E*| values greater than measured values at high temperatures and low loading frequencies.

2.4 Flow Number

The flow number (FN) test is a dynamic creep test in which a compressive haversine load is applied to an HMA sample with rest periods between loadings. Samples used to determine FN exhibit three distinct stages of permanent deformation as shown in Figure 2.3. First, denoted as the primary zone, the specimen experiences a rapid accumulation of strain. The secondary zone follows and is characterized by a constant accumulated strain rate. Finally, the tertiary zone is marked by an increase in strain rate. It is at this juncture, from secondary to tertiary, that the FN is defined (see Figure 2.3). More specifically, the FN for the mixture is the point at which the permanent strain rate is at a minimum and the tertiary flow begins.

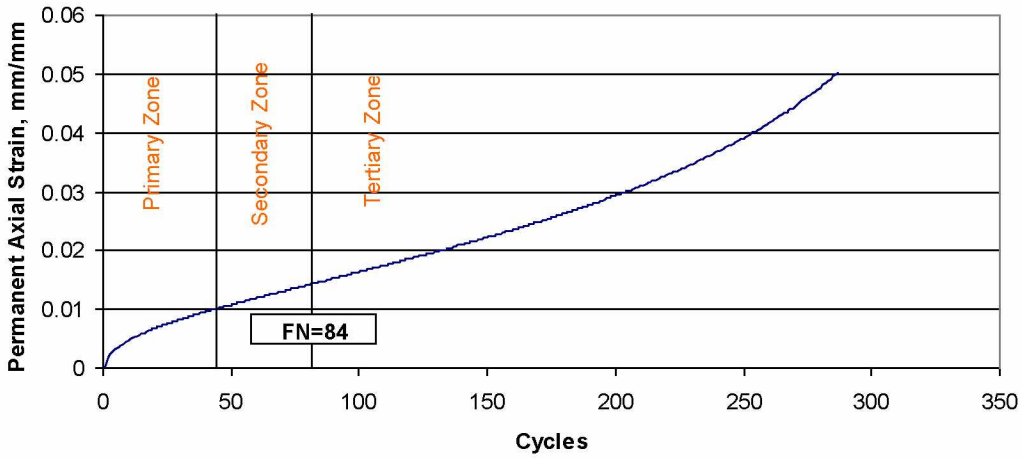

Figure 2.3 Accumulation of permanent strain in flow number test (Huang et al., 2013)

According to Archilla and Diaz, (2008), either permanent deformation model parameters or permanent deformations tests, such as FN, should be included in the permanent deformation analysis of asphalt pavement contained in the MEPDG. Williams et al. (2007) and Apeagyei et al. (2011), found FN to increase with increasing amounts of RAP contained in the mix.

2.4.1 Flow Number Testing

The flow number testing procedure was developed in the NCHRP 9-19 and is defined in AASHTO TP79. |E*| is considered a nondestructive test, therefore, the samples used for |E*| testing are generally used to evaluate flow number. A uniaxial compressive load is applied in haversine form with a loading time of 0.1 seconds and a rest duration of 0.9 seconds for a maximum of 10,000 cycles or until 50,000 microstrain deformation is achieved. Tests may be conducted with or without confining pressure. Testing temperature is generally determined to match local conditions based on the high adjusted binder performance grade of the surrounding area.

2.4.2 Rutting and Flow Number

Rutting is the permanent deformation of pavement along the wheelpath and is caused by densification and shear deformation of the pavement due to repetitive loading. Rutting can be characterized into three types; one-dimensional densification, lateral-plastic flow, and mechanical deformation (Witczak, 2007). The FN test quantifies this type of pavement distress.

Apeagyei et al. (2011) developed nineteen projects to evaluate the rutting resistance of plant produced asphalt mixtures in the laboratory. These mixtures contained RAP amounts that ranged from 0% to 25%. Tests included |E*| at multiple temperatures and FN at 54 °C to characterize the stiffness and rutting resistance, respectively. Mixtures with lower FNs either contained no RAP or had PG 64-22 binder grade designation. Mixtures that contained moderate amounts of RAP (10% to 15%), regardless of binder grade, had higher FNs than mixtures with either high or low RAP amounts. Statistical analysis showed that RAP amount was the most significant factor affecting rutting resistance in the mixtures studied.

2.4.3 Flow Number Prediction Models

The flow number of HMA has been shown to be an effective predictor of the mix's rutting performance. Because of this, researchers (Witczak and Fonseca 1996; Bhasin et al., 2004) have identified the need to develop a model which can accurately identify this material characteristic. While most HMA predictive models have focused on |E*|, some researchers have studied the prediction of flow number based on mix design parameters. It is noted in the literature the benefit of using FN in conjunction with |E*| as inputs to the MEPDG. To accomplish this, a reliable FN model must be developed.

Kvasnak et al. (2007) developed a flow number model based on 17 dense graded mixtures in the state of Wisconsin. The final model is based on six influencing factors. The accuracy of the model was good with a coefficient of determination of 0.90.

$$\log FN = 2.866 + 0.00613Gyr + 3.86Visc - 0.072VMA + 0.0282P_4 - 0.051P_{16} + 0.075P_{200}$$

Equation 2.9

where,

FN = flow number

Gyr = number of gyrations

Visc = binder viscosity at 70°F (106 poise)

VMA = voids in mineral aggregate (%)

P_4 = passing 4.75 mm sieve (%)

P_{16} = passing 1.18 mm sieve (%)

P_{200} = passing 0.075 mm sieve (%)

Apeagyei (2014) developed an empirical FN predictive model based on statistical evaluation of the volumetric and binder properties of an HMA mix. Thirteen mix designs were used in this study with RAP content ranging from 0% to 25%.

$$FN = 5698.1734P_{be} + 423.6569VFA + 924.1876\,G^*/sin\delta - 1001.435P_{25} + 148.0361P_{19} - 4395.186P_{200} + 24751DB + 31393$$

Equation 2.10

where,

FN = flow number at 54 °C (cycles)

P_{be} = effective binder content (%)

VFA = voids filled with aggregate (%)

$G^*/sin\delta$ = rutting parameter at 70 °F (kPa)

P_{25} = passing 25 mm sieve (%)

P_{19} = passing 19 mm sieve (%)

P_{200} = passing 0.075 mm sieve (%)

DB = P_{200} to P_{be} ratio

This model showed an accurate prediction of FN with an R^2 value of 0.94 with the selected HMA mix designs. Binder stiffness ($G^*/\sin\delta$) was the determined to be the most significant factor affecting FN. The authors note the importance of $G^*/\sin\delta$ as the most specified criteria for selecting asphalt binder and propose a model to determine this parameter based on FN test results.

$$G*/\sin\delta = -5.1524P_{be} - 0.3581VFA + 0.0009191FN + 0.8386P_{25} - 0.0901P_{19} + 4.4449P_{200} - 25.1211DB - 21.7312$$

Equation 2.11

where,

Variables as defined previously.

The correlation of predicted binder stiffness ($G^*/\sin\delta$) and measured values were very good with an R^2 value of 0.94. The authors conclude, if FN and binder stiffness can be accurately modeled and predicted, considerable time and effort could be saved in the design process. This is especially true for mixtures containing RAP due to the complications associated with binder extraction.

2.5 Cost Analysis

Due to the economic and environmental benefits of recycling, state agencies are focusing increasing efforts to incorporate higher levels of RAP into new and rehabilitation construction projects. To provide support for this movement, several researchers have studied new methods to analyze the cost (or cost savings) associated with increasing RAP use. Several factors are involved in this analysis, for instance, what technologies are available for the inclusion of RAP and where in the pavement structure can RAP use benefits be maximized. To properly evaluate the life cycle costs of utilizing RAP in highway construction, both economic and environmental aspects must be considered.

The NCAT website (2016) provides an example of the cost savings realized by using 20% RAP into a traditional hot mix with a target binder content of 5%. In this case, as seen in Table 2.2, the cost savings was determined to be \$34.10 - \$28.99 = \$5.11 per ton.

Table 2.2 NCAT cost analysis assumptions

Mix Type	Assumptions
Virgin Mix	Virgin aggregate: \$13/ton; Virgin binder: \$435/ton; Virgin mix cost: \$34.10 per ton
RAP Mix	Virgin aggregate: \$13/ton; Processed RAP: \$9/ton; RAP with 5% binder content; 20% RAP mix cost: \$28.99/ton

Several researchers have identified issues incorporating RAP into cost analysis models. These issues arise due to the various methods RAP can be utilized in the construction process. Morian and Ramirez (2016) have identified three main technologies for this purpose; cold in-place recycling, cold plant recycling and hot in-place recycling. The proposed model

incorporates several costs associated with each construction alternative and provides a methodology for evaluating these costs using a cost/benefit analysis. All HMA containing RAP production costs are compared with that of virgin materials to provide a clear assessment for economic evaluation. From the literature, the proposed model is as follows:

$$TIC = RAP + MC + PC + MobC + HC + PavC$$

Equation 2.12

where,

TIC = total initial cost ($/ton)

RAP = RAP removal cost ($/ton)

MC = recycled mix cost ($/ton)

PC = plant cost ($/ton)

$MobC$ = mobilization cost ($/ton)

HC = hauling cost ($/ton)

$PavC$ = paving cost ($/ton)

Each of the factors considered in this equation represent variables evaluated by the following functions:

RAP = *f(removal depth, equipment cost)*

MC = *g(mix design, RAP%, material costs)*

PC = *h(RAP sizing, RAP stockpiling costs, plant modification cost, laboratory test cost)*

$MobC$ = *i(distance to jobsite, permits cost, cost per mile)*

HC = *j(hauling cycle duration, project length, trucking costs)*

Hauling cycle duration = k(truck capacity, delay at plant, loading time, distance to job site, delay at job site, dump time)

$PavC$ = *l(placement costs, compaction costs)*

Once the total initial cost (TIC) was determined for each construction alternative, an equivalent annual cost (EAC) was calculated. To do this, the performance life of each alternative was estimated based on a literature survey. The proposed EAC equation is as follows:

$$Equivalent\ Annual\ Cost\ (EAC) = \frac{Total\ Initial\ Cost\ \left(\frac{\$}{ton}\right)}{Expected\ performance\ life\ (years)}$$

Equation 2.13

Using the EAC, a cost benefit analysis was conducted to evaluate the economic benefit of each construction alternative compared with conventional, virgin HMA. The following equation shows this procedure:

$$\frac{B}{C} = \frac{(EAC\ Recycling\ Method)}{(EAC\ Virgin\ HMA)}$$

Equation 2.14

The authors further refine this model by incorporating the structural contribution of the various asphalt pavement products to the overall pavement performance. Following recommendations by the 1993 AASHTO Pavement Design Guide; virgin HMA is assigned a structural coefficient of 0.44 per inch of thickness, and underlying asphalt treated base layers are assigned a value of 0.4 per inch of thickness. The authors use a layer coefficient of 0.3 per inch of thickness for recycled asphalt pavement products. Using the structural layer coefficient, the cost benefit equation becomes:

$$\frac{B}{C} = \frac{(EAC\ Recycling\ Method) * (Structural\ Layer\ Coefficient\ Virgin\ HMA)}{(EAC\ Virgin\ HMA) * (Structural\ Layer\ Coefficient\ Recycling\ Method)}$$

Equation 2.15

Using data from the literature, the authors evaluate each construction method on a cost/benefit basis. In general, they conclude that when compared with virgin HMA mixtures, all recycling options are beneficial from an economic standpoint but the greatest cost savings can be realized using hot in-place recycling. The authors are clear to point out that there are several project specific factors which may influence the perceived benefits of using RAP. Some of these factors include; percentage of RAP allowed in the mix design and haul distance to transport RAP. These as well as other project specific variables must be analyzed carefully by the owner and design team to determine the most cost effective alternative. It is also important to keep in mind the technologies available for inclusion of RAP. Some technologies, such as hot in-place recycling, may not be in use at every agency.

Other researchers have investigated the best uses, with regard to the pavement structure, for reclaimed asphalt. Franke and Ksaibati (2014) researched the most cost effective applications for RAP. Using a method proposed by the National Asphalt Pavement Association, they assessed the benefits of using RAP in hot plant mixes. They compared these findings to the benefits of using RAP in gravel roads and as base material. The authors conclude that the most substantial cost savings of using RAP for highway construction projects can be realized in its utilization in the hot plant mix. In this study, a cost savings of $40.87 per ton of mix was determined when RAP was incorporated into the hot plant mix. When RAP was used in the construction of gravel roads, a cost savings of $17.07 was realized and $15.71 per ton of RAP was saved by incorporating RAP into the base materials. It is important to keep in mind project specific variables, such as haul distances, can have a great effect on the results of this type of analysis.

In addition to the economic costs associated with highway construction, environmental costs must also be evaluated. Willis (2015) researched the effect of recycled materials on pavement lifecycle. In this study, the author assessed the environmental impact of highway construction activities based on energy consumption and equivalent emitted carbon. The research database was composed of a 2012 National Center for Asphalt Technology (NCAT) test section designed to reduce the life-cycle costs of the pavement structure. Using the life-cycle assessment software Roadprint, a comparison was made on the material and construction phases of an idealized virgin hot-mix construction project.

Based on this study, Willis concluded that the CO_2 produced during raw material extraction and processing is greatly reduced when recycled materials are used to replace virgin aggregate. CO_2 production was reduced by 5 to 29 percent and energy consumption was reduced by 9 to 26 percent by using recycled materials.

In addition to energy consumption and CO_2 emission, other environmental concerns arise regarding the use of RAP. Issues regarding certain toxic constituents' potential to leach into soil and groundwater have been evaluated. This concern includes the processing and transporting of recycled materials, including RAP. Research by Horvath (2003) shows average metal leachate concentrations and how they compare to the limits established by the Texas Risk Reduction

Program (TRRP). The results of this work show RAP leachate to exceed recommended safe levels of lead and barium as well as high levels of mercury and antimony.

These environmental concerns can be difficult to quantify economically. The author recommends the use of a software package titled, Pavement Life-cycle Assessment Tool for Environmental and Economic Effects (PaLATE, 2003). This software (Horvath, 2003) estimates energy consumption and emissions of CO_2, NO_X, PM_{10}, SO_2, CO and average leachate for various construction materials including RAP. PaLATE can be used to help highway designers evaluate the environmental implications of design alternatives.

CHAPTER 3 EXPERIMENTAL DETAILS

This chapter provides the research details including, materials collection, specimen fabrication and laboratory tests. The laboratory tests (binder, |E*| and FN) were conducted to characterize HMA mixtures containing RAP.

3.1 Materials

For this project, materials from the Central and Northern regions of ADOT&PF were selected for characterization. Six mixes were characterized for the Central region and five for the Northern region. The materials and their job mix formulas (JMFs) studied in this experiment are summarized in Table 3.1.

All aggregate was collected from the same contractors who selected the JMFs. Binders were provided by the contractors according to their availability. Recycled asphalt pavement used in both the Central and Northern region mixes was collected from the Northern region as RAP from Central region was not fractionated. Ignition test and sieving analysis were conducted to verify binder content and gradation of the selected RAP. The binder content of RAP was determined to be 4.75%. The JMFs can be found in Appendix A.2

Table 3.1 Matrix of HMA mixtures

Mix #	Region	Mix Type	Mix Name	RAP %	Binder PG Supplier	Aggregate Source	Project Name / Nbr / Contractor / Year
1	Central	Control	Type II-B	0	PG 52-28 Tesoro	MP 78 Parks Pit (KASH)/C Str. QAP	A-Street Resurfacing/ 56000/ QAP/ 2014
2		Control	Type II-B	0	PG 58-34 EP	MP 78 Parks Pit (Dyno-Nobel)/C Str. QAP	Lab Produced
3		Control	Type II-A	0	PG 58-34 Denali	MP 39 Glenn Hwy / AS&G	Lake Hood A&B Parking Rehab / 54465 / Granite / 2015
4		RAP25	Type II-A	25	PG 58-34 Denali	MP 39 Glenn Hwy / AS&G	AIA 7L/25R Runway Rehab/ 53598 / Granite / 2015
5		RAP25	Type II-B	25	PG 58-34 Denali	MP 39 Glenn Hwy / AS&G	W. Dowling Ph.II Recon. / 51030 / Granite / 2015
6		RAP35	Type II-B	35	PG 52-28 Tesoro	MP 78 Parks Pit (Dyno-Nobel)/C Str. QAP	Lab Produced
7	Northern	Control	Type II-B	0	PG 52-28 EP	Tanana River Valley (Exclusive Paving)	Lab Produced
8		Control	Type II-B	0	PG 52-40 EP	Tanana River Valley (Exclusive Paving)	Lab Produced
9		RAP25	Type II-B	25	PG 52-28 EP	Tanana River Valley (Exclusive Paving)	Lab Produced
10		RAP25	Type II-B	25	PG 52-40 EP	Tanana River Valley (Exclusive Paving)	Lab Produced
11		RAP35	Type II-B	35	PG 52-28 EP	Tanana River Valley (Exclusive Paving)	Lab Produced

** Type II: NMAS 19mm; Class A: 75 blows; Class B: 50 blows*

The Central region mixes used two binder grades; PG 52-28 and PG 58-34, and two mix designations; Type II-A and Type II-B. Type II-A was tested with 25% RAP and the binder designation PG 58-34. This mix was acquired from the field as a plant produced mix. Type II-B was tested with 25% RAP with the PG 58-34 binder and 35% RAP with the PG 52-28 binder. The mixture with 25% RAP was acquired from the field and the mixture with 35% RAP was produced in the lab. All mixtures were tested against a control containing no RAP. Control specimens Type II-A with PG 58-34 binder and Type II-B with PG 52-28 binder were acquired in the field. Control Type II-B with binder designation PG 58-34 was produced in the lab.

The majority (4) of the Central region mixes were obtained from the field from active paving projects as plant produced mixes. Two mixes were produced in the lab due to unavailability of paving work, mix #2 Type-II B 0% RAP PG 58-34 and mix #6 Type II-B 35% RAP PG 52-28. These lab produced mixtures were produced by first sieving the aggregate into appropriate sizes and then manufacturing blends corresponding to the JMF. Figure 3.1 - Figure 3.4 show the blended aggregate gradations and their conformity to the JMF. The asphalt binder was obtained from various suppliers as outlined in Table 3.1.

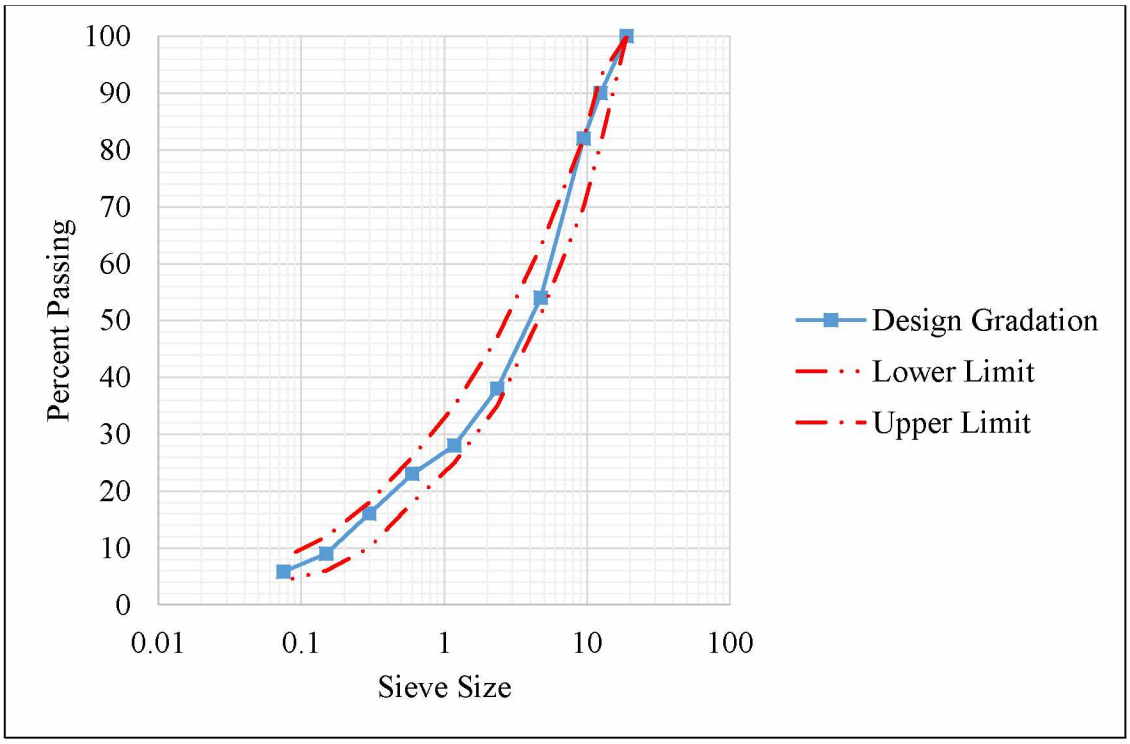

Figure 3.1 Aggregate gradation (mix #1 & #6) with PG 52-28 Type II-B (Central)

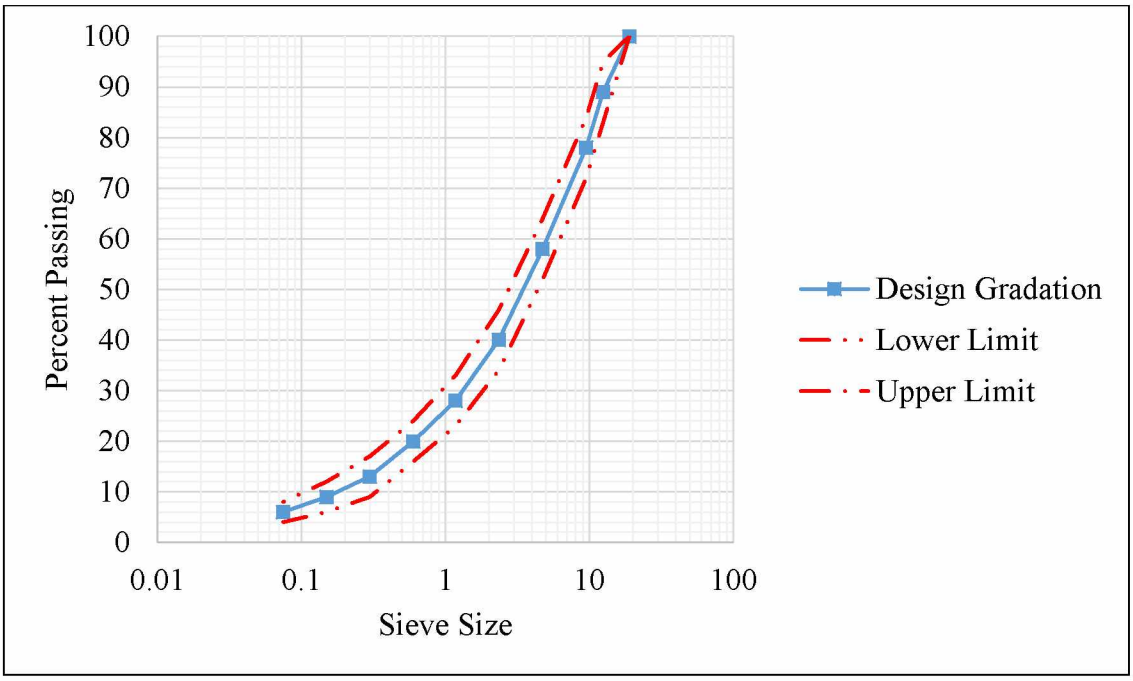

Figure 3.2 Aggregate gradation (mix # 2 & #5) with PG 58-34 Type II-B (Central)

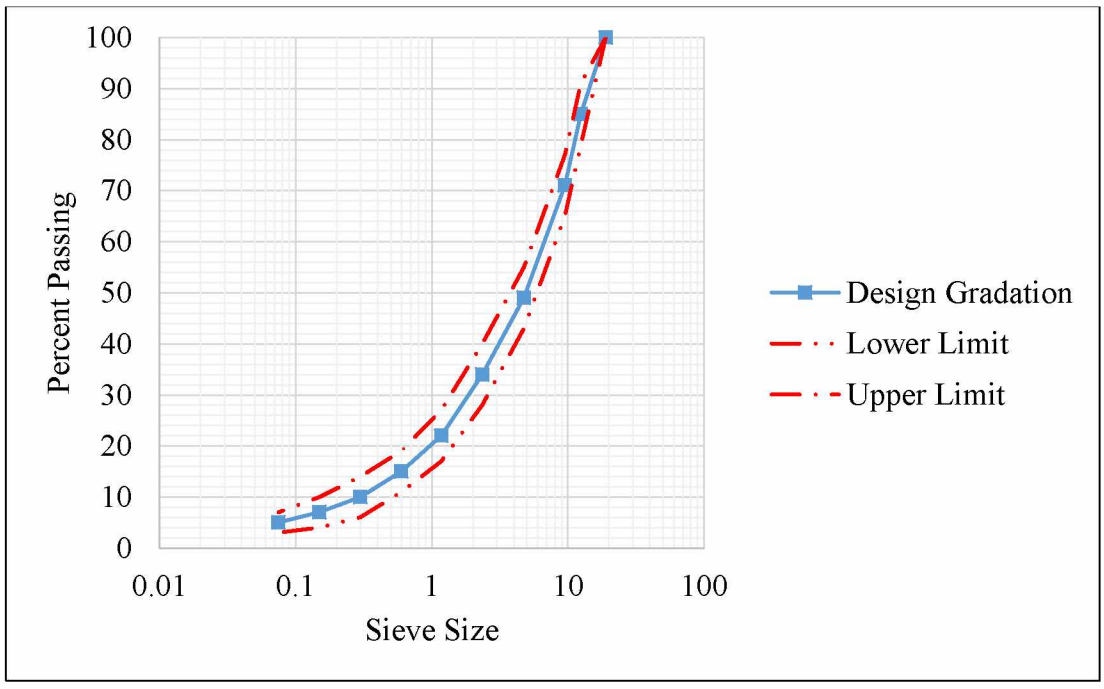

Figure 3.3 Aggregate gradation (mix #3) with PG 58-34 Type II-A (Central)

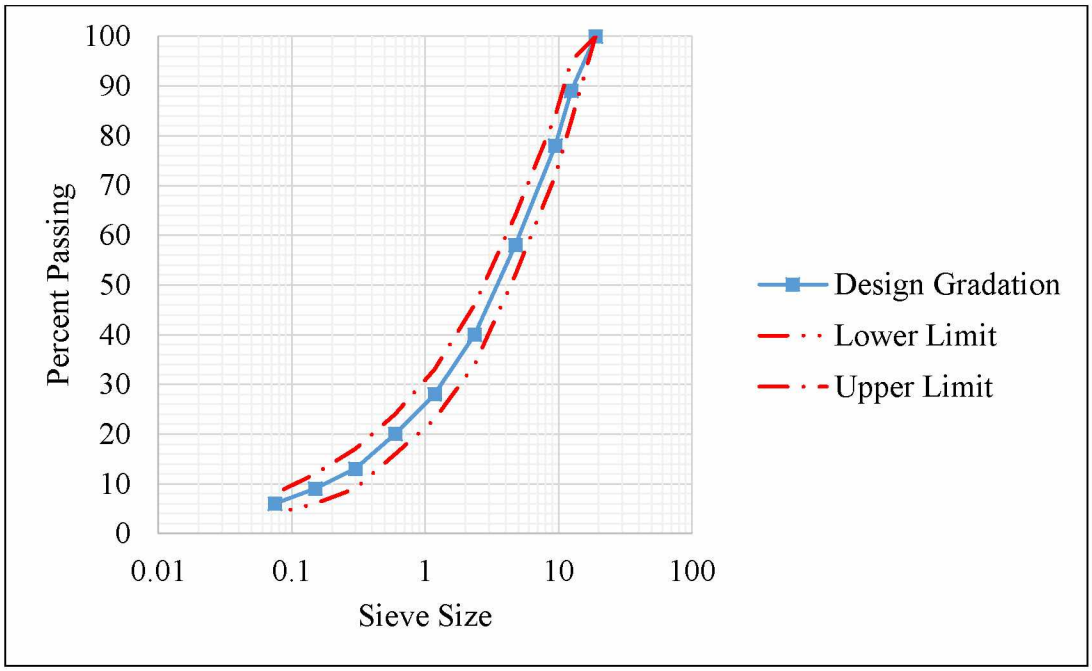

Figure 3.4 Aggregate gradation (mix #4) with PG 58-34 Type II-A 25% RAP (Central)

Plant produced HMA was collected by ADOT&PF at the paving site. Ten boxes containing approximately 12 kg of asphalt were obtained for each mix design collected and stored at the DOT office in Anchorage. The materials were then delivered to the University of Alaska Fairbanks by Lynden Transport or by ADOT employees. The plant produced HMA samples were re-heated at 160°C for 2 hours and compacted using the gyratory compactor. The specimens were compacted using air void control following AASHTO PP 60 to a design AV of 7.0 ± 0.5%. The details of specimen fabrication are discussed in section 3.4.

The Northern region mixes used two different binder grades, PG 52-28 and PG 52-40. The Type II-B mix designation was used for all mixes from this region with differing amounts of RAP. The PG 52-28 mixes were tested with 25 and 35 percent RAP while the PG 52-40 was tested at 25 percent. Both mixtures were tested against a control containing 0% RAP. Due to the lack of highway construction projects in the Northern region, all asphalt mixtures were produced in the laboratory. The virgin aggregate and RAP were obtained from a single contractor, Exclusive Paving, and collected at the Tanana River Valley stockpile. The asphalt binder was obtained from Emulsion Products Co. Table 3.1 provides a summary of the Northern region mixes studied in this experiment.

Virgin aggregate and RAP for all Northern region mixes were obtained from Exclusive Paving's Tanana River Valley stockpiles. The coarse, intermediate and fine aggregate as well as the RAP were collected from separate stockpiles and their respective gradations were determined. These gradations can be found in Appendix A.

Using the job mix formulae, blends were created to adhere to the specific design gradations based on the JMF percent passing criteria. Figure 3.5 shows the blended aggregate gradations and their conformity to the JMF for mixes with the PG 52-28 binder designation. Figure 3.6 show the blended aggregate gradations and their conformity to the JMF for mixes with the PG 52-40 binder designation.

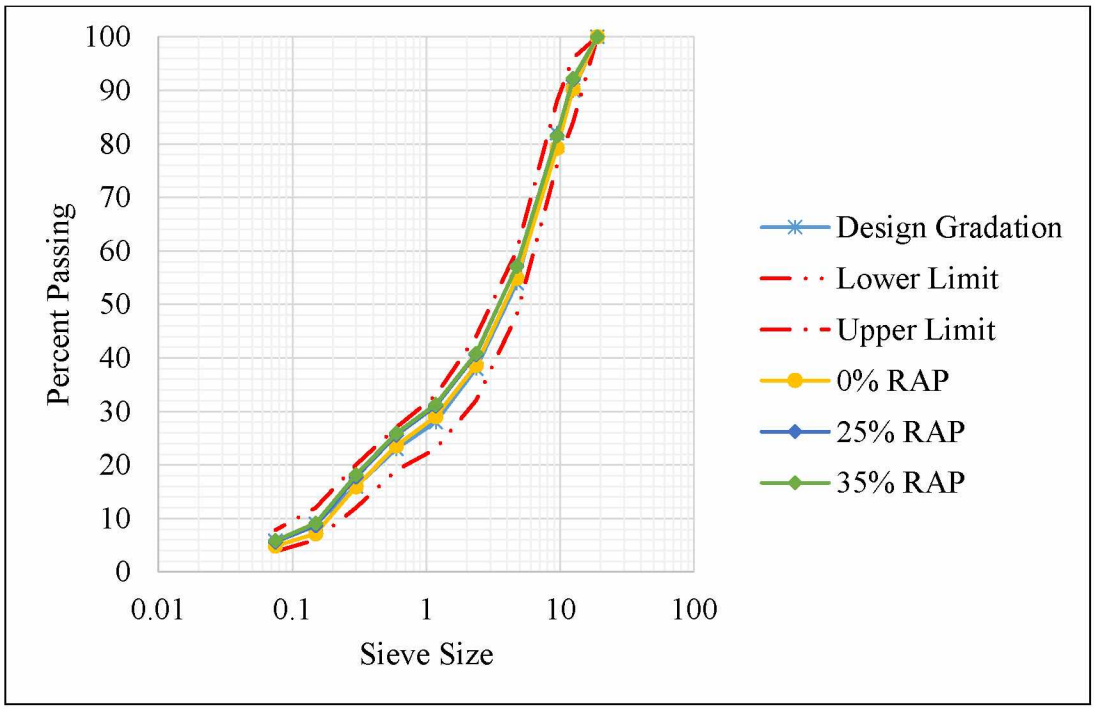

Figure 3.5 Aggregate gradation (mix #7, 9, 11) PG 52-28 binder (Northern)

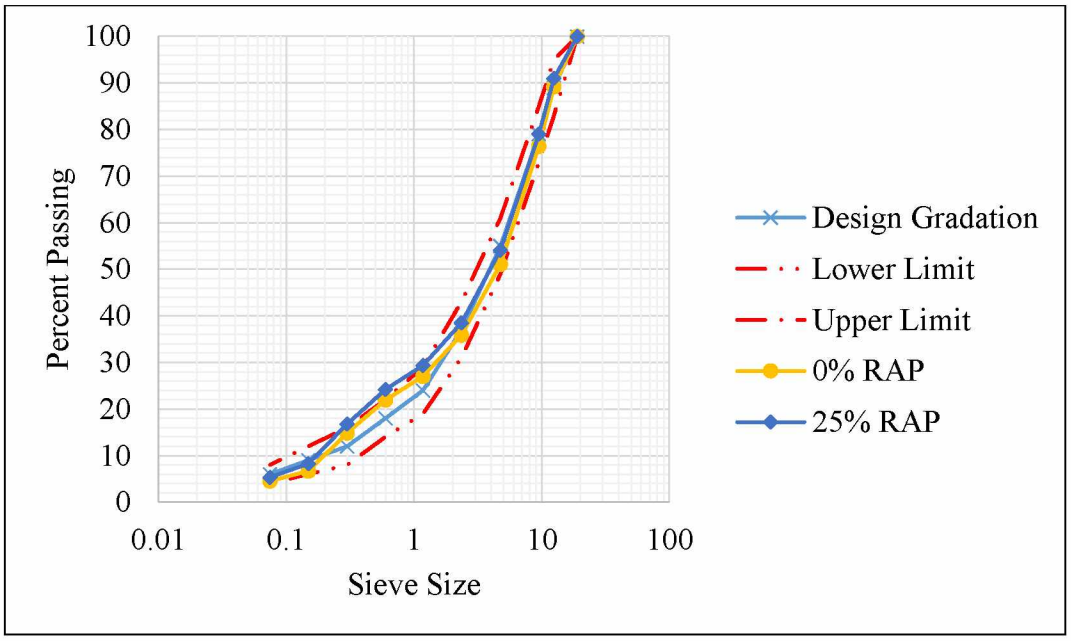

Figure 3.6 Aggregate gradation (mix #8 & #10) PG 52-40 binder (Northern)

RAP was added to the laboratory mixtures by first determining its gradation and binder content. Once this information was known, it was used to replace aggregate and binder based on the particular gradation and RAP content of the mixture. Table 3.2 shows a summary of mix designs based on the JMF.

Table 3.2 Summary of mix properties from JMFs

Mix	Type	Binder		Volumetrics			Gradation % Passing										D/A
		PG	Binder Content (%)	VTM (%)	VFA (%)	VMA (%)	3/4	1/2	3/8	#4	#8	#16	#30	#50	#100	#200	
1	II-B	52-28	5.4	3.2	78	14.6	100	87	76	57	41	30	22	14	9	6.2	1.3
2	II-B	58-34	5.3	3.1	78	13.8	100	89	78	58	40	28	20	13	9	6.0	1.4
3	II-A	58-34	5.3	3.8	75	15.0	100	85	71	49	34	22	15	10	7	5.0	1.1
4	II-A	58-34	5.0	3.1	77	13.8	100	89	78	58	40	28	20	13	9	6.0	1.4
5	II-B	58-34	5.3	3.1	78	13.8	100	89	78	58	40	28	20	13	9	6.0	1.4
6	II-B	52-28	5.4	3.2	78	14.6	100	87	76	57	41	30	22	14	9	6.2	1.3
7	II-B	52-28	5.5	3.6	76	14.7	100	90	82	54	38	28	23	16	9	5.8	1.3
8	II-B	52-40	5.5	3.9	73	14.4	100	89	79	55	37	24	18	12	9	6.0	1.4
9	II-B	52-28	5.5	3.6	76	14.7	100	90	82	54	38	28	23	16	9	5.8	1.3
10	II-B	52-40	5.5	3.9	73	14.4	100	89	79	55	37	24	18	12	9	6.0	1.4
11	II-B	52-28	5.5	3.6	76	14.7	100	90	82	54	38	28	23	16	9	5.8	1.3

** Type II: NMAS 19mm; Class A: 75 blows; Class B: 50 blows*

3.3 Binder Tests

The asphalt binders used in this study were collected from Emulsion Products Co. and include PG 52-28, PG 58-34 and PG 52-40. Testing of all binders used in this project was conducted by researchers at the University of Tennessee Knoxville (UTK) for the ADOT&PF project (Liu et al., 2016). Table 3.3 summarizes the binder-testing matrix. A dynamic shear rheometer (DSR) was used to verify the high-temperature grading and to test viscoelastic behavior.

Table 3.3 Testing matrix (tests conducted in triplicate)

Properties	Parameters	Equip.	Binder status	Binders	Testing T (°C)	Standard
Binder Grading	G*/sinδ	DSR	Original RTFO	PG 52-28 PG 52-40 PG 58-34	Binder Dependent	ASTM D 7643
Viscoelastic behavior	complex modulus *(G*)* and phase angle *(δ)*	DSR	RTFO	PG 52-28 PG 52-40 PG 58-34	Three for each (± 6°C and high PG)	AASHTO T 315

The DSR test was used to determine the viscoelastic behavior at mid-to-high-level temperatures. Following ASTM D7643 and AASHTO T 315, the selected binders were subjected to DSR testing (Figure 3.7). Six specimens per binder grade were tested, with three specimens as original and three undergoing RTFO aging. Figure 3.9 shows the DSR specimens and Figure 3.8 shows the RTFO oven. For each binder grade group, a mid and high temperature was chosen and applied to the control group and RTFO-aged specimens. For the test, a thin film of binder was placed between two plates of the DSR device with the lower plate fixed. Torque was applied to the upper plate at a frequency of 10 radians per second. The applied torque and resulting shear strain measured by the DSR are used to calculate the complex modulus (G*) and phase angle (δ) of the binder. The G* is a measurement of total resistance to deformation under constant shear, while δ defines the interval between the applied shearing stress and resulting shear strain due to the applied torque. The original binder specification requires a minimum value of 1.0 kPa for G*/sinδ for the corresponding temperature. The RTFO-aged binder specification requires a

minimum value of 2.20 kPa for G*/sinδ at the corresponding temperature. G* and δ values tested at all the high temperatures were recorded to display the viscoelastic behavior of the binders.

Figure 3.7 DSR equipment (courtesy of UTK)

Figure 3.8 Rolling thin film oven (RTFO) (courtesy of UTK)

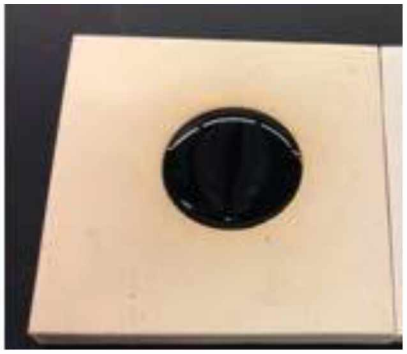

Figure 3.9 DSR specimen (courtesy of UTK)

3.4 Sample Preparation

The laboratory-produced mixtures were fabricated following the JMF. Each aggregate gradation was weighed and placed in an oven at 165 °C for two hours. Asphalt binder was heated at 165 °C for one hour. RAP was heated in a separate oven at 110 °C for one hour. The three components (aggregate, binder and RAP) were then mixed using a commercial grade mixer manufactured by Hobart (Figure 3.10). The loose asphalt mix was then placed in the oven at 165 °C for an additional two hours to simulate short-term aging. The HMA test specimens (both lab and field produced) were fabricated following AASHTO PP 60, *Preparation of Cylindrical Performance Test Specimens Using the Superpave Gyratory Compactor (SGC)* (Figure 3.11). The design air voids (VTM) for this experiment was 7.0 ± 0.5%. The following method was followed to achieve target air void content.

The maximum specific gravity, G_{mm}, was either provided on the JMF or measured following AASHTO T209, *Theoretical Maximum Specific Gravity (G_{mm}) and Density of Hot Mix Asphalt (HMA)*. An estimate of the HMA required was determined using the G_{mm}, target height and target air void content using Equation 3.1.

$$\text{Mass} = \left[\frac{100 - (Va_t + F)}{100}\right] * G_{mm} * 176.7147 * H$$

Equation 3.1

where,

Mass = estimated mass of mixture to prepare a test specimen to target air voids

Va_t = target air void content for the test specimen, percent by volume

G_{mm} = maximum specific gravity of the mixture

H = height of the gyratory specimen, cm

F = air void adjustment factor: 1.0 for fine-graded; 1.5 for coarse-graded

Using the estimated mass from Equation 3.1, a trial specimen was prepared. The bulk specific gravity was measured and the air void content was determined. The mass was then adjusted using the following equation:

$$Mass_{adj} = \left[\frac{100 - Va_t}{100 - Va_m}\right] * Mass$$

Equation 3.2

where,

$Mass_{adj}$ = adjusted gyratory specimen mass, g

Va_t = target air void content for the test specimen, percent by volume

Va_m = measured trial test specimen air void content, percent by volume

$Mass$ = mass used to prepare the gyratory specimen for the trial test specimen

Using the adjusted mass from Equation 3.2, a second trial gyratory specimen was fabricated. The bulk specific gravity was measured and the air void content was determined as before. If the air void tolerance was not satisfied, the mass was again adjusted using Equation 3.2. The process was repeated until the air void content was within the acceptable range. Once the target AV had been achieved, the specimens were produced in triplicate and their AV was confirmed.

Figure 3.10 Asphalt mixer

Figure 3.11 Superpave gyratory compactor

The specimens produced for AMPT tests from the SGC had a dimeter of 150mm and were compacted to a height of 170mm (Figure 3.12). The compacted samples were then cored using a floor mounted coring drill (Figure 3.13) to a final diameter of 100mm and cut to a final height of 150mm using a masonry saw (Figure 3.14). Studs for mounting LVDT's were then attached to the AMPT specimens using the Gauge Point Fixing Jig supplied by IPC Global (Figure 3.15). The studs were placed radially at 120°. The specimens used for |E*| tests were also used for FN testing.

Figure 3.12 Representative specimens for AMPT tests

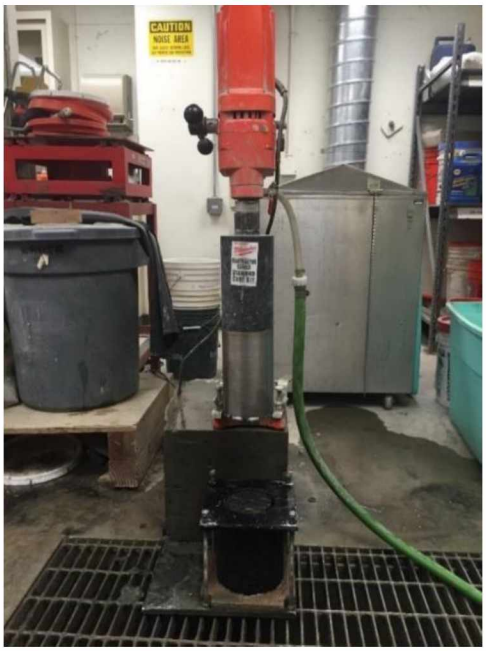

Figure 3.13 Asphalt specimen core drill

Figure 3.14 Masonry saw

Figure 3.15 Gauge point fixing jig

The air voids of all test specimens were confirmed following AASHTO T 269, *Percent Air Voids in Compacted Dense and Open Asphalt Mixtures*. The target air voids for this project

was 7% ± 0.5%. The results of these tests can be found in Appendix B. The air voids of test specimens were determined as follows:

$$Percent\ Air\ Voids = 100\left(1 - \frac{G_{mb}}{G_{mm}}\right)$$

Equation 3.3

where,

G_{mb} = bulk specific gravity

G_{mm} = maximum (Rice) specific gravity

3.5 Dynamic Modulus Test

The SPT tests (dynamic modulus and flow number) were performed utilizing the AMPT apparatus manufactured by IPC Global of Australia (Figure 3.16). The testing system consists of a digital servo hydraulic control with a continuous electronic control and data acquisition system (CDAS). Two AMPT tests were used to evaluate the materials of this study; the dynamic modulus and flow number.

Figure 3.16 AMPT

The Dynamic Modulus test procedure was derived from AASHTO T 342, *Standard Method of Test for Determining Dynamic Modulus of Hot Mix Asphalt (HMA)*. This test is stress controlled, meaning the test is conducted in such a way that the strain increases at a given rate. For this study, the load induced approximately 100 microstrain in the specimen. Three linear variable displacement transducers (LVDT) were placed radially at 120°. The LVDT's measured and recorded the deformation (strain) during loading. The applied load (stress) was a continuous sinusoidal compression. The specimens were placed in an environmental chamber at the appropriate temperature to ± 0.5° C. Response and performance analysis were conducted at loading frequencies of 0.1, 0.5, 1, 2, 5, 10, 20 and 25 Hz and at temperatures of 4.4, 21.1, 37.8 and 54° C (40, 70, 100 and 130° F).

The precision of |E*| test results was evaluated following AASHTO TP 79, *Determining the Dynamic Modulus and Flow Number for Asphalt Mixtures Using the Asphalt Mixture Performance Tester (AMPT).* The coefficient of variation was determined (Equation 3.4) and compared to the recommended limits for three test replicates, single-operator precision. This evaluation provides support for the repeatability of the test results.

$$S_r\% = \left[29.8e^{(0.014\times NMAS)}\right]\times|E*|^{-\left[0.189e^{(0.012\times NMAS)}\right]}$$

Equation 3.4

where,

Sr% = repeatability coefficient of variation for |E*|, %

NMAS = mixture nominal maximum aggregate size, mm

|E|* = average dynamic modulus, MPa

Master curves for the dynamic modulus were created using the time-temperature superposition (t-TS) principle as defined in section 2.3 of this document and presented in section 4.2, Figures 4.6 – 4.10.

3.6 Flow Number Test

The flow number (FN) test procedure was derived from AASHTO TP79 (2013). The samples used to determine the dynamic modulus were also used to test FN (Figure 3.17). The

testing was performed in triplicate. The FN test is used to evaluate the creep characteristics of HMA and results in the permanent deformation of the test specimen. The specimen was a cored cylinder 100 mm in diameter and 150 mm in height. A uniaxial compressive load was applied in haversine form with a loading time of 0.1 seconds and a rest duration of 0.9 seconds for a maximum of 10,000 cycles or until a 50,000 microstrain deformation is reached. No confining stress was applied. Tests were conducted at 40 °C which closely matched the High Adjusted PG Temperature for Fairbanks, AK and surrounding areas. Average maximum effective pavement temperature was determined using LTPP Bind Version 3.1 software.

Figure 3.17 AMPT specimens following FN testing

CHAPTER 4 RESULTS AND ANALYSIS

The results and analysis of binder specifications, HMA mixture performance tests and cost analysis are summarized in this chapter. Testing of all binders used in this study (PG 52-28, PG 58-34 and PG 52-40) was conducted by researchers at the University of Tennessee Knoxville (UTK) for the ADOT&PF project (Liu et al. 2016). The analysis of data was conducted by this researcher. AMPT tests including |E*| and FN were conducted on the 11 mixtures. The |E*| master curves were constructed from measured |E*|. Predictive models were investigated on seven of the eleven mixtures (based on the availability of job mix formulae) at the MEPDG Level 2 and Level 3. In Level 2, the |E*| was calculated based on both measured binder and mix volumetric properties. In Level 3, the |E*| was calculated based on mix volumetric properties (from the JMF) and default binder properties, which were determined according to the binder's PG. A preliminary cost analysis based on material inputs was conducted on a typical Alaskan HMA mix containing 0% and 25% RAP.

4.1 Binder Tests

The asphalt binders used in this study included PG 52-28, PG 58-34 and PG 52-40. The true high temperature grades were verified for each original and RTFO aged binder using a DSR and the results are presented in Table 4.1. The viscoelastic behavior (complex modulus (G*) and phase angle (δ)) was determined using a DSR and the results are presented in Table 4.2. These binder parameters were determined at three test temperatures, including the high PG temperature and ± 6 °C of the high PG. Detailed testing data can be found in Appendix C. This data was used to predict |E*| using the original and modified Witczak |E*| predictive models. The binder properties of asphalt mixtures containing RAP were not evaluated.

Table 4.1 True high temperature grades of binders

Binder	True High Temperature Grade (Original) (°C)	True High Temperature Grade (RTFO) (°C)	High PG (°C)
PG 52-28	56.6	56.9	52
PG 58-34	64.3	61.4	58
PG 52-40	60.6	56.4	52

Table 4.2 Viscoelastic behavior in terms of |G*| and δ at RTFO

Binder	T (°C)	|G*| (kPa)	δ (rad)
PG 52-28	46	10.53	1.46
	52	4.39	1.49
	58	1.88	1.51
PG 58-34	52	4.50	1.09
	58	2.56	1.08
	64	1.54	1.06
PG 52-40	46	4.36	1.05
	52	2.65	1.03
	58	1.65	1.01

4.2 Dynamic Modulus

The |E*| test was performed as detailed in Chapter 3. Eleven mixes (see Table 3.1) were evaluated for |E*|. The following figures summarize the |E*| testing for this project: Figure 4.1 (a-d) are Central region mixes Type II-B with PG 52-28 binder (mixes #1, #6). Figure 4.2 (a-d) are Central region Type II-B with PG 58-34 binder (mixes #3, #4). Figure 4.3 (a-d) are Central region Type II-A with binder designation PG 58-34 (mixes #2, #5). Figure 4.4 (a-d) are Northern region with PG 52-28 binder (mixes #7, #9 and #11). Figure 4.5 (a-d) are Northern region PG 52-40 binder (mixes #8, #10).

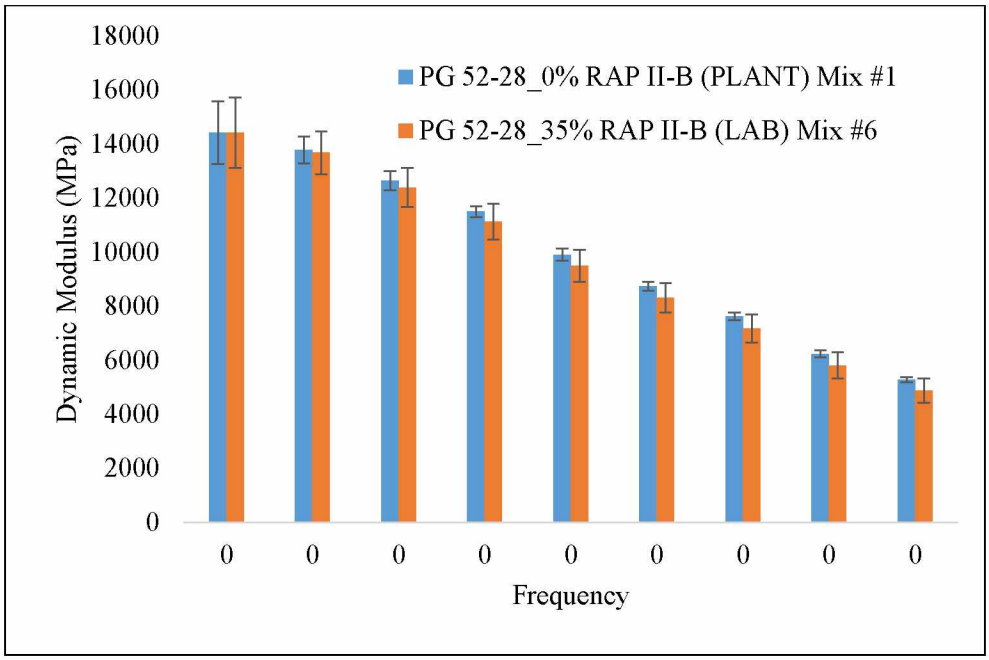

(a) PG 52-28 Type II-B, 4.4 °C

Figure 4.1 |E*| data for Central region mixes #1 and #6

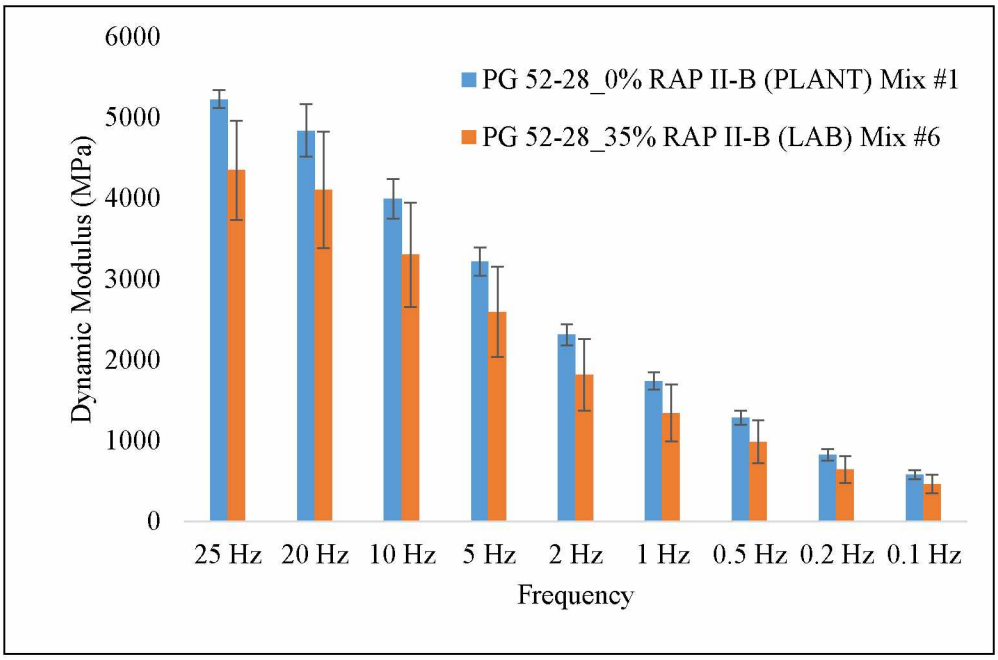

(b) PG 52-28 Type II-B, 21.1 °C

Figure 4.1 continued

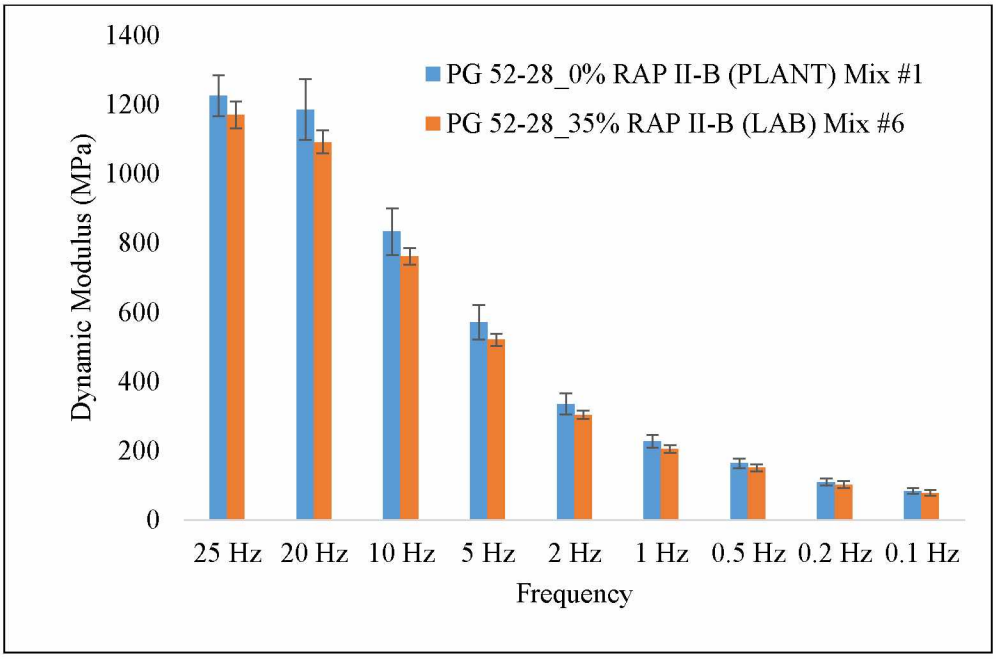

(c) PG 52-28 Type II-B, 37.8 °C

Figure 4.1 continued

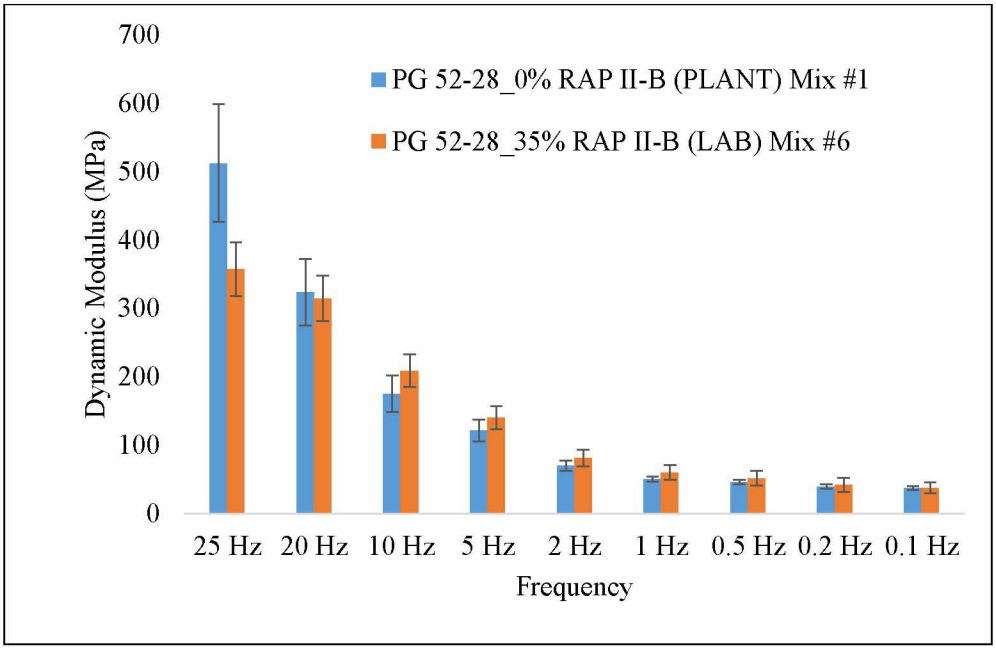

(d) PG 52-28 Type II-B, 54.0 °C

Figure 4.1 continued

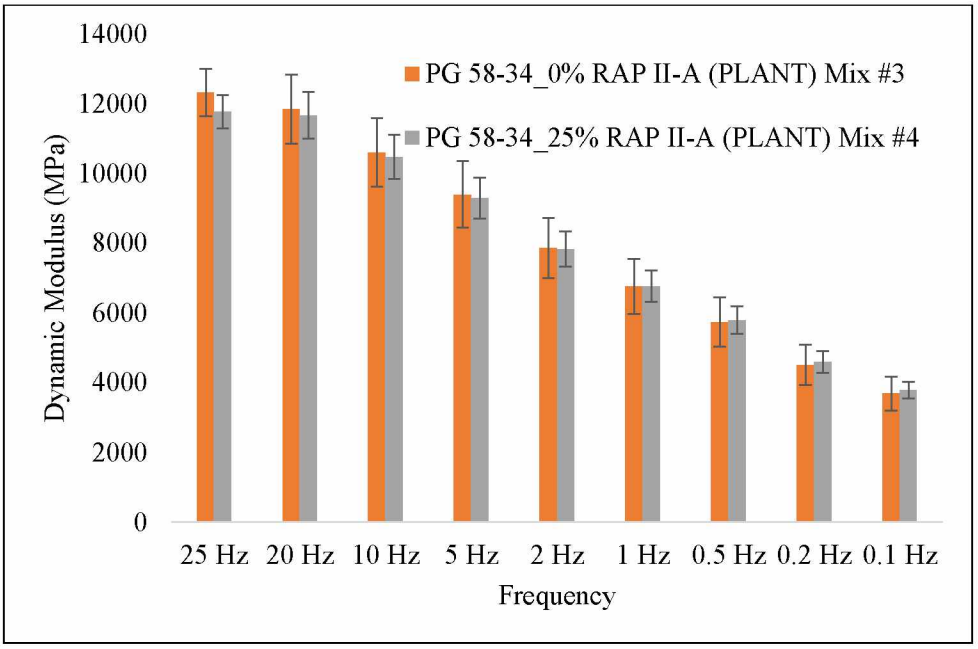

(a) PG 58-34 Type II-A, 4.4 °C

Figure 4.2 |E*| data for Central region mixes #3 and #4

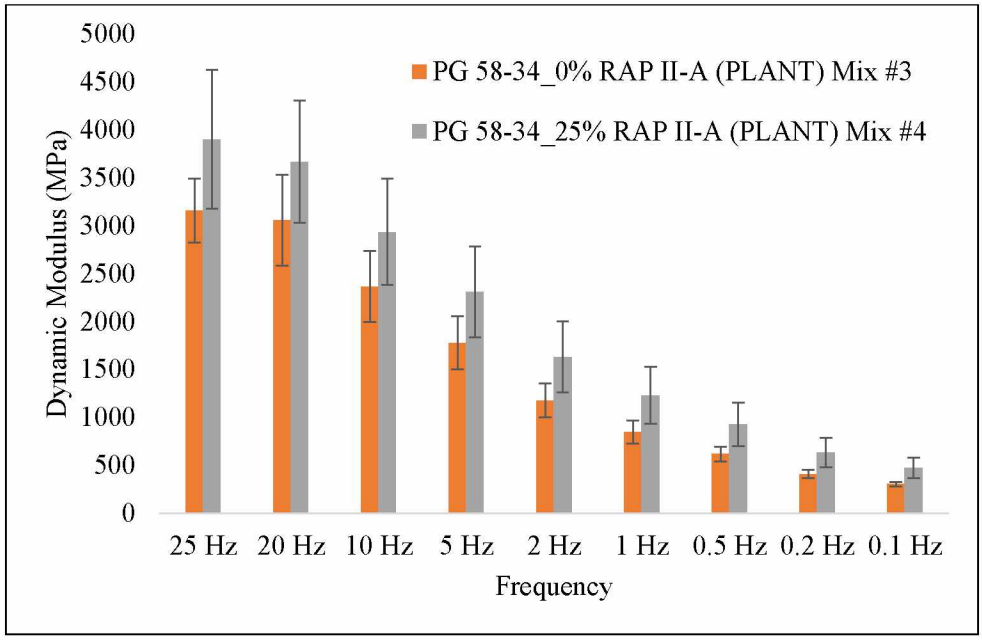

(b) 58-34 Type II-A, 21.1 °C

Figure 4.2 continued

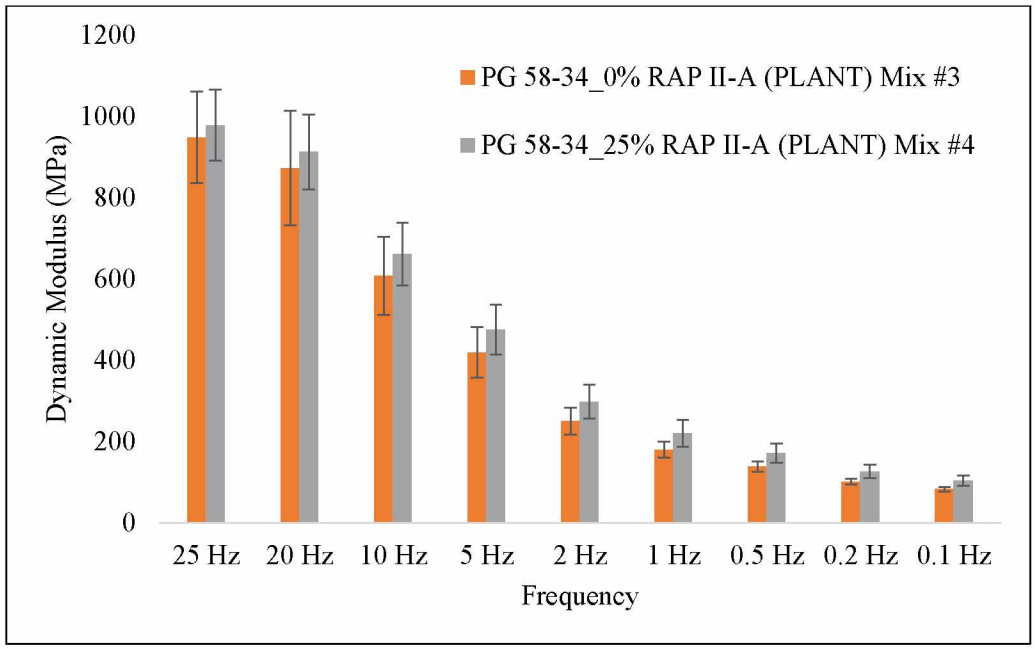

(c) PG 58-34 Type II-A, 37.8 °C

Figure 4.2 continued

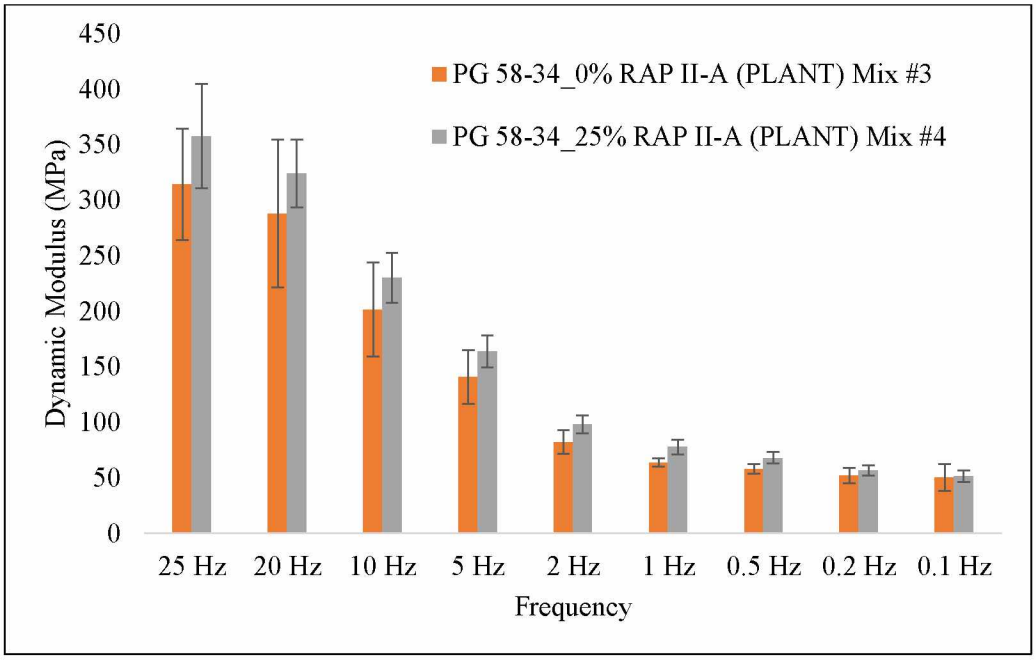

(d) PG 58-34 Type II-A, 54.0 °C

Figure 4.2 continued

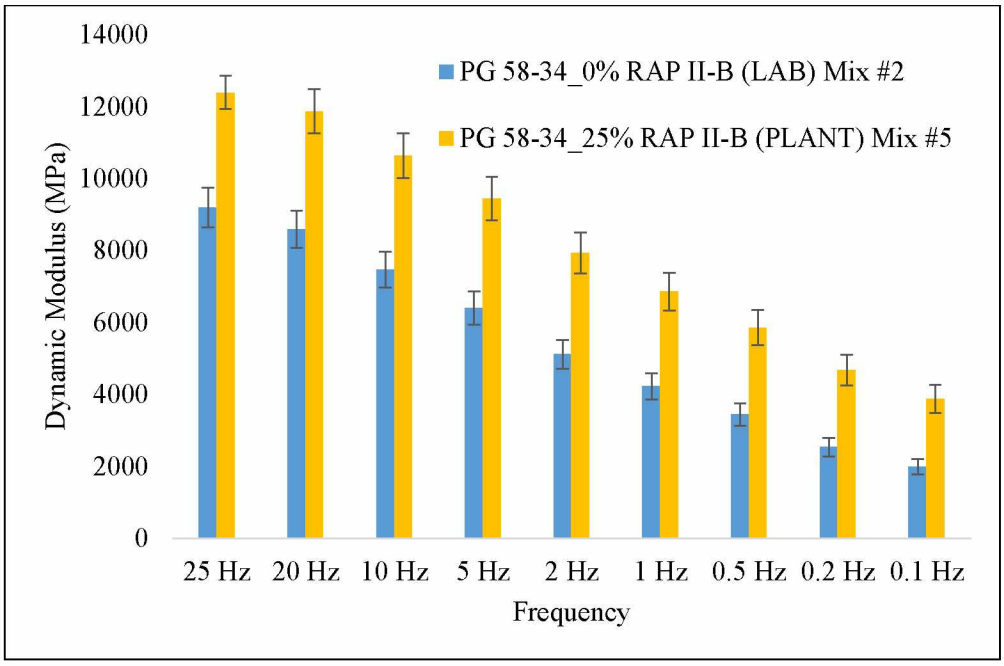

(a) PG 58-34 Type II-B, 4.4 °C

Figure 4.3 |E*| data for Central region mixes #2 and #5

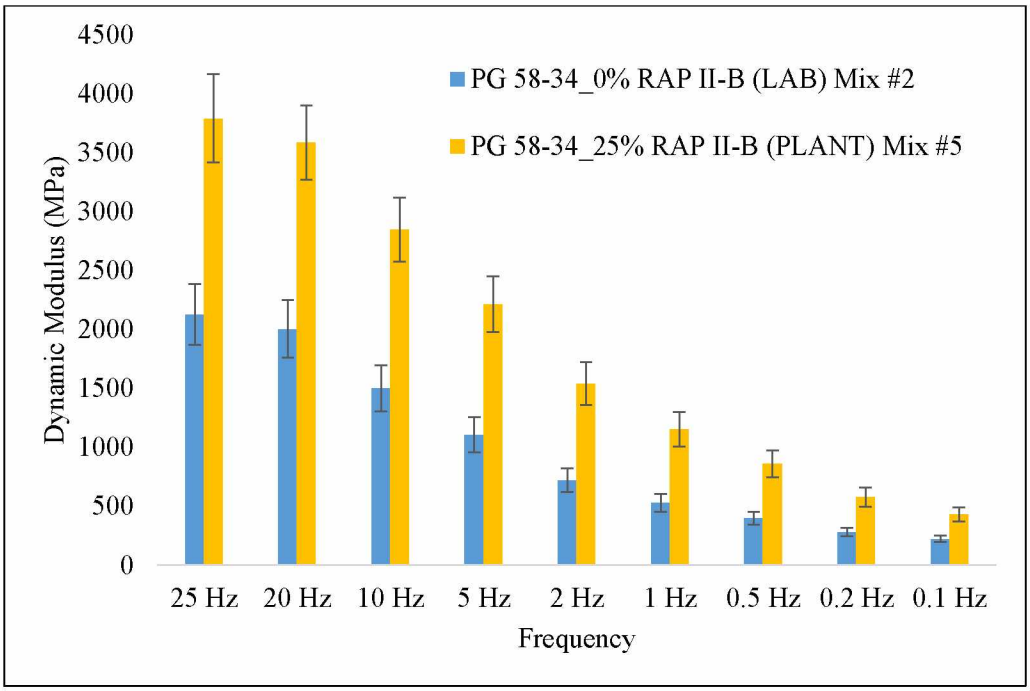

(b) PG 58-34 Type II-B, 21.1 °C

Figure 4.3 continued

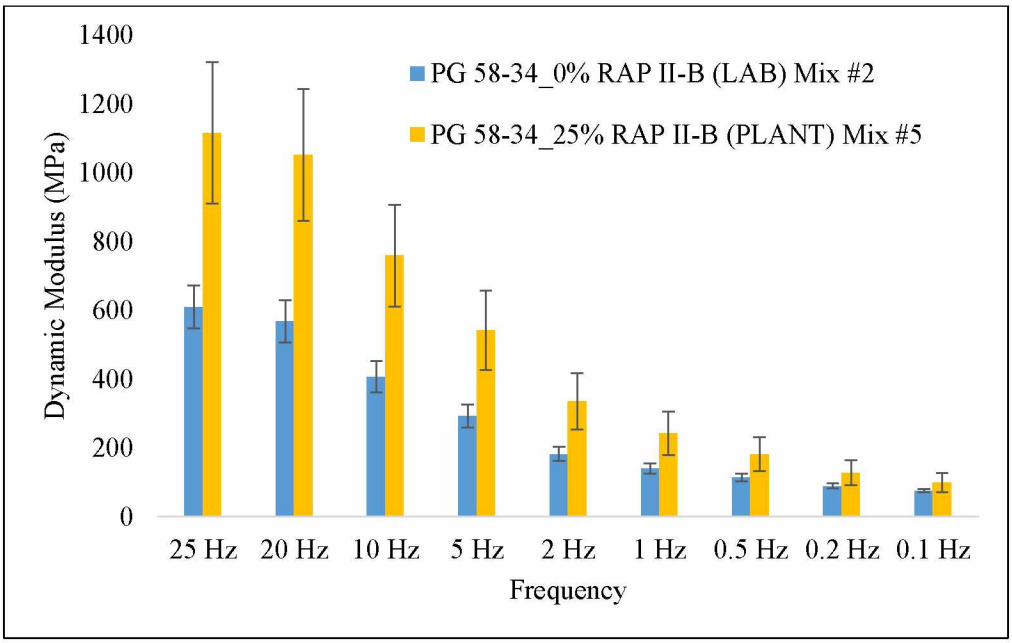

(c) PG 58-34 Type II-B, 37.8 °C

Figure 4.3 continued

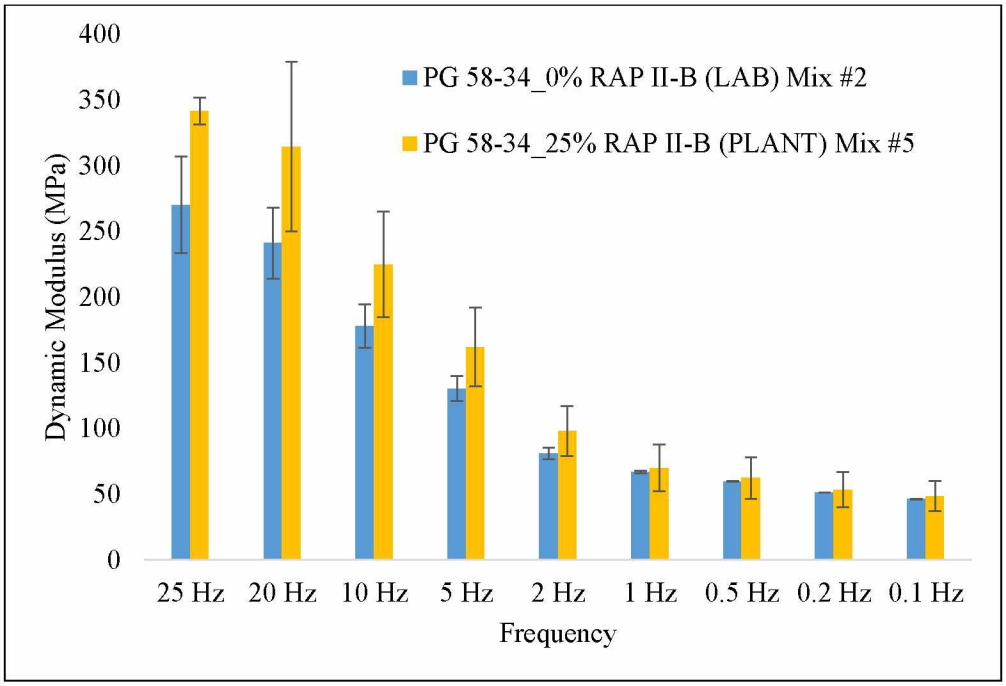

(d) PG 58-34 Type II-B, 54.0 °C

Figure 4.3 continued

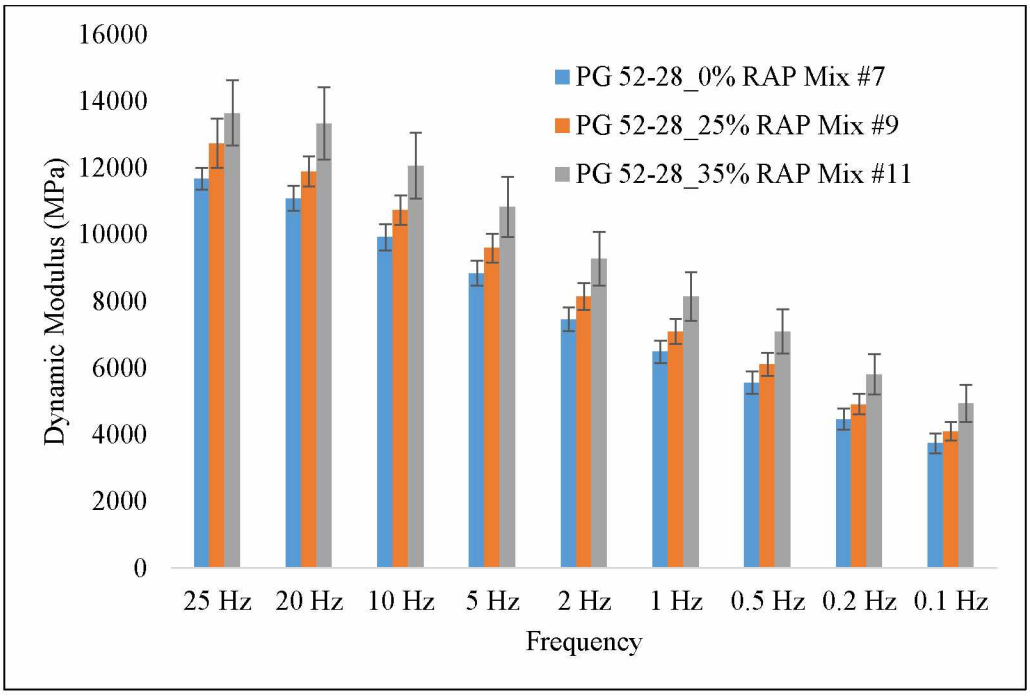

(a) PG 52-28, 4.4 °C

Figure 4.4 |E*| data for Northern region mixes #7, #9 and #11

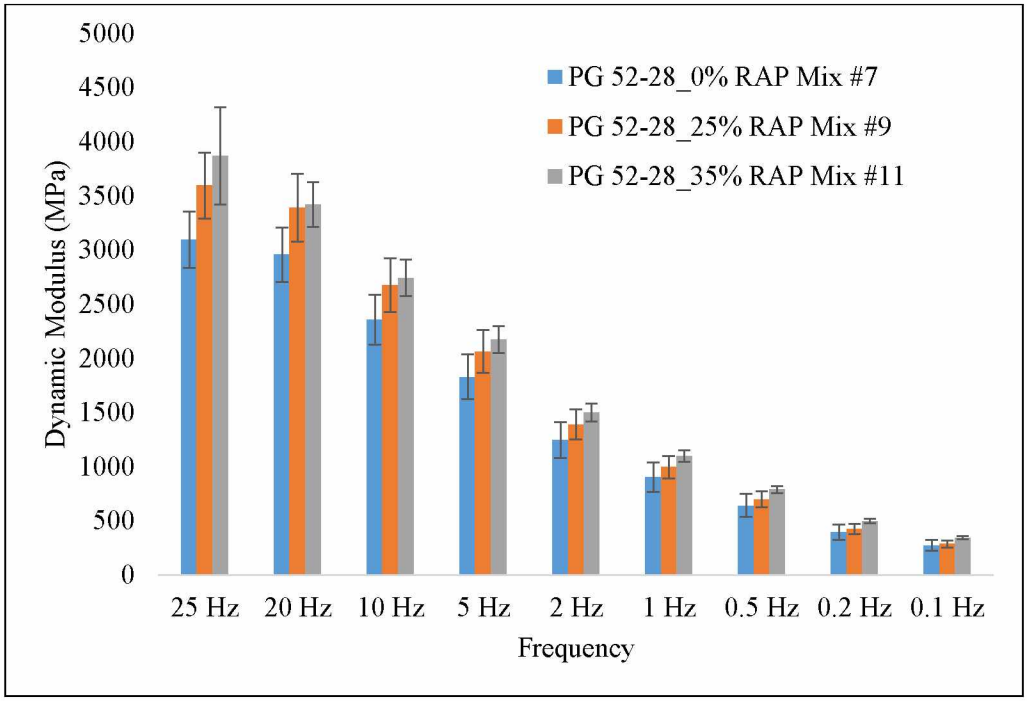

(b) PG 52-28, 21 °C

Figure 4.4 continued

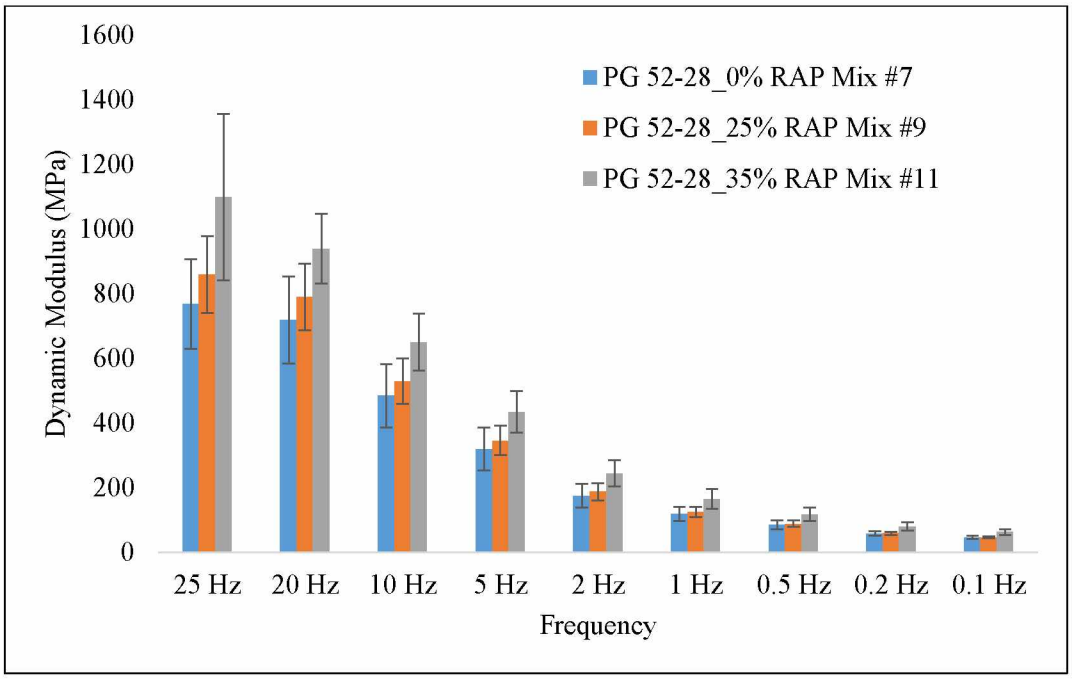

(c) PG 52-28, 37.8 °C

Figure 4.4 continued

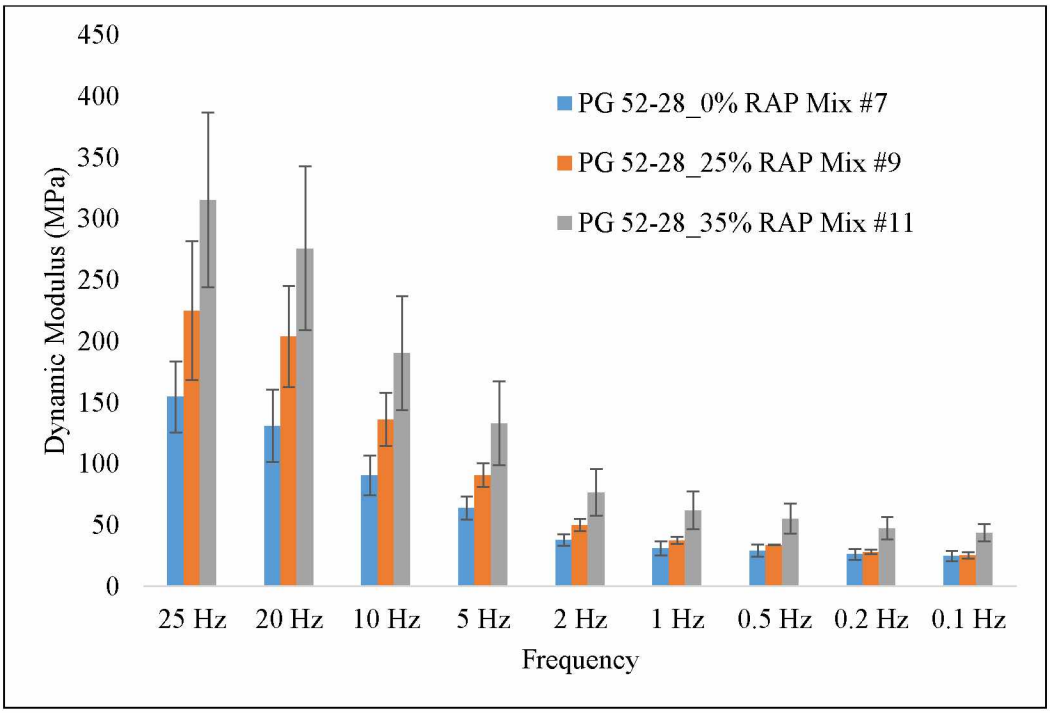

(d) PG 52-28, 54 °C

Figure 4.4 continued

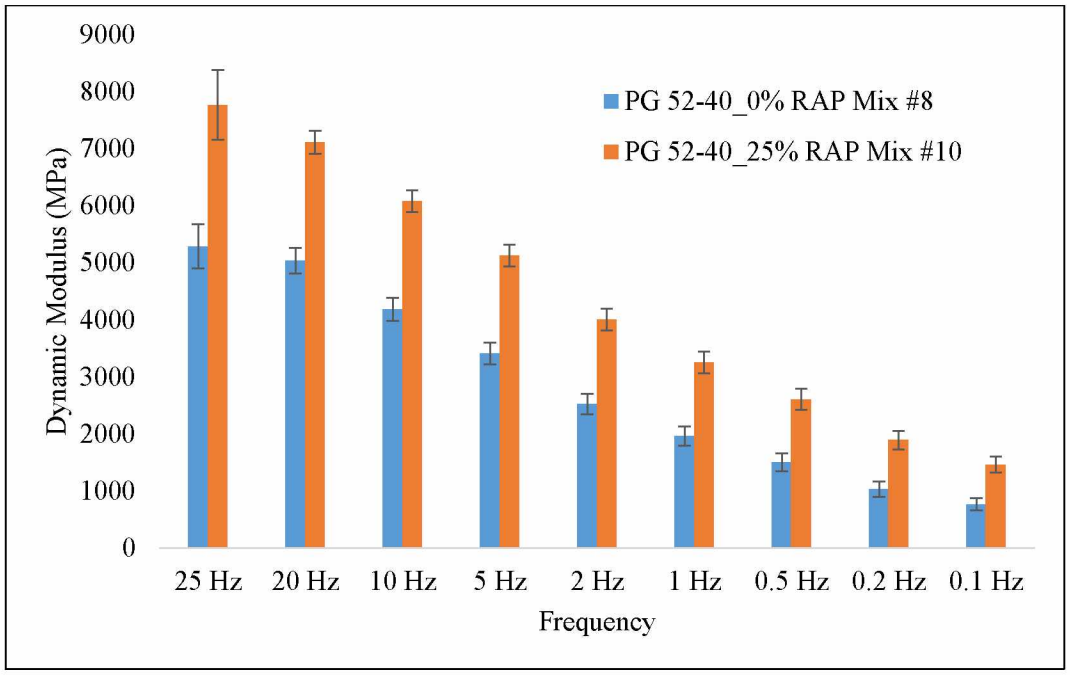

(a) PG 52-40, 4.4 °C

Figure 4.5 |E*| data for Northern region mixes #8 and #10

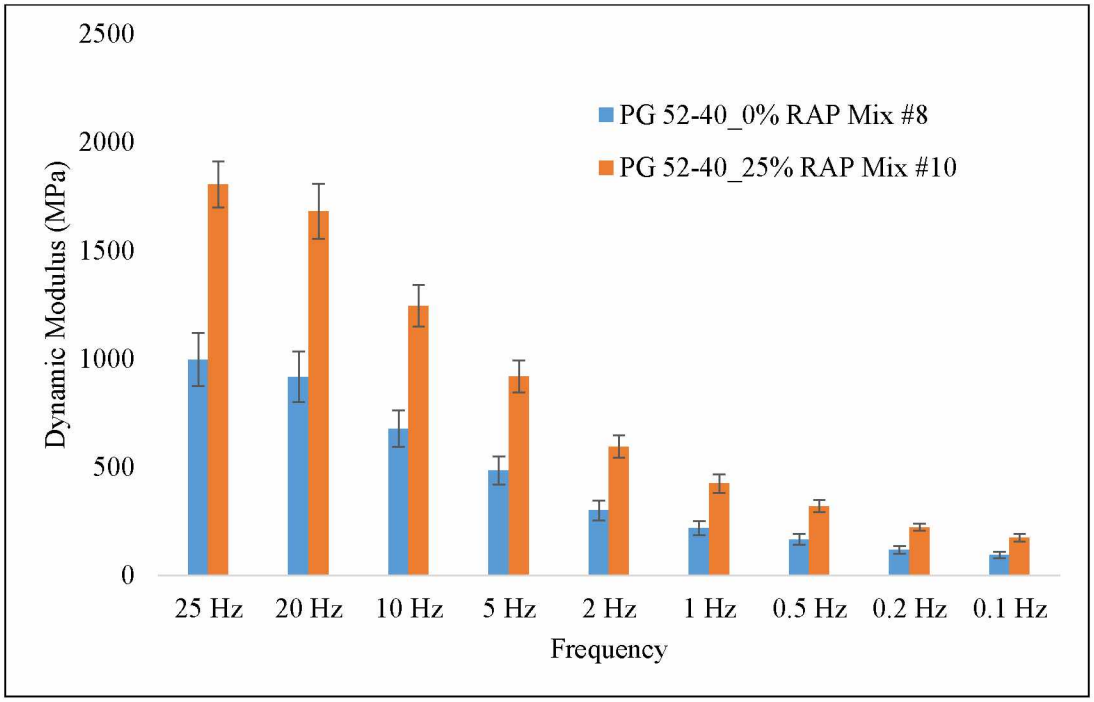

(b) PG 52-40, 21 °C

Figure 4.5 continued

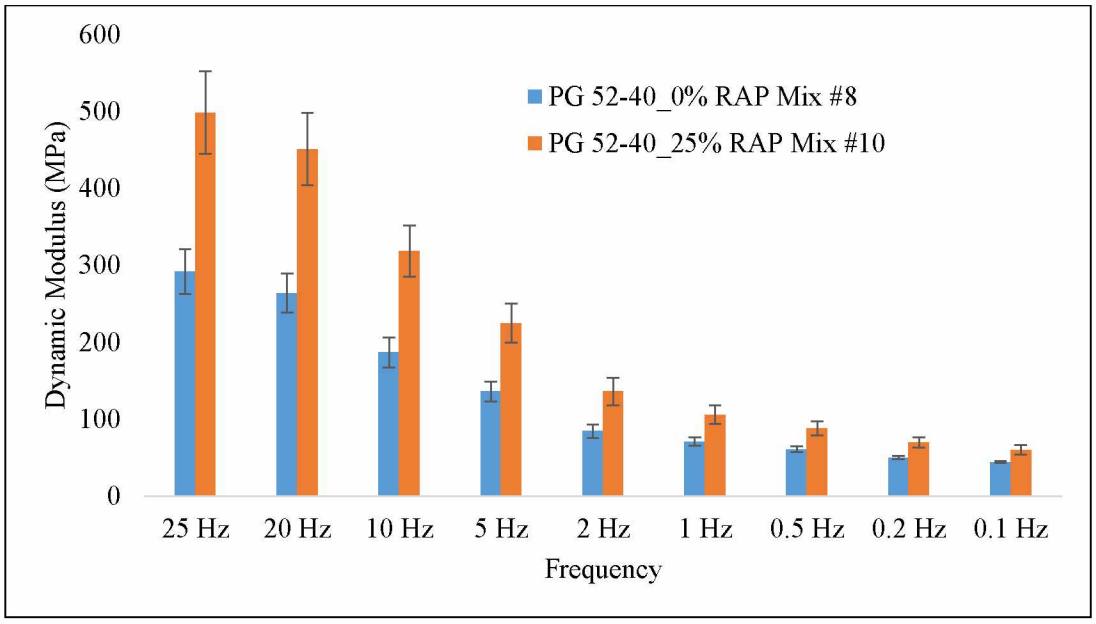

(c) PG 52-40, 37.8 °C

Figure 4.5 continued

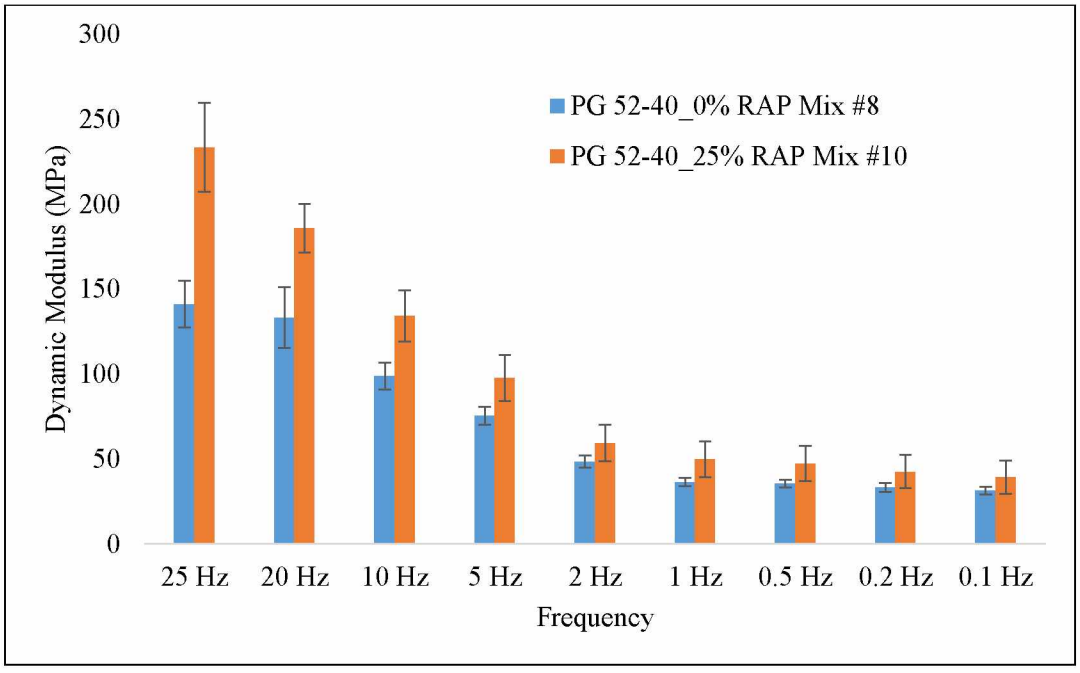

(d) PG 52-40, 54 °C

Figure 4.5 continued

The data show a general trend; the dynamic modulus increases with increasing frequency (i.e. loading time). The dynamic modulus of most mixes increased with the inclusion of RAP. In general, the higher the RAP content, the higher the dynamic modulus. One exception was observed regarding the PG 52-28 mixes (mix #1 and mix #6) from the Central region. Note that the control mix (#1) in this pair was produced in the field and the 35% RAP mix (#6) was produced in the lab. Testing on additional specimens should be done to validate this observation.

Figures 4.6 – 4.8 show the master curves for the Central Region mixtures. Table 4.3 – Table 4.8 show the summary of measured |E*| and the corresponding master curve coefficients. The individual |E*|curves were shifted into one master curve at a reference temperature of 21.1 °C using the time-temperature superposition principle as described in section 2.3. The mixture |E*| master curves were consistent with the |E*| testing results.

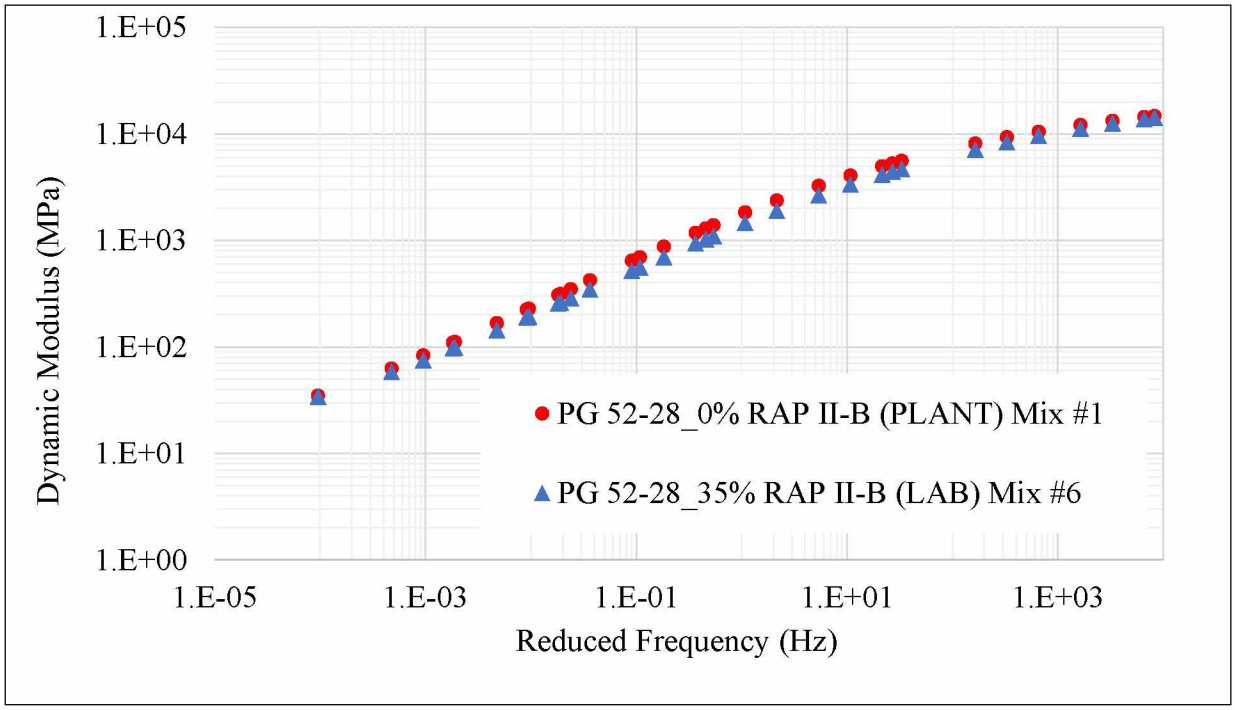

Figure 4.6 Central region master curve PG 52-28 II-B (mixes #1 & #6)

Table 4.3 Summary of measured |E*| and master curve coefficients (Mix #1)

	Measured Dynamic Modulus (MPa)							
Temperature (°C)	25 Hz	20 Hz	10 Hz	5 Hz	2 Hz	1 Hz	0.5 Hz	0.1 Hz
4	14415	13777	12641	11488	9905	8728	7616	5275
21	5226	4837	3991	3215	2312	1740	1282	576
37	1225	1186	832	571	335	227	163	84
54	512	323	175	121	70	50	46	37

Master Curve Coefficients							R^2 (Logarithmic)
δ	α	β	γ	a	b	c	
0.63214	3.7618431	-0.826054	0.490689	0.001116	-0.171323	3.06167	0.9998

Table 4.4 Summary of measured |E*| and master curve coefficients (Mix #6)

	Measured Dynamic Modulus (MPa)							
Temperature (°C)	25 Hz	20 Hz	10 Hz	5 Hz	2 Hz	1 Hz	0.5 Hz	0.1 Hz
4	14422	13682	12391	11121	9491	8303	7169	4871
21	4347	4104	3300	2596	1815	1342	984	463
37	1170	1092	761	520	304	205	150	78
54	357	315	209	140	81	60	52	38

Master Curve Coefficients							R^2 (Logarithmic)
δ	α	β	γ	a	b	c	
0.68385060	3.7585498	-0.646575	0.467550	0.001430	-0.176008	2.99628	0.9997

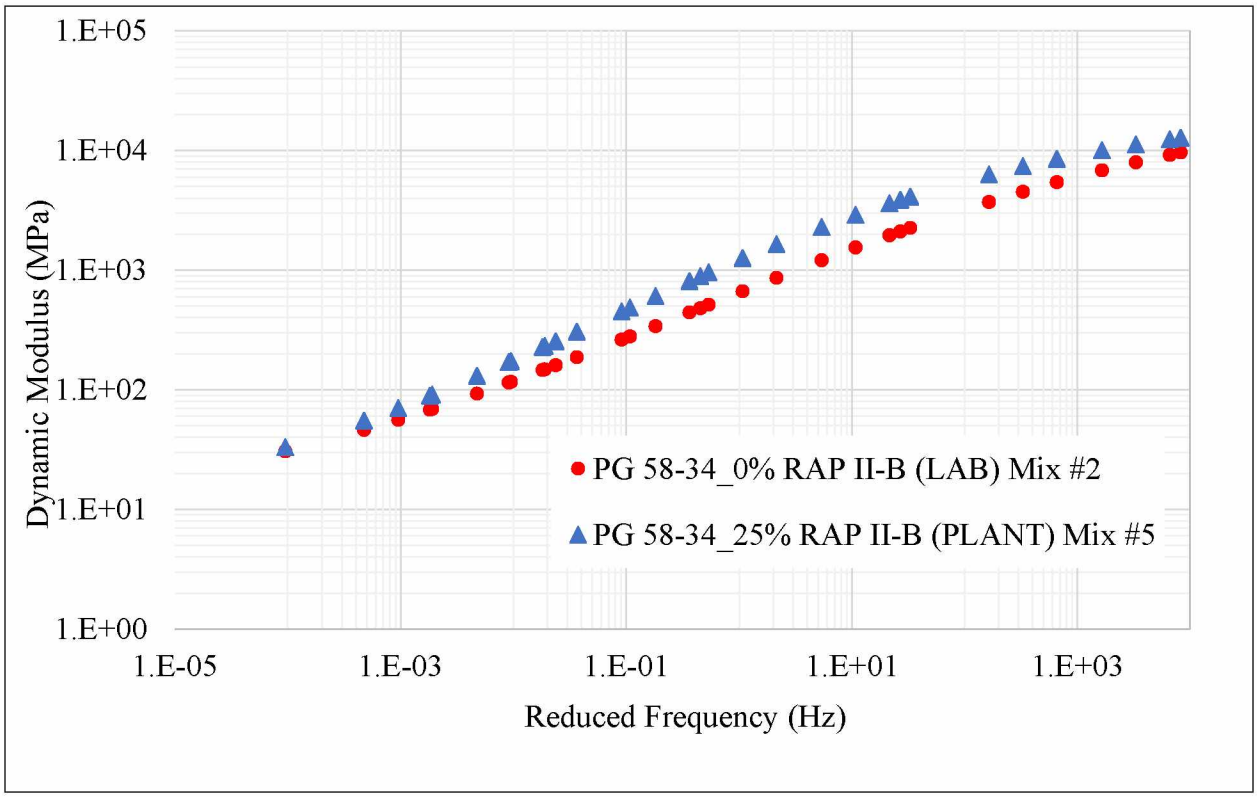

Figure 4.7 Central region master curve PG 58-34 II-B (mixes #2 & #5)

Table 4.5 Summary of measured |E*| and master curve coefficients (Mix #2)

	Measured Dynamic Modulus (MPa)							
Temperature (°C)	25 Hz	20 Hz	10 Hz	5 Hz	2 Hz	1 Hz	0.5 Hz	0.1 Hz
4	9200	8597	7468	6401	5110	4225	3437	1991
21	2126	2002	1499	1105	721	527	397	221
37	610	568	408	293	183	141	115	76
54	270	241	178	130	81	67	60	46

Master Curve Coefficients							R^2 (Logarithmic)
δ	α	β	γ	a	b	c	
0.76143509	3.7952089	-0.160661	0.399347	0.001430	-0.176008	2.99628	0.9995

Table 4.6 Summary of measured |E*| and master curve coefficients (Mix #5)

	Measured Dynamic Modulus (MPa)							
Temperature (°C)	25 Hz	20 Hz	10 Hz	5 Hz	2 Hz	1 Hz	0.5 Hz	0.1 Hz
4	12391	11876	10635	9441	7936	6861	5864	3872
21	3789	3584	2846	2213	1541	1152	859	429
37	1117	1052	759	542	337	242	182	99
54	342	314	225	162	98	70	62	49

Master Curve Coefficients							R^2 (Logarithmic)
δ	α	β	γ	a	b	c	
0.72881621	3.686498	-0.573897	0.4652323	0.001430	-0.176008	2.99628	0.9998

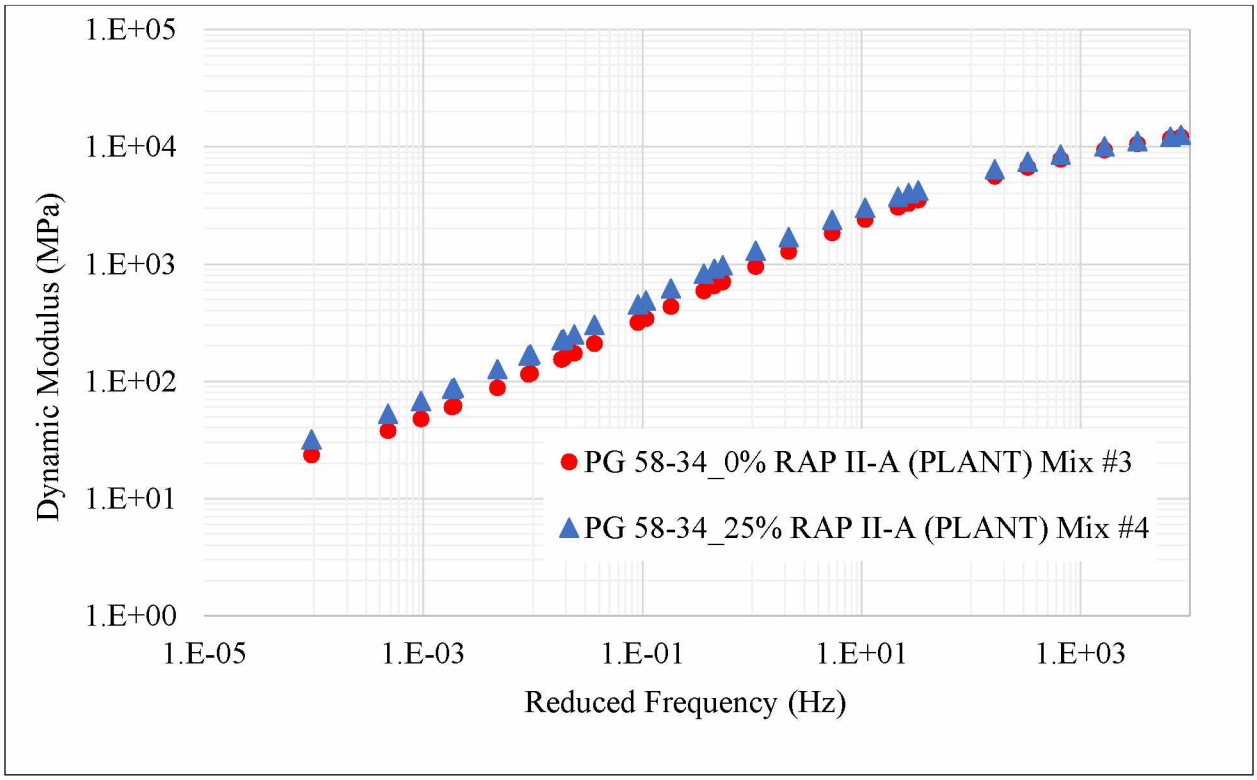

Figure 4.8 Central region master curve PG 58-34 II-A (mixes #3 & #4)

Table 4.7 Summary of measured |E*| and master curve coefficients (Mix #3)

	Measured Dynamic Modulus (MPa)							
Temperature (°C)	25 Hz	20 Hz	10 Hz	5 Hz	2 Hz	1 Hz	0.5 Hz	0.1 Hz
4	12321	11848	10604	9393	7857	6765	5741	3688
21	3154	3056	2362	1777	1175	846	617	303
37	948	873	608	419	250	180	138	83
54	314	288	202	141	82	64	58	50

Master Curve Coefficients							R^2 (Logarithmic)
δ	α	β	γ	a	b	c	
0.72199098	3.667757	-0.452476	0.495473	0.0014302	-0.176008	2.99628	0.9999

Table 4.8 Summary of measured |E*| and master curve coefficients (Mix #4)

	Measured Dynamic Modulus (MPa)							
Temperature (°C)	25 Hz	20 Hz	10 Hz	5 Hz	2 Hz	1 Hz	0.5 Hz	0.1 Hz
4	11776	11663	10470	9297	7827	6771	5787	3784
21	3902	3667	2933	2307	1630	1230	927	473
37	978	913	661	475	298	220	171	104
54	358	324	230	164	98	78	68	51

Master Curve Coefficients							R^2 (Logarithmic)
δ	α	β	γ	a	b	c	
0.76834460	3.594537	-0.61075	0.4909171	0.0014302	-0.176008	2.99628	0.999903

Figures 4.9 and 4.10 show the master curves for the Northern Region mixtures. Table 4.9 – 4.13 show the summary of measured |E*| and the corresponding master curve coefficients. The individual |E*| curves were shifted into one master curve using the time-temperature superposition principle. From the following figures a trend can be observed; |E*| increases with increasing RAP content.

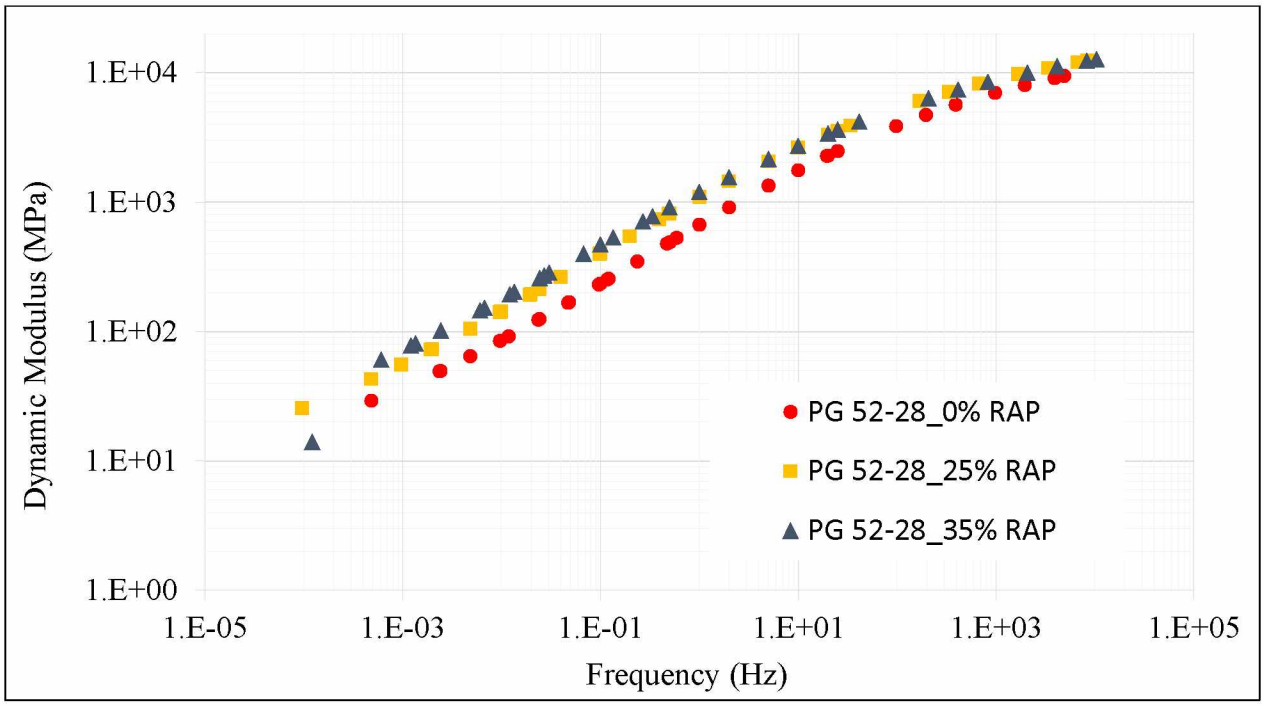

Figure 4.9 Northern region master curve PG 52-28 (mixes #7, #9 & #11)

Table 4.9 Summary of measured |E*| and master curve coefficients (Mix #7)

	Measured Dynamic Modulus (MPa)							
Temperature (°C)	25 Hz	20 Hz	10 Hz	5 Hz	2 Hz	1 Hz	0.5 Hz	0.1 Hz
4	11672	11084	9926	8843	7464	6483	5557	3738
21	3096	2955	2354	1827	1244	900	639	273
37	768	718	484	318	174	119	85	46
54	155	131	91	64	38	31	29	25

Master Curve Coefficients							R^2 (Logarithmic)
δ	α	β	γ	a	b	c	
1.2	3.172717	-0.28364	0.488064	0.000848	-0.16949	3.21673	0.9994

Table 4.10 Summary of measured |E*| and master curve coefficients (Mix #9)

	Measured Dynamic Modulus (MPa)							
Temperature (°C)	25 Hz	20 Hz	10 Hz	5 Hz	2 Hz	1 Hz	0.5 Hz	0.1 Hz
4	12740	11897	10739	9597	8143	7097	6111	4100
21	3595	3392	2674	2062	1389	996	697	286
37	858	789	530	345	187	124	88	45
54	225	204	136	91	50	38	34	25

Master Curve Coefficients							R^2 (Logarithmic)
δ	α	β	γ	a	b	c	
0.7237166	3.643315	-0.54978	0.500212	0.000977	-0.16812	3.15248	0.9993

Table 4. 11 Summary of measured |E*| and master curve coefficients (Mix #11)

	Measured Dynamic Modulus (MPa)							
Temperature (°C)	25 Hz	20 Hz	10 Hz	5 Hz	2 Hz	1 Hz	0.5 Hz	0.1 Hz
4	13645	13334	12064	10830	9276	8148	7091	4938
21	3869	3419	2741	2173	1497	1096	788	344
37	1099	939	650	434	244	164	118	62
54	315	276	190	133	77	62	55	44

Master Curve Coefficients							R^2 (Logarithmic)
δ	α	β	γ	a	b	c	
1.1996693	3.198037	-0.35531	0.506922	0.001154	-0.17717	3.33606	0.9995

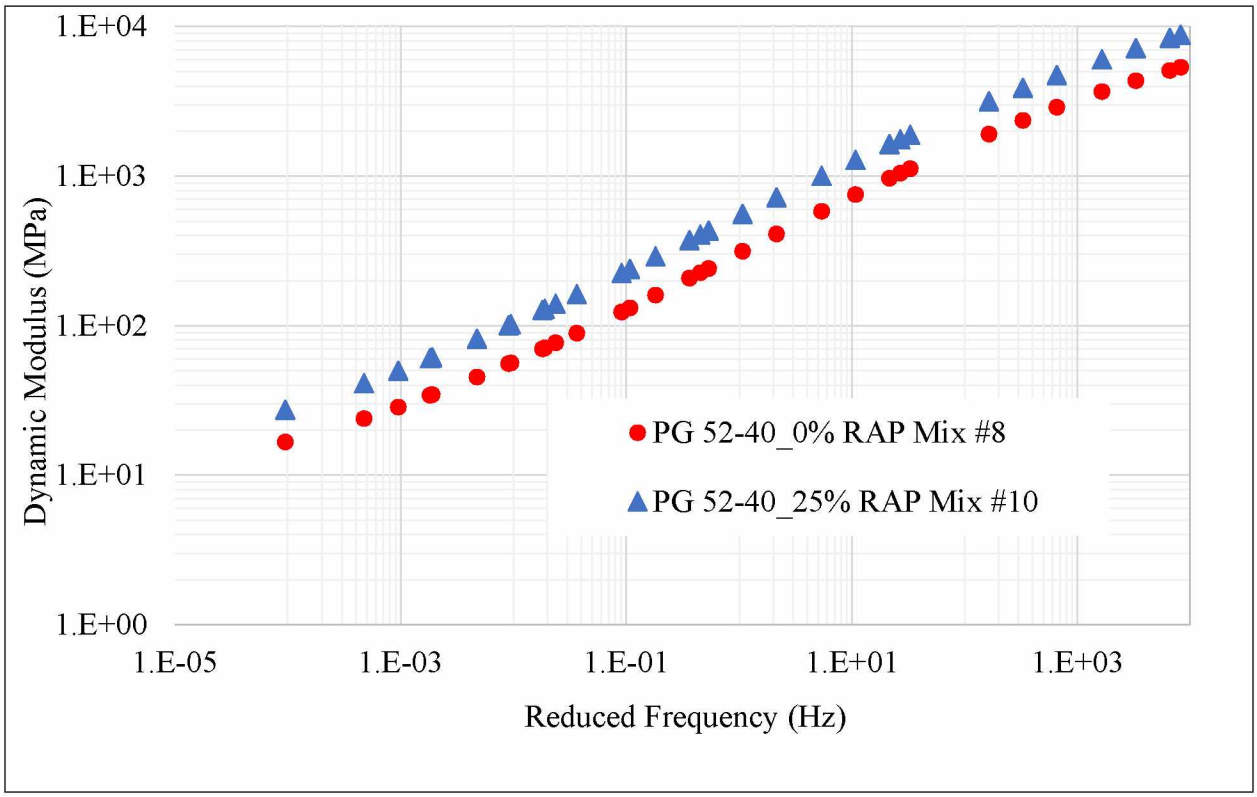

Figure 4.10 Northern region master curve PG 52-40 (mixes #8 & #10)

Table 4.12 Summary of measured |E*| and master curve coefficients (Mix #8)

	Measured Dynamic Modulus (MPa)							
Temperature (°C)	25 Hz	20 Hz	10 Hz	5 Hz	2 Hz	1 Hz	0.5 Hz	0.1 Hz
4	5285	5035	4182	3410	2525	1964	1506	769
21	997	918	678	485	301	219	166	95
37	292	264	187	136	84	71	61	44
54	141	133	99	75	49	36	36	31

Master Curve Coefficients							R^2 (Logarithmic)
δ	α	β	γ	a	b	c	
0.63214	3.5485656	0	0.553335	0.0012594	-0.151334	2.61405	0.9988

Table 4.13 Summary of measured |E*| and master curve coefficients (Mix #10)

	Measured Dynamic Modulus (MPa)							
Temperature (°C)	25 Hz	20 Hz	10 Hz	5 Hz	2 Hz	1 Hz	0.5 Hz	0.1 Hz
4	7770	7112	6078	5127	4001	3256	2609	1461
21	1805	1681	1245	919	595	425	320	174
37	499	451	318	225	136	106	88	60
54	233	186	134	98	59	50	47	39

Master Curve Coefficients							R^2 (Logarithmic)
δ	α	β	γ	a	b	c	
0.63214	3.7985638	-0.158319	0.456390	0.0011697	-0.155207	2.7474	0.9995

4.3 Comparison with Witczak |E*| Predictive Models

According to the MEPDG, there are three hierarchical input levels to determine |E*|. Level 1 uses laboratory measured |E*|. Levels 2 and 3 use |E*| as predicted by empirical models. In Level 2, |E*| is calculated based on both measured binder and mix volumetric properties, and in Level 3, |E*| is calculated based on JMF mix volumetric properties and default binder properties. The default binder properties are determined according to PG grade. In this study, the Original (1996) Witczak model and the modified (2006) Witczak model were evaluated at both MEPDG Levels 2 and 3 for |E*| prediction. Seven of the mixes evaluated in this study were provided with job mix formulae, therefore, were selected for analysis using the Witczak model. These mixes include; #1, #3, #4, #5, #7 and #8. The details of these mixes can be found in Tables 3.1 and 3.2. The JMFs can be found in Appendix A.

4.3.1 Verification of Level 2 Inputs – Original Witczak Model

The Level 2 model verifications were performed for the original Witczak model (Equation 2.11). At Level 2, the model requires rheological properties measured on short-term (RTFO) aged binder and mix volumetric properties. The binder rheological properties were determined using the viscosity-temperature susceptibility (A-VTS) method as described in section 2.4.3. Using the DSR results in combination with the A-VTS method, the binder viscosity was estimated at each of the dynamic modulus testing temperatures (4.4, 21.1, 37.8 and 54 °C). The details of viscosity testing at each test temperature is provided in Appendix C. The

A-VTS results are summarized in Table 4.14 and shown graphically in Figure 4.11. The resulting binder viscosities at the specified testing temperatures are summarized in Table 4.15.

Table 4.14 Calculated A-VTS coefficients of binder

Binder	A	VTS
PG 52-28	21.979	-7.7904
PG 58-34	12.664	-4.4089
PG 52-40	10.755	-3.7276

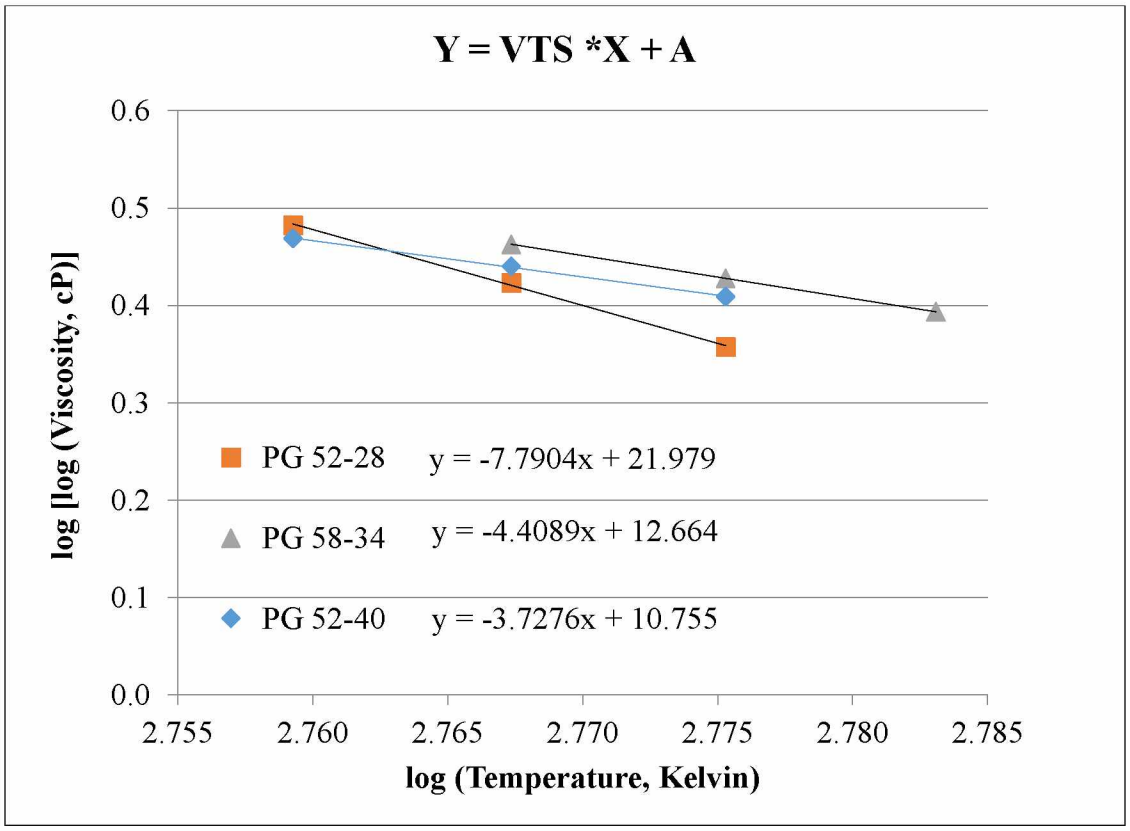

Figure 4.11 A-VTS curves for asphalt binder

Table 4.15 Calculated binder viscosity

PG 52-28	
Temp. (°C)	Viscosity (10^6 P)
4.4	1.36E+01
21.1	5.54E-03
37.8	6.34E-05
54	3.23E-06
PG 58-34	
Temp. (°C)	Viscosity (10^6 P)
4.4	7.46E-03
21.1	3.29E-04
37.8	3.77E-05
54	6.71E-06
PG 52-40	
Temp. (°C)	Viscosity (10^6 P)
4.4	9.74E-04
21.1	9.90E-05
37.8	1.91E-05
54	4.88E-06

Figure 4.12 shows the predicted |E*| versus measured |E*| for the original Witczak model. The correlation between predicted and measured values (R^2) was 0.96, however the observed trend line indicates the model grossly under predicts |E*| through the mid-range of temperatures and loading frequencies. The data also indicate a poor prediction of |E*| for modified binders.

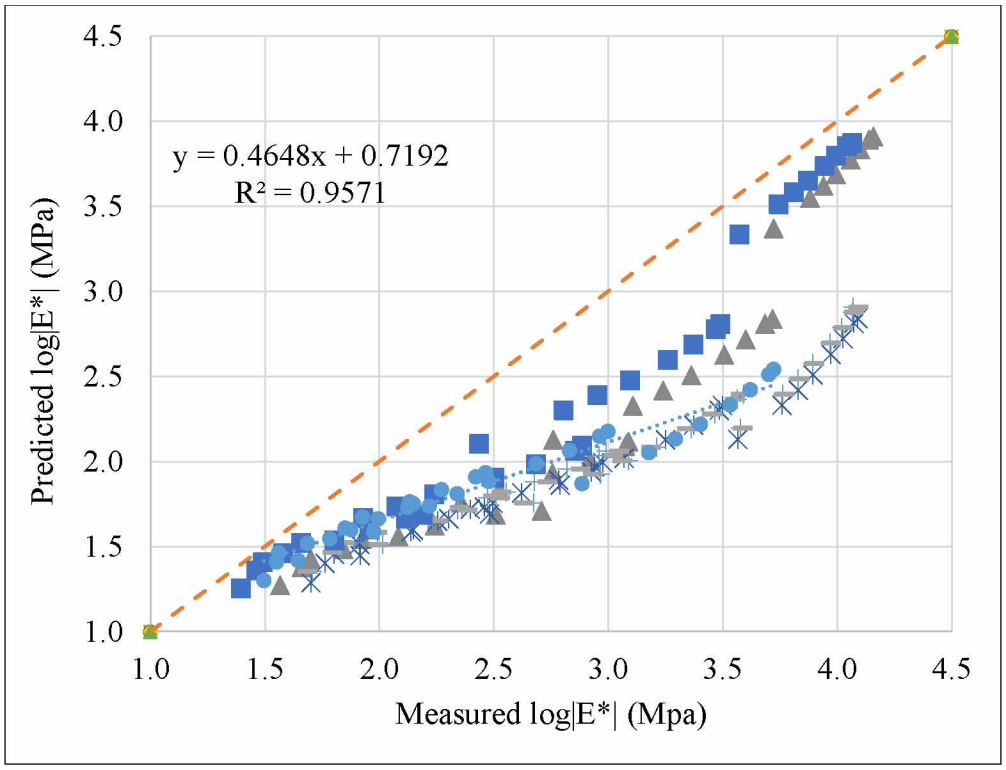

Figure 4.12 Predicted vs. measured |E*| (original Witczak model, Level 2)

Figures 4.10 to 4.12 below show predicted versus measured |E*| for all binders used in this study; PG 52-28, PG 58-34 and PG 52-40, respectively. It has been noted in the literature (2002 Design Guide, 2004) that the use of the A-VTS method to determine binder viscosity can be problematic with modified binders. As seen below, the predicted |E*| was consistently lower than measured. This is especially true for the modified binders (PG 58-34, PG 52-40). While the accuracy of the |E*| prediction is low for the original Witczak model at Level 2, the correlation coefficient is relatively high for neat as well as modified binders. This suggests the data could be further analyzed and a local calibration function could be applied to make the prediction more accurate. The need for calibration of the Witczak models to local conditions and materials has been noted extensively in the literature (2002 Design Guide, 2004; Bari and Witczak, 2006; Andrei et al., 1999; Caliendo, 2012; Garcia and Thompson, 2007; Yu, 2012).

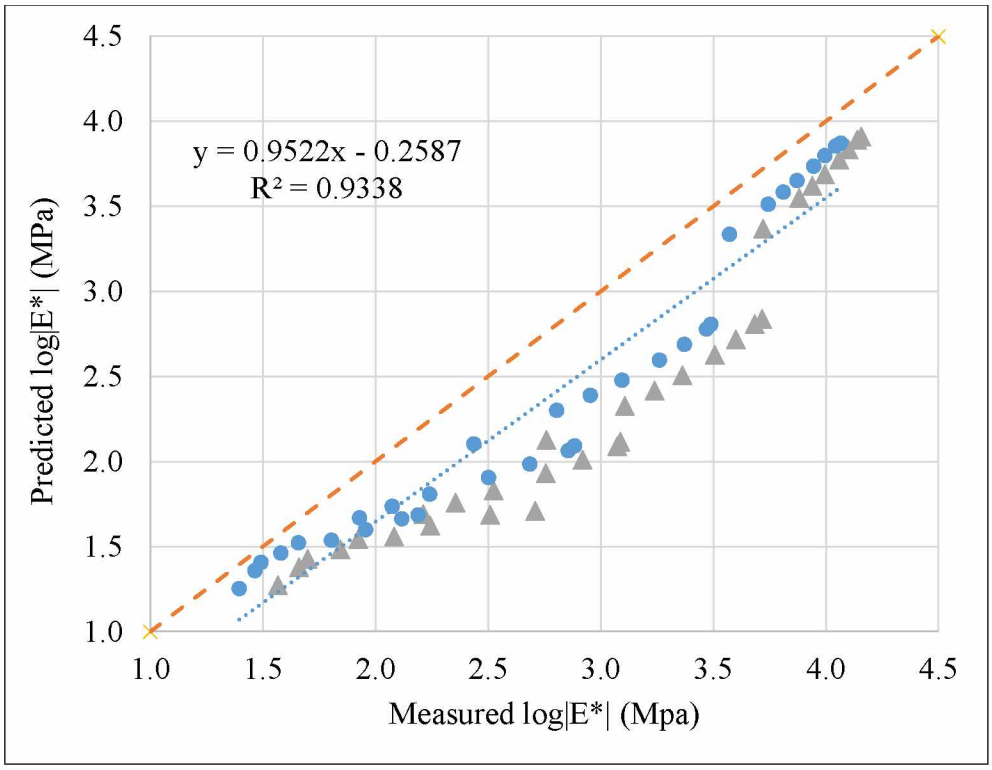

Figure 4.13 Predicted vs. measured |E*| Level 2 (PG 52-28 binder)

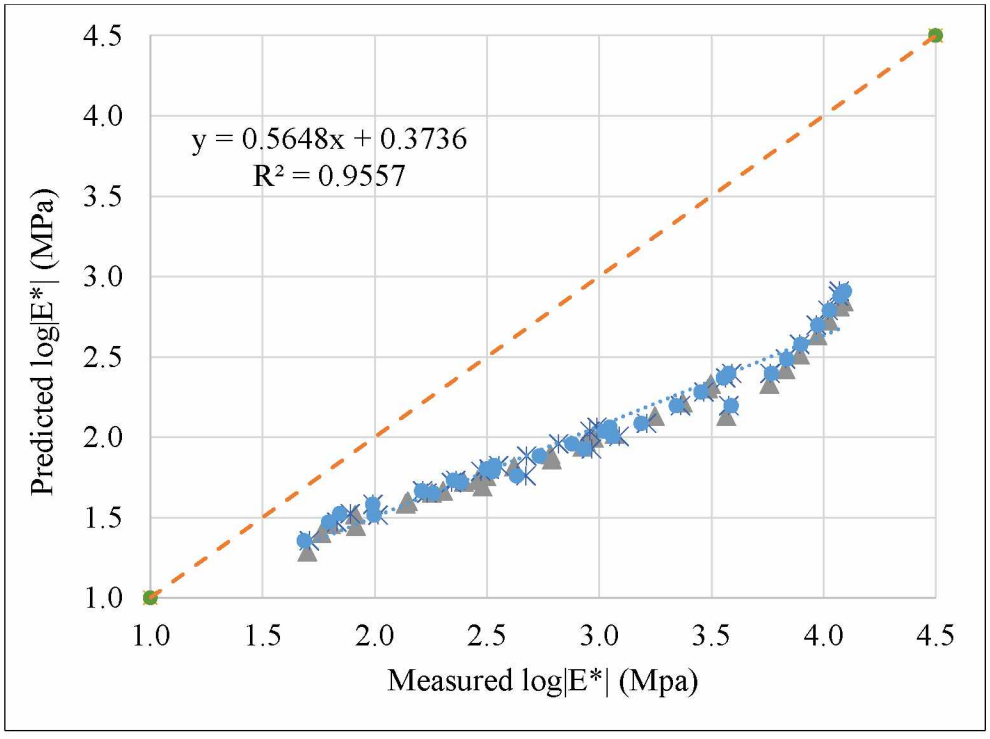

Figure 4.14 Predicted vs. measured |E*| Level 2 (PG 58-34 binder)

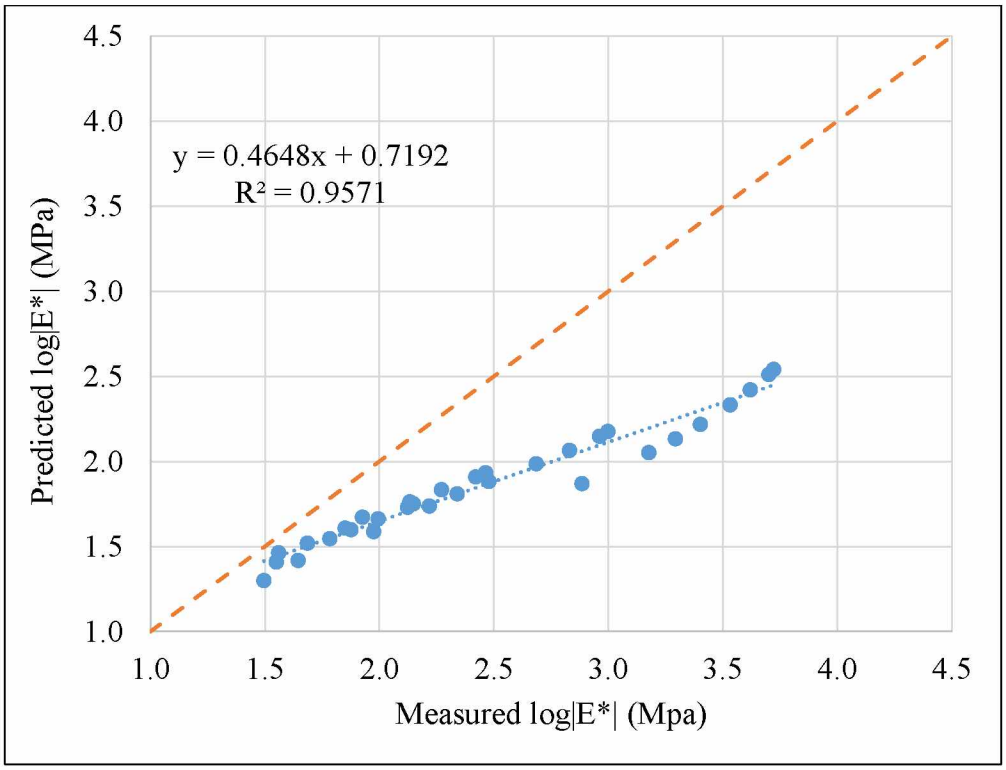

Figure 4.15 Predicted vs. measured |E*| Level 2 (PG 52-40 binder)

4.3.2 Verification of Level 3 Inputs – Original Witczak Model

The verification of the original Witczak model at MEPDG Level 3 was conducted using volumetric properties obtained from the JMF and default rheological properties based on the PG grade of the asphalt binder. The default values of A and VTS for the RTFO aged binder based on PG are provided in Table 4.16. The table includes all binder grades used in this study and the default values are recommended by MEPDG (2002 Design Guide, 2004). The asphalt binders' temperature sensitivity is represented by the parameter VTS. The absolute value of VTS decreases as the span between higher and lower PG increases. The parameter A is the intercept. The value of A will decrease as the low end of PG decreases. The mix volumetric properties are listed in Table 3.2. Table 4.17 shows the resulting binder viscosities at the specified testing temperatures.

Table 4.16 Default values of A and VTS based on PG (2002 Design Guide, 2004)

Binder	A	VTS
PG 52-28	11.84	-4.012
PG 58-34	10.035	-3.35
PG 52-40	9.496	-3.164

Table 4.17 Calculated binder viscosity for Level 3

PG 52-28	
Temp. (°C)	Viscosity (10^6 P)
4.4	2.03E+02
21.1	1.42E+00
37.8	3.42E-02
54	2.14E-03
PG 58-34	
Temp. (°C)	Viscosity (10^6 P)
4.4	7.54E+01
21.1	1.32E+00
37.8	5.63E-02
54	4.95E-03
PG 52-40	
Temp. (°C)	Viscosity (10^6 P)
4.4	1.17E+01
21.1	3.46E-01
37.8	2.14E-02
54	2.46E-03

Figure 4.16 illustrates predicted |E*| versus measures |E*| by the original Witczak model. The results show that the predicted |E*| is close to the laboratory measured values through a wide range of temperatures and frequencies. The correlation between predicted and measured values (R^2) was 0.96. The regression trend line indicates the model overestimates |E*| at higher temperatures and lower loading frequencies. This observation is consistent with previous studies reported by Li and Liu (2014) and Mohammad et al. (2005). Individual mix results are presented in Appendix D.

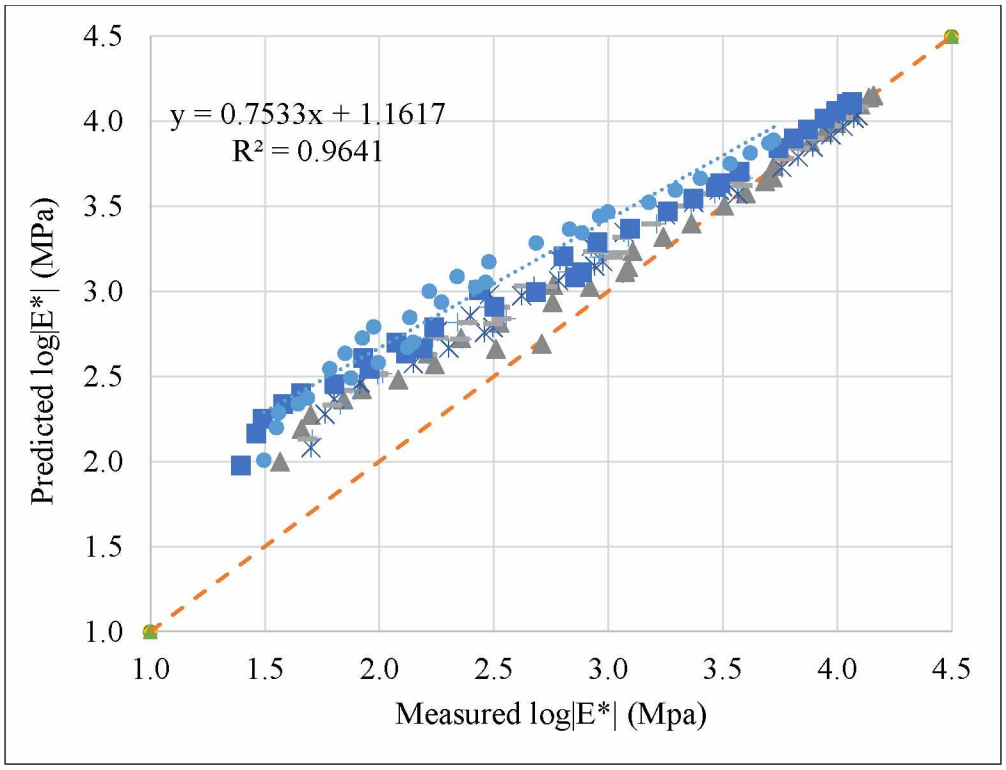

Figure 4.16 Predicted vs. measured |E*| (original Witczak model, Level 3)

4.3.3 Verification of Level 2 Inputs – Modified Witczak Model

The Level 2 model verifications were performed for the modified Witczak model (Equation 2.15). As with the original Witczak model verification, the modified Witczak model was verified using binder rheological properties estimated using the A-VTS method. The modified Witczak model uses binder shear modulus (|G*|) and phase angle (δ) as inputs. These parameters are estimated for both Levels 2 and 3 analysis using Equations 4.1 to 4.5 shown below. In addition, the modified Witczak model requires frequency be converted from compressive mode to shear mode. This is accomplished following Equation 4.6.

$$|G^*|_b = 0.0051 f_s \eta_{f_{s,T}} (\sin \delta_b)^{7.1542 - 0.4929 f_s + 0.0211 f_s^2}$$

Equation 4.1

$$\delta_b = 90 + (-7.3146 - 2.6162 VTS') \times \log\left(f_s \times \eta_{f_{s,T}}\right) + (0.1124 + 0.2029 VTS') \times \log\left(f_s \times \eta_{f_{s,T}}\right)^2$$

Equation 4. 2

$$\log\log \eta_{f_{s,T}} = A' + VTS' \log T_R$$

Equation 4.3

$$A' = 0.9699 f_s^{-0.0527} A$$

Equation 4.4

$$VTS' = 0.9668 f_s^{-0.0575} VTS$$

Equation 4.5

where,

f_s = loading frequency in shear mode (Hz)

$\eta fs,T$ = viscosity at reference shear loading frequency and temperature (cP)

A' = adjusted A (adjusted for frequency)

VTS' = adjusted VTS (adjusted for frequency)

and,

$$f_s = \frac{f_c}{2\pi}$$

Equation 4.6

where,

f_c = loading frequency in compression mode (Hz)

The |E*| values predicted by the modified Witczak model for Level 2 are plotted in Figure 4.17 versus the measured |E*|. The overall correlation (R^2) between measured and predicted was 0.72 which is lower than that of the original Witczak model. This observation is consistent with the findings of previous studies that the modified model does not improve the accuracy of the prediction (Kim et al., 2011).

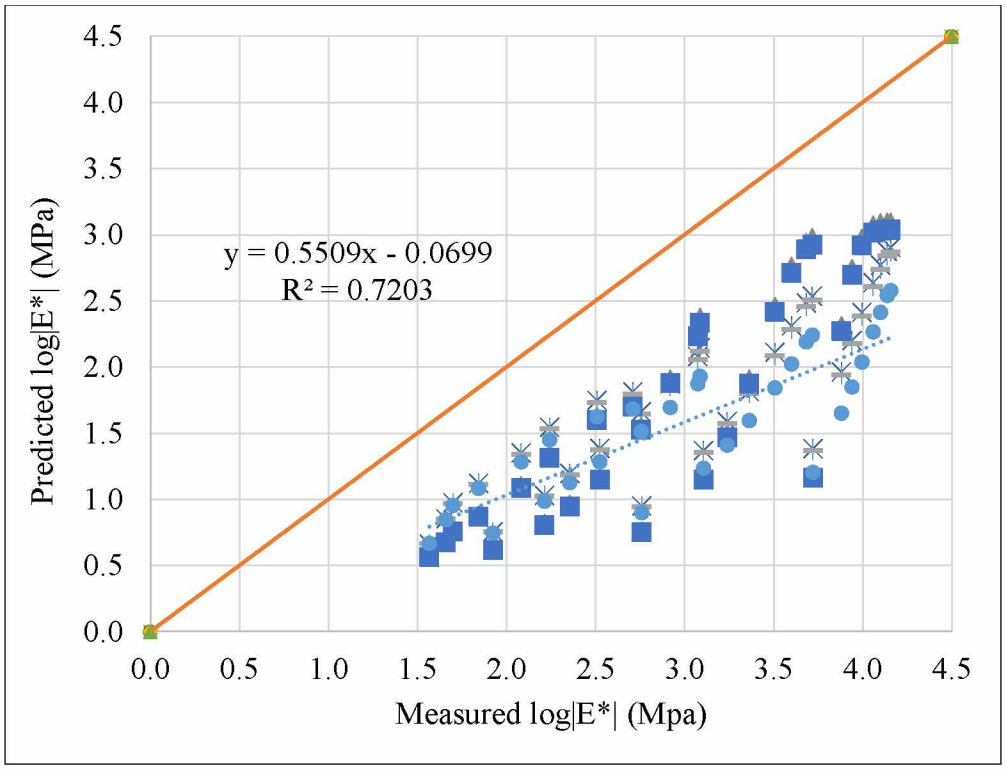

Figure 4.17 Predicted vs. Measured |E*| (modified Witczak model, Level 2)

4.3.4 Verification of Level 3 Inputs – Modified Witczak Model

The Level 3 model verifications were performed for the modified Witczak model. The binder rheological properties, G* and δ, were estimated using the method defined for Level 2. The |E*| values predicted by the modified Witczak model for Level 3 are plotted in Figure 4.18 versus the measured |E*|. The overall correlation (R^2) between measured and predicted was 0.88 which is lower than that of the original Witczak model.

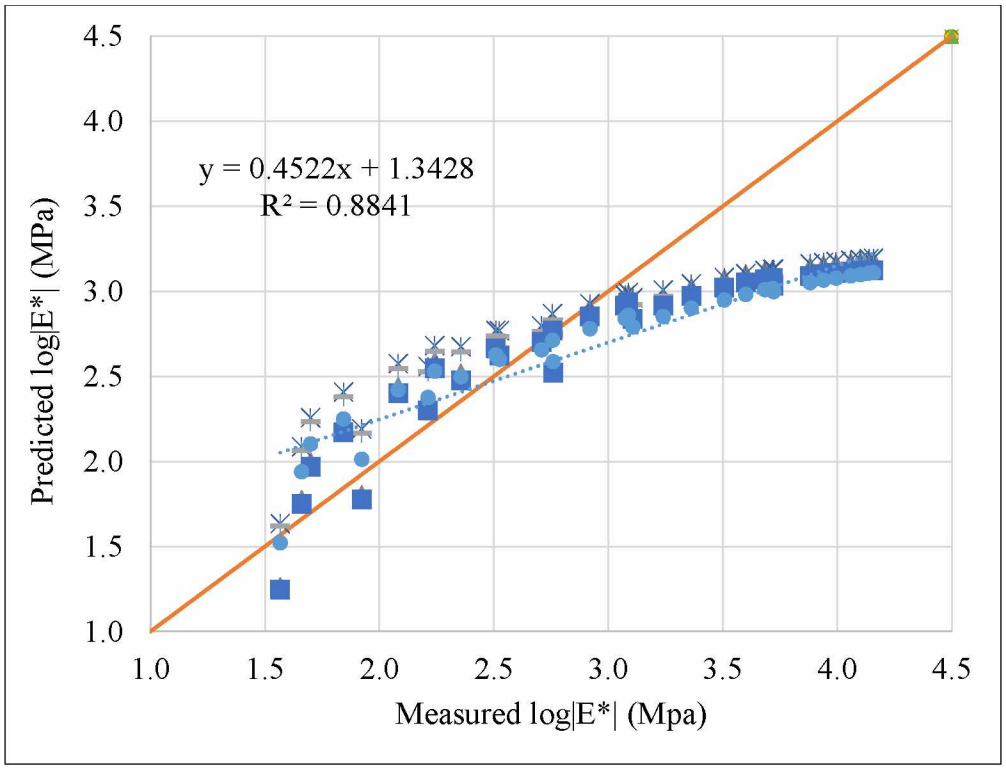

Figure 4.18 Predicted vs. Measured |E*| (modified Witczak model, Level 3)

Previous research (Li and Liu, 2014) studying the Witczak |E*| predictive equations with reference to typical Alaskan HMA mixtures, show similar findings: at Level 3 input, the most accurate estimation of |E*| was observed from the original (η-based) model. None of the mixtures studied previously contained RAP, however, the results are comparable to the findings of this project.

4.4 Analysis of RAP Mixture E* Prediction

The rheological properties of extracted binder from RAP mixtures were not evaluated in this study. To account for this, a literature search was conducted to evaluate the possible effects of varying amounts of RAP to binder rheology. TecleMariam and Saboundjian (2010) studied the effect to combined binder PG of typical Alaskan asphalt using extracted RAP binder at 15%, 20% and 25%. According to their study, up to 25% RAP can be added without changing the original PG. Esfandiarpour et al. (2015), conducted a study evaluating the E* prediction of the original Witczak model. According to this research, the mix rheology of a virgin binder PG 58-28 was unaffected by the inclusion of 10% RAP and the high grade of the combined binder was

one grade higher while the low grade was two grades higher for a 50% RAP mix, resulting in a PG 64-16 designation. Jeong and Younghan (2015) studied the effect of 15% and 20% RAP content on the E* prediction of both the original and modified Witczak models. The binder PG was un-changed for 15% RAP and the high temperature grade was found to be one grade higher for the 20% RAP mix. The authors conclude that there is no significant effect of RAP on the accuracy of both versions of the Witczak predictive equation.

For this study, one control (mix #3) and one RAP mix (mix #4) were provided with JMFs. For this reason, they were selected for evaluation of |E*| prediction for mixtures containing RAP by the original and modified Witczak model. A sensitivity analysis was conducted to evaluate the prediction variance due to changes in binder PG grade. The control PG grade for these mixes is PG 58-34. Following results found in the literature, the PG was adjusted accordingly. Due to the lack of DSR data for this binder designation, only Level 3 analysis was conducted. Table 4.18 shows the estimated binder PG adjustment.

Table 4.18 Adjusted binder PG grade

Mix #	Type	PG	A	VTS
3	Control	58-34*	10.035	-3.35
4	25% RAP	58-34*	10.035	-3.35
4	25% RAP	64-22**	10.98	-3.68

* Original virgin binder PG designation

** PG adjusted following recommendations from the literature

Figure 4.19 shows original Witczak predicted E* for Mix #3 and Mix #4 with PG 58-34 as well as Mix #4 with adjusted binder grade PG 64-22. Figure 4.20 is shown to compare the effects PG adjustment on E* prediction of Mix #4. The adjustment of binder rheology decreased the accuracy of the model.

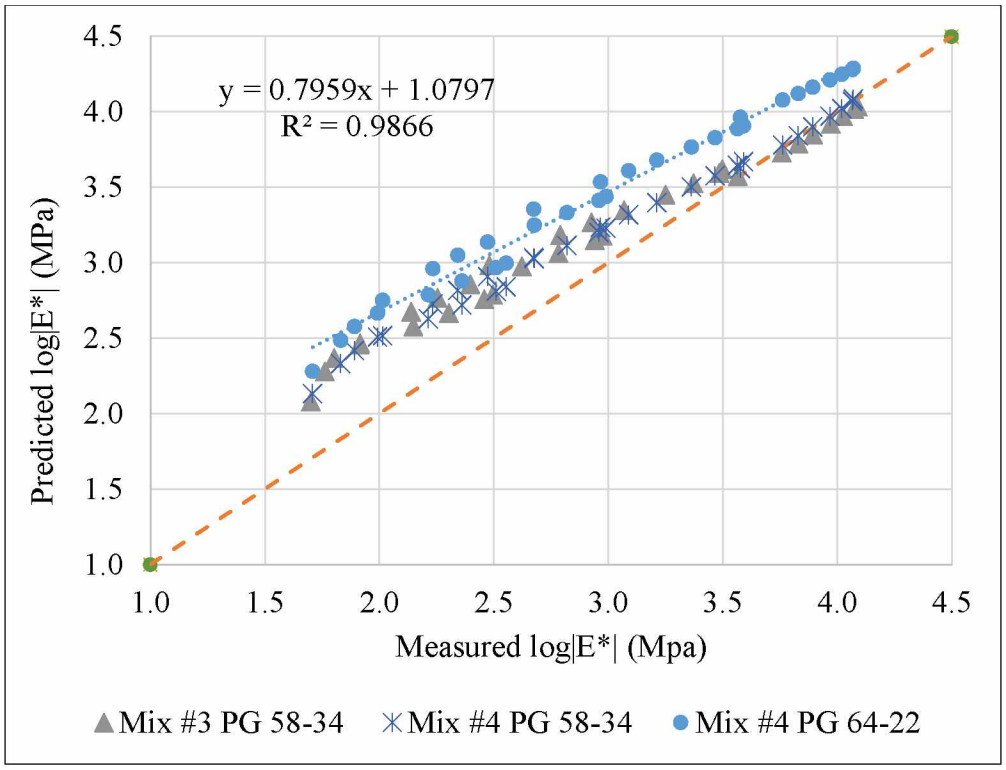

Figure 4.19 Predicted vs. Measured |E*| (original Witczak model, Mix #3, #4, mod. #4)

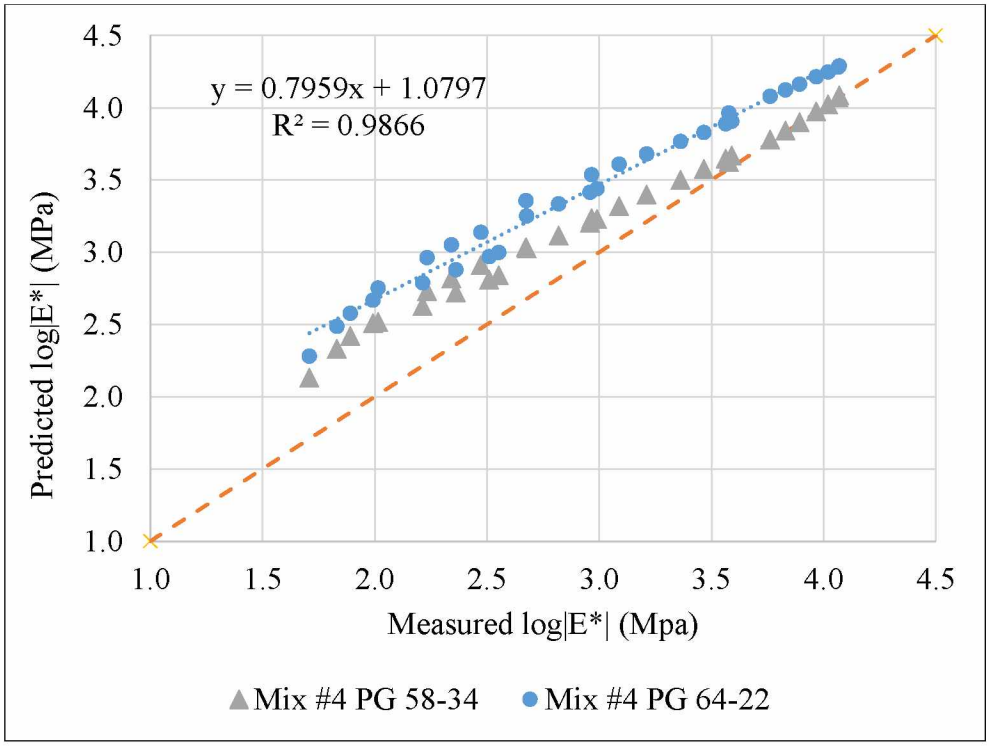

Figure 4.20 Predicted vs. Measured |E*| (original Witczak model, Mix #4, mod. #4)

Figure 4.21 shows the modified Witczak predicted E* for Mix #3 and Mix #4 with PG 58-34 as well as Mix #4 with adjusted binder grade PG 64-22. Figure 4.22 is shown to compare the effects PG adjustment on E* prediction of Mix #4. It can be seen that the adjustment of binder rheology has negligible effects to the prediction accuracy.

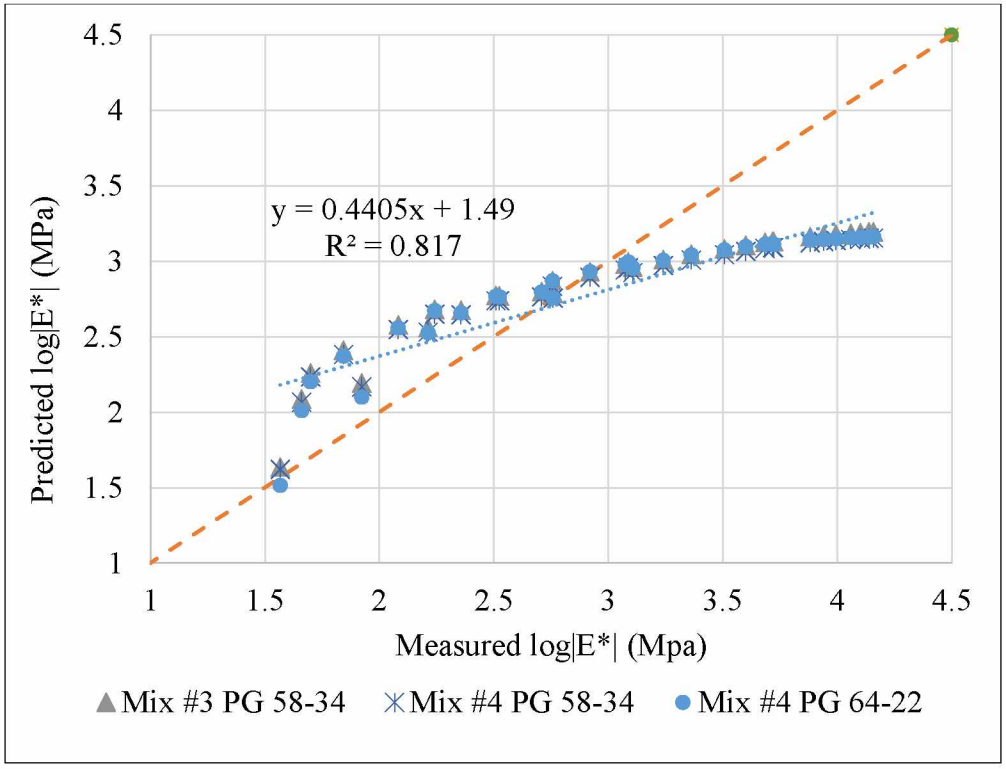

Figure 4.21 Predicted vs. Measured |E*| (modified Witczak model, Mix #3, #4, mod. #4)

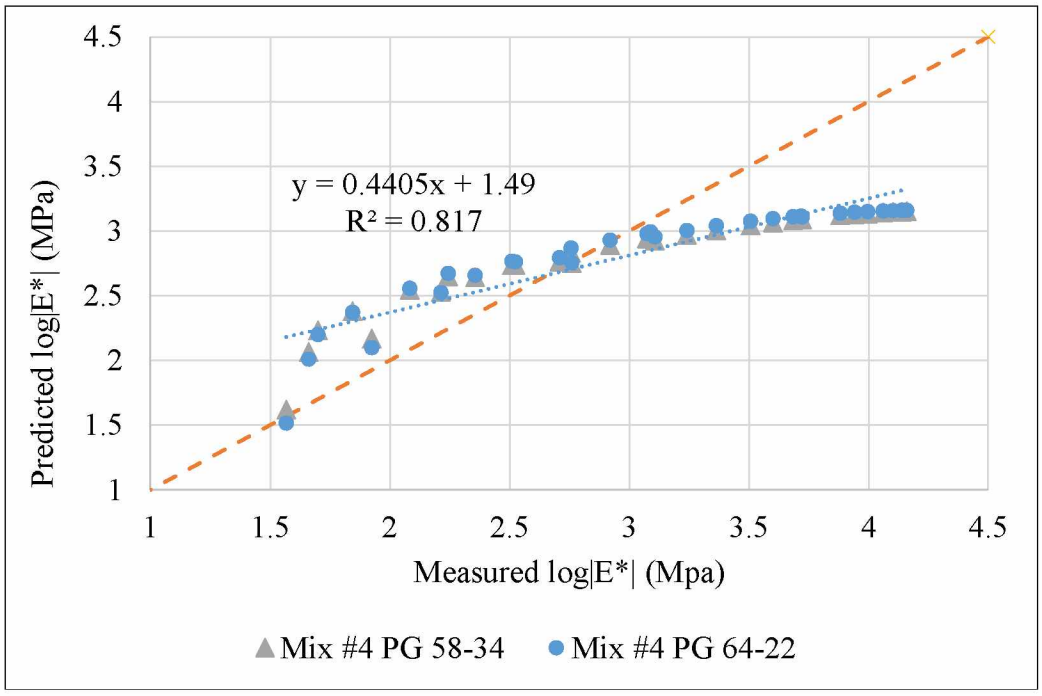

Figure 4.22 Predicted vs. Measured |E*| (modified Witczak model, Mix #4, mod. #4)

4.5 Flow Number

The FN test was used to evaluate the rutting resistance of the HMA mixtures. This test examines the permanent deformation characteristics by applying a repeated dynamic load. The FN for the mixture is the point at which the permanent strain rate is at a minimum.

Figure 4.23 shows the FN data for the Central Region mixtures. Two pairs out of three show that the flow number of the control mix is lower than the flow number of the RAP mix. The pair of type II-B PG 58-34 mixes is the exception. However, the control mix in this pair was produced in the laboratory and the RAP mix was produced in the field. This difference might cause a significant difference in the mixture's performance. A comparison of more mixes is recommended for improved understanding of RAP's effect on flow number variation.

Figure 4.24 shows the FN data for the five Northern Region HMA mixes. The addition of RAP was found to increase the flow number of both PG 52-28 and PG 52-40 mixes, with higher RAP content leading to higher flow number, namely higher rut resistance. This finding was consistent with that from dynamic modulus results. With higher RAP content, a higher flow number is observed.

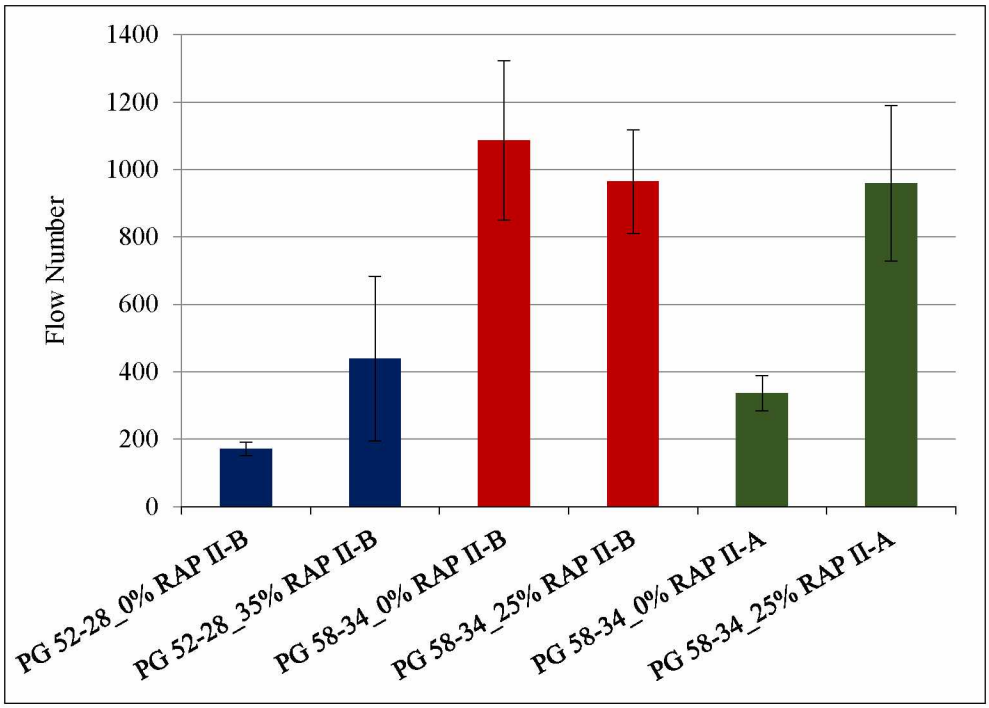

Figure 4.23 FN for Central region mixes

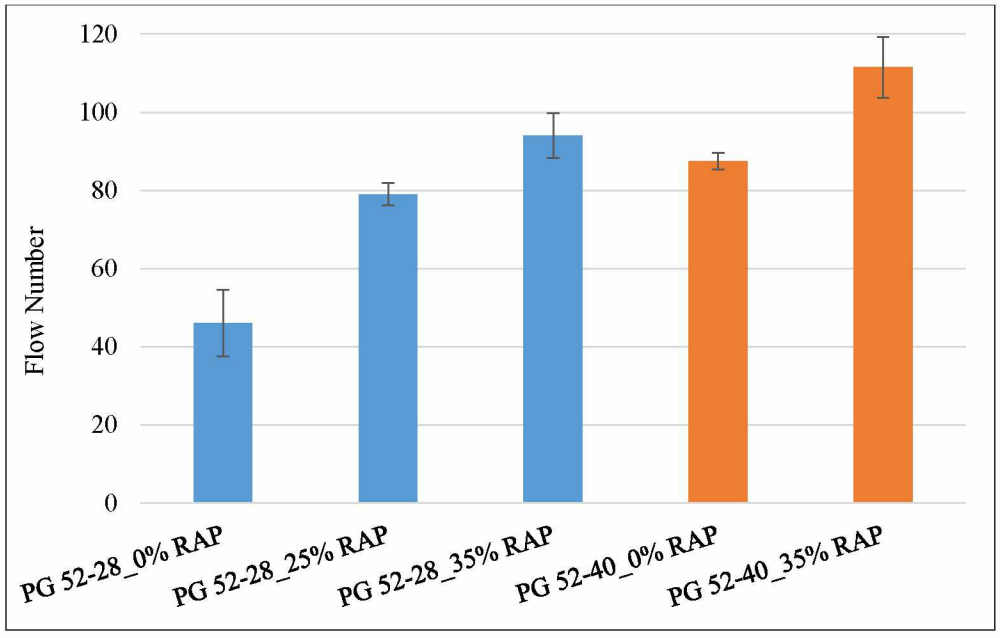

Figure 4.24 FN for Northern region mixes (all lab produced)

4.5 Preliminary Cost Analysis

The cost analysis was to investigate the potential cost savings of a 25% RAP mixture compared to a control mix containing 0% RAP. Table 4.19 shows the calculation process. For this analysis, RAP was considered free of charge as typically in Alaska contractors use RAP stockpiled from previous projects. The assumptions for calculation were presented in table 3.1. As shown in Table 4.19, a cost savings of $13.60/ton can be achieved using a RAP content of 25%.

Table 4.19 HMA material cost estimate

Cost Assumptions	
Aggregate:	15 $/ton
Asphalt binder:	603 $/ton
Virgin HMA binder content:	6.0%
Markup:	15.0%
Aggregate hauling:	$3.00
Asphalt binder hauling:	$18.00
RAP fractionation:	2 $/ton

Table 4.19 continued

Mix Alternatives					
	Mix 1		Mix 2		
RAP %:	0.0%		25.0%		
RAP binder content:	0.0%		5.0%		
Aggregate $/ton, delivered to plant					
Material		Trucking	Net	Markup 15%	Total
$15.00	+	$3.00	$18.00	2.7	$20.70
Aggregate Cost Saving					
	Aggregate Cost		Aggregate savings		
Mix 1	$20.70	X	0	=	0
Mix 2	$20.70	X	25%	=	$5.18
Asphalt binder $/ton, delivered to plant					
Material		Trucking	Net	Markup 15%	Total
$603.00	+	$18.00	$621.00	$93.15	$714.15
	RAP binder content	RAP %	Binder replacement	Virgin binder	Adjusted virgin
Mix 1	0.0%	0.0%	0.0%	6.0%	6.0%
Mix 2	5.0%	25.0%	1.3%	6.0%	4.8%
Binder Cost Saving					
	Binder Cost				
Mix 1	$714.15	X	6.0%	=	$42.85
Mix 2	$714.15	X	4.8%	=	$33.92
Total Material Cost					
	Binder cost		Aggregate cost		
Mix 1	$42.85	+	20.7	=	$63.55
Mix 2	$33.92	+	15.525	=	$49.45
Additional Costs					
	RAP fractionation				
Mix 1	$2.00	X	0	=	$0.00
Mix 2	$2.00	X	0.25	=	$0.50
Final Estimated Cost					
Mix 1	$63.55		Total ($/ton)		
					Total savings
Mix 2	$49.95		Total ($/ton)		**$13.60/ton**

Using the method described above, the estimated cost savings per lane-mile was evaluated. For this analysis, a typical (18 ft. wide, 1 in. thick, 1 mi. long) lane was considered. The estimate assumptions, cost and cost savings are presented in Table 4.20. The cost savings for a lane-mile of 1 in. HMA was determined to be; $8,405 and $10,487 for 25% and 35% RAP, respectively. That is equivalent to 21% and 27% savings for 25% and 35% RAP, respectively, when compared to the conventional virgin (no RAP) mix.

Table 4.20 Cost savings per lane-mile

Assumptions					
G_{mb}	Density (lb/ft^3)	Lane Width (ft)	Length (ft)	Thickness (in)	Quantity (ton)
2.5	156	18	5280	1	618
Total Cost per Lane Mile					
RAP %	Quantity (ton)	$/ton	Total Cost/Lane Mile		
0	618	63.55	$39,273.90		
25	618	49.95	$30,869.10		
35	618	46.58	$28,786.44		
Cost Savings					
RAP %	Quantity (ton)	Unit Savings	Total Savings/Lane Mile		% Savings
25	618	13.60	**$8,404.80**		**21.4**
35	618	16.97	**$10,487.46**		**26.7**

CHAPTER 5 CONCLUSIONS AND RECOMMENDATIONS

The research for this thesis is part of a research project titled "Characterization of Alaskan Hot-Mix Asphalt containing Reclaimed Asphalt Pavement Material" (Liu et al., 2016), funded by the CESTiCC and the ADOT&PF. The goal of this thesis was to characterize the material properties of Alaskan HMA materials containing RAP. The asphalt binders included one neat binder (PG 52-28) and two modified binders (PG 58-34 and PG 52-40). Eleven HMA mixtures were either collected from active paving projects or produced in the laboratory. The materials were collected from the Central and Northern regions of the ADOT&PF and consisted of two mix types, RAP content up to 35%, and the asphalt binders mentioned previously. The binder tests in this study included DSR for verification of binder grading and evaluation of viscoelastic behavior. The mixture performance tests included AMPT tests for dynamic modulus and flow number. An evaluation of the original and modified Witczak |E*| predictive equations was conducted. A cost analysis of a 25% RAP mix was conducted assuming typical Alaskan conditions. Based on the testing results and analysis and analysis, the following conclusions were made:

- The high-temperature grades of the three binders used in this study were verified. The true grades of PG 52-28 binder before and after RTFO aging were 56.6 °C and 56.9 °C; the true grades of PG 58-34 binder before and after RTFO aging were 64.3 °C and 61.4 °C; the true grades of PG 52-40 binder before and after RTFO aging were 60.6 °C and 56.4 °C.
- The shear complex modulus (|G*|) and phase angle (δ) of the three binders were characterized to evaluate their viscoelastic behavior.
- With the incorporation of RAP into the evaluated HMA mixtures, an increase in the dynamic modulus and flow number was observed. This indicates that the addition of RAP, at the ratios evaluated, may increase the rut resistance of HMA in Alaska. Typically, the greater the RAP content, the greater the increase. Only one exception was found in flow number results from one pair of mixes; the control mix and RAP mix were produced in the field and plant, respectively. The inconsistent flow number trend is attributed to this difference in production method.

- The original (η-based) Witczak |E*| predictive model under predicted |E*| at Level 2 analysis. This observation was most prominent with the modified binders.
- The original Witczak |E*| predictive model was observed to be the most accurate predictor of |E*| in this study. The model over predicted |E*| at high temperatures and low loading frequencies at Level 3 analysis. This result is consistent with other research found in the literature.
- The modified (G*, δ-based) Witczak |E*| predictive model under predicted |E*| at Level 2 analysis for all mixtures evaluated in this study. The overall correlation between measured and predicted |E*| was lower than that observed with the original model. This observation is consistent with the findings of previous studies.
- At Level 3 analysis, the modified Witczak predictive model over predicted |E*| at high temperatures and low loading frequencies and under predicted |E*| at low temperatures and high loading frequencies.
- The A-VTS method was used to determine binder rheological properties for all model evaluations.
- The effect on |E*| prediction for extracted RAP binder was estimated following recommendations from the literature. It was concluded that adjusting the binder viscosity either had negative or negligible affects on |E*| prediction.
- A savings of $13.60/ton for HMA consisting of 25% RAP was estimated based on aggregate and binder costs.
- The cost savings for a lane-mile of 1 in. HMA was determined to be; $8,405 and $10,487 for 25% and 35% RAP, respectively. That is equivalent to 21% and 27% savings for 25% and 35% RAP, respectively, when compared to the virgin (no RAP) mix.

The following recommendations are made based on the conclusions of this study:

- It is recommended that the binders of RAP mixes be extracted to compare their properties with control binders for performance evaluation. Also, extracted binders should be used to evaluate |E*| predictive models.
- According to this study, the inclusion of RAP should not be of concern to the rut resistance of HMA.

- A local calibration should be determined for use of predictive models. This calibration may be determined using a statistical multivariate analysis of regression constants of the original and modified Witczak models.
- More Alaskan RAP mixtures should be tested to verify the conclusions of this study.
- To correlate the laboratory testing results with actual field performance, it is recommended that trial sections with RAP mix and control mix should be developed.

REFERENCES

AASHTO T 315 (2013). "Determining the Rheological Properties of Asphalt Binder Using the Dynamic Shear Rheometer (DSR)." American Association of State Highway and Transportation Officials.

Al-Qadi, L., Elseifi, A., and Carpenter, H. (2007). "Reclaimed Asphalt Pavement – A Literature Review." Research Report FHWA-ICT-07-001, Federal Highway Administration, Washington, DC.

Andrei, D., Witczak, M., and Mizra, M. (1999). "Development of a Revised Predictive Model for the Dynamic (Complex) Modulus of Asphalt Mixtures." NCHRP Report 1-37A.

Apeagyei, A. (2014). "Flow Number Predictive Models from Volumetric and Binder Properties." Construction and Building Materials, Volume 64, 14 August 2014, Pages 240-245.

Apeagyei, A., Diefenderfer, B. and Diefenderfer, S. (2011). "Rutting Resistance of Asphalt Concrete Mixtures That Contain Recycled Asphalt Pavement." Transportation Research Record: Journal of the Transportation Research Board, 2208, 9-16.

Archilla, R. and Diaz, G. (2008). "Using Permanent Deformation Tests and the MEPDG to Quantify Permanent Deformation Improvements from Modified Binders (with discussion)." Journal of the Association of Asphalt Paving Technologists, 77.

Aurangzeb, Q. and Al-Qadi, I.L. (2014). "Asphalt Pavements with High RAP Content: Economic and Environmental Perspectives." Presented at the 93rd Transportation Research Board Annual Meeting, Washington, D.C., No. 14-3488.

Azari, H., Al-Khateeb, G., Shenoy, A., and Gibson, H. (2007). "Comparison of simple performance test |E*| of accelerated loading facility mixtures and prediction |E*|: Use of NCHRP 1-37A and Witczak's new equations." Transportation Research Record: Journal of the Transportation Research Board, Issue 1998.

Bari, J. and Witczak, M.W. (2006). "Development of a New Revised Version of the Witczak E* Predictive Model for Hot Mix Asphalt Mixtures." Journal of the Association of Asphalt Paving Technologists, p. 385.

Bhasin, A., Button, J., and Chowdhury, A. (2004). "Evaluation of Simple Performance Tests on Hot-Mix Asphalt Mixtures from South Central United States." Transportation Research Record 1891, 2004.

Bhasin, A., Button, J.W., and Chowdhury, A. (2005). "Evaluation of Selected Laboratory Procedures and Development of Databases for HMA." FHWA/TX-05/0-4203-3 Texas Department of Transportation, Texas Transportation Institute.

Blankenship, P.B., and Anderson, R.M. (2010). "Laboratory Investigation of HMA Modulus, Flow Number and Flexural Fatigue on Samples of Varying Density." Journal of the Association of Asphalt Paving Technologists, 79.

Bonaquist, R.F. (2008). "NCHRP Report 629: Ruggedness Testing of the Dynamic Modulus and Flow Number Tests with the Simple Performance Tester." National Cooperative Highway Research Program, Washington, D.C.

Boriack, P.C., Katicha, S.W., Flintsch, G.W. and Tomlinson, C.R. (2014). "Laboratory Evaluation of Asphalt Concrete Mixtures Containing High Contents of Reclaimed Asphalt Pavement (RAP) and Binder." Report FHWA/VCTIR 15-R8, Virginia Center for Transportation Innovation and Research, Charlottesville, Virginia.

Brown, R., Kandhal, S. and Zhang, J. (2004). "Performance Testing for Hot-Mix Asphalt, Transportation Research E-Circular E-C068." Transportation Research Record, National Research Council, Washington, D.C.

Brown, E.R., Kandhal, P.S., Roberts, F.L., Kim, Y.R., Lee, D., and Kennedy, T.W. (2009). "Hot Mix Asphalt Materials, Mixture Design and Construction, Third Edition." NAPA Research and Education Foundation, Lanham, MD.

Brock, J. D. and Richmond, J. L. (2007). "Milling and Recycling." Chattanooga, TN: ASTEC, Technical Paper T-127.

Caliendo, C. (2012). "Local Calibration and Implementation of the Mechanistic-Empirical Pavement Design Guide for Flexible Pavement Design." Journal of Transportation Engineering 138.3: 348-360. Web.

Connor, B., and Li, P. (2009). "Evaluation of the Addition of 15% Recycled Asphalt Pavement." Research Report, Alaska Transportation Research Center, AK.

Copeland, A. (2011). "Reclaimed Asphalt Pavement in Asphalt Mixtures: State of the Practice." McLean, VA: Turner-Fairbank Highway Research Center, U.S. Department of Transportation Federal Highway Administration Report Number FHWA-HRT-11-021.

Esfandiarpour, S., Ahammed, M., Shalaby, A., Liske, T. and Kass, S. (2015). "An Evaluation of Pavement ME Design Dynamic Modulus Prediction Model for Asphalt Mixes Containing RAP." Paper prepared for the 2015 Conference of the Transportation Association of Canada, Charlottetown, PEI.

FHWA. (1993). "Study of the Use of Recycled Paving Materials: A Report to Congress." FHWARD-93-417, Federal Highway Administration (FHWA), Washington, DC.

Franke, R., and Ksaibati, K. (2014). "A Methodology For Cost-Benefit Analysis Of Recycled Asphalt Pavement (RAP) In Various Highway Applications." International Journal of Pavement Engineering 16.7 (2014): 660-666. Web.

Garcia, G. and Thompson, M. (2007). "HMA Dynamic Modulus Predictive Models – A Review." Illinois Center for Transportation. Research report FHWA-ICT-07-005.

Gedafa, D.S., Hossain, M.R., and Romanoschi, S.A. (2009). "Field Verification of KDOT's Superpave Mixture Properties to Be Used as Inputs in the NCHRP Mechanistic Empirical Pavement Design Guide." Kansas Department of Transportation, Topeka, KS.

Horvath, A. (2003). "Life-Cycle Environmental and Economical Assessment of Using Recycled Materials for Asphalt Pavements." Technical Report: University of California Transportation Center (UCTC).

Huang, B., Shu, X. and Zhao, S. (2013). "Laboratory and Field Evaluation of Warm Mix Asphalt Pavements in Tennessee (Phase II)." Report to Tennessee Department of Transportation Research Development and Technology Program, December 2013.

Huang, B., Shu, X., Shrum, E. and Zhao, S. (2011). "Evaluation of Durability of Asphalt Mixtures Containing Fractionated High RAP Content." Report to Tennessee Department of Transportation Research Development and Technology Program, September 2011.

Jeong, M. and Younghan, J. (2015). "Dynamic Complex Modulus Prediction of Non-Conventional Asphalt Mixes." 51st ASC Annual International Conference Proceedings. The Associated Schools of Construction.

Kandhal, P., and Mallick, B. (1997). "Pavement Recycling Guidelines for State and Local Governments – Participant's Reference Book." Report No. FHWA-SA-98-042, Federal Highway Administration, Washington, D.C.

Kandhal, P., and Parker, Jr. F. (1998). "Aggregate Tests Related to Asphalt Concrete Performance in Pavements." NCHRP Report 405, Transportation Research Board, National Research Council, Washington, DC.

Kennedy, T. W., Tam, W. O., and Solaimanian, M. (1998). "Optimizing use of Reclaimed Asphalt Pavement with the SuperPave System." Journal of the Association of Asphalt Paving Technologists, 67, 311–333.

Kim, Y.R., and King, M. (2005). "Typical Dynamic Moduli for North Carolina Asphalt Concrete Mixes." FHWA/NC/2005-03, Federal Highway Administration, Washington, D.C.

Kim, Y.R., Seo, Y., King, M., and Momen, M. (2004). "Dynamic modulus testing of asphalt concrete in indirect tension mode." Transportation Research Record: Journal of the Transportation Research Board, Issue 1891.

Kim, Y.R., Underwood, B., Sakhaei, M.F., Jackson, N., and Puccinelli, J. (2011). "LTPP Computed Parameter: Dynamic Modulus." FHWA-HRT-10-035, Turner-Fairbank Highway Research Center, McLean, VA.

Kvasnak, A., Robinette, J., Williams, C. (2007). "Statistical Development of a Flow Number Predictive Equation for the Mechanistic-Empirical Pavement Design Guide." TRB Annual Meeting Paper 07-1000.

Li, P. and Liu, J. (2014). "Characterization of Alaskan HMA Mixtures with the Simple Performance Tester." Report to Alaska Department of Transportation & Public Facilities and Alaska University Transportation Center, May 2014.

Li, X., Marasteanu, M.O. Williams, R.C. and Clyne. T.R. (2008). "Effect of Reclaimed Asphalt Pavement (Proportion and Type) and Binder Grade on Asphalt Mixtures." Transportation Research Record: Journal of the Transportation Research Board, 2051, 90-97.

Li, X., Clyne, T. R. and Marasteanu, M.O. (2004). "Recycled Asphalt (RAP) Effects on Binder and Mixture Quality." MN/RC-2005-02. University of Minnesota, Twin Cities. http://www.cts.umn.edu/Publications/ResearchReports/reportdetail.html?id=973

Liu, J., Zhao, S., and Li, L. (2016). "Characterization of Alaskan Hot-Mix Asphalt Containing Reclaimed Asphalt Pavement Material." Report to Alaska Department of Transportation & Public Facilities and Alaska University Transportation Center, CESTiCC Project No. 101418. http://www.dot.state.ak.us/stwddes/research/assets/pdf/4000-137.pdf

McDaniel, R., and Anderson, R. M. (2001). "Recommended Use of Reclaimed Asphalt Pavement in the Superpave Mix Design Method: Technician's Manual." NCHRP Report No. 452, Transportation Research Board, Washington, D.C.

Mohammad, L. N., Wu, Z., Myers, L., Cooper, S., Abadie, C., Chehab, G., and Davis, R. (2005). "A Practical Look at the Simple Performance Tests: Louisiana's Experience." Journal of the Association of Asphalt Paving Technologists, 74.

Mohammad, L. N., Wu, Z., Obulareddy, S., Cooper, S., and Abadie, C.D. (2006). "Permanent Deformation Analysis of Hot Mix Asphalt Mixtures Using the Simple Performance Tests and 2002 Mechanistic-Empirical Design software." Transportation Research Record: Journal of the Transportation Research Board, Issue 1970: 133-142.

Morian, D., and Ramirez, L. (2016). "Economic Consideration for asphalt Pavement Recycling Techniques." Submitted to the 95th Annual Meeting of the Transportation Research Board.

Muthadi, R., and Kim, Y. (2007)." Local Calibration of the MEPDG for Flexible Pavement Design." A thesis submitted to, the Department of Civil, Construction, and Environmental Engineering, North Carolina State University, Raleigh, NC.

NCHRP REPORT 673 (2011). Advanced Asphalt Technologies, LLC. "A Manual for Design of Hot Mix Asphalt with Commentary." Transportation Research Board, National Research Council, Washington, DC.

Obulareddy, S. (2006). "Fundamental Characterization of Louisiana HMA Mixtures for the 2002 Mechanistic-Empirical Design Guide." Thesis, B.E., Andhra University, India.

Pavement Life-cycle Assessment Tool for Environmental and Economic Effects (PaLATE) (2003). Consortium on Green Design and Manufacturing. University of California, Berkeley. http://www.ce.berkeley.edu/~horvath/palate.html

Pellinen, K. (2001). "Investigation of the use of dynamic modulus as an indicator of hot-mix asphalt performance." Ph.D. thesis, Arizona State University, Tempe, AZ.

Pellinen, T., and Witczak, M. (2002). "Stress Dependent Master Curve Construction for Dynamic (Complex) Modulus." Journal of the Association of Asphalt Paving Technologists, 71.

Shen, S. and Yu, H. (2012). "An Investigation of Dynamic Modulus and Flow Number Properties of Asphalt Mixtures in Washington State." Washington State Transportation Center (TRAC). A report for Transportation Northwest (TransNow), University of Washington, Seattle Washington. Report No. TNW2012-02.

Stuart, K.D., and Izzo, R.P. (1995). "Correlation of G*/sin Delta with Rutting Susceptibility from Laboratory Mixture Tests." Transportation Research Record: Journal of the Transportation Research Board, Issue 1891.

Teclemariam, S. and Saboundjian, S. (2010). "Determining the Effective Performance Grade of Blends of Recovered Asphalt from RAP with Neat Asphalt Cement." Research Report No. FHWA-AK-RD-11-01. ADOT&PF, AK.

West, R. C., Rada, G. R., Willis, J. R., and Marasteanu, M. O. (2013). "Improved Mix Design, Evaluation, and Materials Management Practices for Hot Mix Asphalt with High Reclaimed Asphalt Pavement Content." Transportation Research Board.

Williams, R.C., Robinette, C.J., Bausano, J., and Breakah, T. (2007). "Testing Wisconsin Asphalt Mixtures for the AASHTO 2002 Mechanistic Design Procedure." WHRP 0092-04-07.

Willis, R. (2015). "Effect of Recycled Materials on Pavement Life-Cycle Assessment: A Case Study." Submitted to the 94th Annual Meeting of the Transportation Research Board.

Willis, J. R., Turner, P., Julian, G., Taylor, A. J., Tran, N., and Padula, F. (2012). "Effects of Changing Virgin Binder Grade and Content on RAP Mixture Properties." Auburn, AL: National Center for Asphalt Technology, Report Number NCAT, 12-03.

Witczak, M. W., and Fonseca, O. A. (1996). "Revised Predictive Model for Dynamic (Complex) Modulus of Asphalt Mixtures." Transportation Research Record 1540, 15-23.

Witczak, M.W. (2002). "Simple Performance Test for Superpave Mix Design." Transportation Research Board, 2002.

Witczak, M.W. (2007). "Superpave Support and Performance Models Management." NCHRP Report 9-19, Transportation Research Board, National Research Council, Washington, DC.

Witczak, M.W., Kaloush, K., Pellinen, T., El-Basyouny, M., and Vonquintus, H. (2002). "Simple Performance Test for Superpave Mix Design." NCHRP Report 465, Transportation Research Board, National Research Council, Washington, DC.

Yu, J. (2012). "Modification of Dynamic Modulus Predictive Models for Asphalt Mixtures Containing Recycled Asphalt Shingles." Graduate Thesis and Dissertations. Iowa State University. Paper 12540.

2002 Design Guide for New & Rehabilitated Pavements (Final Report) (2004). "Part 2-Design Inputs, Chapter 2 Material Characterization." NCHRP Project 1-37A. March 2004. http://www.trb.org/mepdg/guide.htm

Latest News. (n.d.). Retrieved May 20, 2016, from National Center for Asphalt Technology (NCAT) website: (http://eng.auburn.edu/research/centers/ncat/

Virginia Department of Transportation – Home. (n.d.). Retrieved May 20, 2016, from *http://www.virginiadot.org/* (Figure 2.1)

APPENDIX A JOB MIX FORMULAE

State of Alaska
Department of Transportation & Public Facilities
Central Materials Lab
5750 East Tudor Road
Anchorage, AK 99507
Phone (907) 269-6200 FAX (907) 269-6201

Laboratory Report

Quality
Laboratory No.: 2014A-1760

Name: AMATS: Ast Resurfacing: Northern Lts. To 9th Ave Project No.: 56000 / 0527023
Sample: HMA Type IIB Item/Spec No.: 401(1B) Field No.: Q-ATBIIB-MD-2
Sampled From: Manufacturer's Stock Date Sampled: 07/27/2014
Source MP 78 Parks Pit (KASH)/ Cst QAP Quantity Represented: Source Date Received: 07/30/2014
Location: Anchorage Submitted By: QAP Date Completed: 08/06/2014
Examined For: Bituminous Mix Design Date Reported: 08/06/2014

AGGREGATE

Blend Ratio 27:50: :13:10: :
CA:IA:NF:CF:BS:MF:RP

Blend Specific Gravity Bulk 2.685 Effective 2.734

Sieve	% Pass		Specs
1"			
3/4"	100		100
1/2"	87		81-93
3/8"	76		70-82
#4	57		51-63
#8	41		35-47
#16	30		25-35
#30	22		18-26
#50	14		10-18
#100	9		6-12
#200	6.2		4.2-8.2
FA FM		2.96	
FA Angularity			
CA Absorption		0.7	2.0 max
% Fracture			
Single Face		100	80 min
% Flat / Elongated			
@ 1:3		18	
@ 1:5		2	8 max
Plastic Index		NP	4 max

ASPHALT

Brand & Typ	Tesoro PG 52-28
Specific Gravity	1.011
Mixing Temp. Range	277-287°F
Comp. Temp. Range	254-264°F

ANTI-STRIP ADDITIVE

Brand & Type	Adhere 6500
Minimum Required	0.25%

ATM 417
50 Blow

Related Tests
2014A-1762
2014A-0554

ASPHALT CONTENT, %

@ 4.0% Voids Total Mix	5.2
Approved Optimum	5.4
Specifications	5.0-5.8

PROPERTIES @ OPTIMUM		Specs
Max. SpG (AASHTO T209)	2.504	
Max. SpG Unit Wt., pcf	155.9	
Voids		
Filled	78	65-78
Total Mix	3.2	3-5
In Mineral Aggregate	14.6	12.0+
In Coarse Aggregate		
Stability, lbs	2330	1200+
Flow, 0.01 inches	10	8-16
Unit Weight, pcf	150.9	
Dust/Asphalt Ratio	1.3	0.6-1.4
Rut Index		

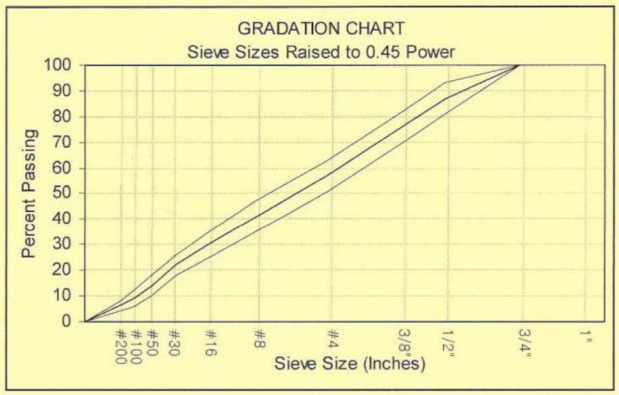

Remarks:

D1 The Material as Submitted Conforms to Specifications
Yes [X] No [ ] NA [ ]
THE TEST RESULTS ARE ONLY REPRESENTATIVE OF THE MATERIAL AS SUBMITTED

Signature: Newton Bingham
Newton J. Bingham, PE
Regional Materials Engineer

Appendix A 1. JMF for PG 52-28 Mixes Central Region (#1 and #6 in Table 3.2)

State of Alaska
Department of Transportation & Public Facilities
Central Materials Lab
5750 East Tudor Road
Anchorage, AK 99507
Phone (907) 269-6200 FAX (907) 269-6201

Laboratory Report

Quality

Laboratory No.: 2014A-0904

Name: W. Dowling Phase II
Project No.: 51030 / 0532(008)
Sample: ATB Type IIB Mix with 25% RAP
Item/Spec No.: 306(1)
Field No.: Q-ATBIIB-MD-2
Sampled From: Manufacturer's Stock
Source MP 39 Glenn Highway / AS&G
Quantity Represented: Source
Location: 11195 Lang St. / Anchorage
Submitted By: Granite Const.
Examined For: Bituminous Mix Design

Date Sampled: 05/13/2014
Date Received: 05/17/2014
Date Completed: 06/12/2014
Date Reported: 06/12/2014

AGGREGATE

Blend Ratio 18:15: :42: : :25
CA:IA:NF:CF:BS:MF:RP

Blend Specific Gravity Bulk 2.688
Effective 2.759

Sieve	% Pass		Specs
1"			
3/4"	100		100
1/2"	89		83-95
3/8"	78		72-84
#4	58		52-64
#8	40		34-46
#16	28		23-33
#30	20		16-24
#50	13		9-17
#100	9		6-12
#200	6.0		4.0-8.0
FA FM		3.10	
FA Angularity			
CA Absorption		0.9	2.0 max
% Fracture			
Single Face		99	80 min
% Flat / Elongated			
@ 1:3			
@ 1:5		4	8 max
Plastic Index		NP	4 max

ASPHALT

Brand & Typ Denali PG 58-34
Specific Gravity 1.007
Mixing Temp. Range 325-335°F

ANTI-STRIP ADDITIVE

Brand & Type Morlife 5000
Minimum Required 0.25%

ATM 417
50 Blow

Related Tests
2014A-0826
2014A-1163

ASPHALT CONTENT, %

@ 4.0% Voids Total Mix	5.0
Approved Optimum	5.3
Specifications	4.9-5.7

PROPERTIES @ OPTIMUM		Specs
Max. SpG (AASHTO T209)	2.526	
Max. SpG Unit Wt., pcf	157.2	
Voids		
Filled	78	65-78
Total Mix	3.1	3-5
In Mineral Aggregate	13.8	12.0+
In Coarse Aggregate		
Stability, lbs	3480	1200+
Flow, 0.01 inches	12	8-16
Unit Weight, pcf	152.5	
Dust/Asphalt Ratio	1.4	0.6-1.4
Rut Index		

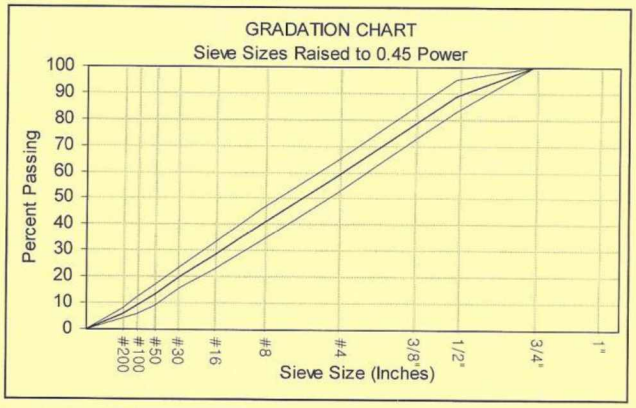

Remarks:

D1 The Material as Submitted Conforms to Specifications
Yes [X] No [ ] NA [ ]

THE TEST RESULTS ARE ONLY REPRESENTATIVE OF THE MATERIAL AS SUBMITTED

Signature: Newton Bingham
Newton J. Bingham, PE
Regional Materials Engineer

Appendix A 2. JMF for PG 58-34 Mixes Central Region (#2 and #5 in Table 3.2)

State of Alaska
Department of Transportation & Public Facilities
Central Materials Lab
5750 East Tudor Road
Anchorage, AK 99507
Phone (907) 269-6200 FAX (907) 269-6201

Laboratory Report

Quality

Laboratory No.: **2015A-1242**

Name: **Lake Hood A&B Parking Rehabilitation** Project No.: **54465 / 3-02-0013-XXX-2014**
Sample: **HMA Type IIA** Item/Spec No.: **P-401a** Field No.: **Q-HMAIIA-MD-1**
Sampled From: **Manufacturer's Stock** Date Sampled: **05/26/2015**
Source **MP 39 Glenn Highway / AS&G** Quantity Represented: **Source** Date Received: **05/30/2015**
Location: **Anchorage** Submitted By: **Granite Const.** Date Completed: **06/29/2015**
Examined For: **Bituminous Mix Design** Date Reported: **06/29/2015**

AGGREGATE

Blend Ratio **24:26: :50: : :**
CA:IA:NF:CF:BS:MF:RP

Blend Specific Gravity Bulk **2.709** Effective **2.761**

Sieve	% Pass		Specs
1"			
3/4"	100		100
1/2"	85		79-91
3/8"	71		65-77
#4	49		43-55
#8	34		28-40
#16	22		17-27
#30	15		11-19
#50	10		6-14
#100	7		4-10
#200	5.0		3.0-7.0
FA FM		3.20	
FA Angularity			
CA Absorption		0.7	2.0 max
% Fracture Double Face		99	90 min
% Flat / Elongated @ 1:3		16	
% Flat / Elongated @ 1:5		2	8 max
Plastic Index		NP	6 max

ASPHALT

Brand & Typ **Denali PG 58-34**
Specific Gravity **1.007**
Mixing Temp. Range **325-335°F**
Comp. Temp. Range **305-315°F**

ANTI-STRIP ADDITIVE

Brand & Type **Morelife 5000**
Minimum Required **0.25%**

ATM 417
75 Blow

Related Tests
2015A-1243
2015A-1195

ASPHALT CONTENT, %

@ 4.0% Voids Total Mix	5.2
Approved Optimum	5.3
Specifications	4.9-5.7

PROPERTIES @ OPTIMUM		Specs
Max. SpG (AASHTO T209)	2.528	
Max. SpG Unit Wt., pcf	157.4	
Voids		
Filled	75	
Total Mix	3.8	2.8-4.2
In Mineral Aggregate	15.0	13.0+
In Coarse Aggregate		
Stability, lbs	3210	2150+
Flow, 0.01 inches	12	10-14
Unit Weight, pcf	151.4	
Dust/Asphalt Ratio	1.1	
Rut Index		

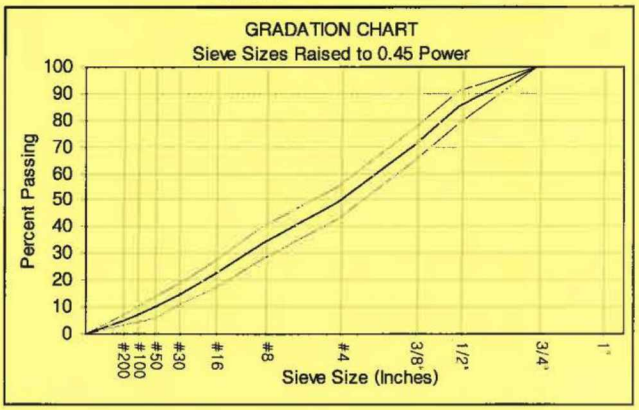

Remarks:

D9 The Material as Submitted Conforms to Specifications
Yes [X] No [ ] NA [ ]

THE TEST RESULTS ARE ONLY REPRESENTATIVE OF THE MATERIAL AS SUBMITTED

Signature: Newton Bingham
Newton J. Bingham, PE
Regional Materials Engineer

Appendix A 3. JMF for PG 58-34 Type II-A Mixes Central Region (#3 in Table 3.2)

State of Alaska
Department of Transportation & Public Facilities
Central Materials Lab
5750 East Tudor Road
Anchorage, AK 99507
Phone (907) 269-6200 FAX (907) 269-6201

Laboratory Report

Quality

Laboratory No.: 2014A-1207

Name: AIA 7L/25R Runway Rehabilittion
Sample: HMA Type IIA Mix Design
Sampled From: Manufacturer's Stock
Source: MP 39 Glenn Highway / AS&G
Location: Anchorage
Examined For: Bituminous Mix Design

Project No.: 53598 / AIP 3-02-0016-171-2014
Item/Spec No.: P-401a(2).n1
Field No.: Q-HMAIIA-MD-1
Quantity Represented: Source
Submitted By: Granite Const.

Date Sampled: 06/17/2014
Date Received: 06/25/2014
Date Completed: 07/09/2014
Date Reported: 07/10/2014

AGGREGATE

Blend Ratio 18:15: :42: : :25
CA:IA:NF:CF:BS:MF:RP

Blend Specific Gravity Bulk 2.707
Effective 2.755

Sieve	% Pass		Specs
1"			
3/4"	100		100
1/2"	89		83-95
3/8"	78		72-84
#4	58		52-64
#8	40		34-46
#16	28		23-33
#30	20		16-24
#50	13		9-17
#100	9		6-12
#200	6.0		4.0-8.0
FA FM		3.10	
FA Angularity			
CA Absorption		0.8	2.0 max
% Fracture			
Double Face		100	90 min
% Flat / Elongated			
@ 1:3		20	
@ 1:5		1	8 max
Plastic Index		NP	6 max

ASPHALT

Brand & Typ	Denali PG 58-34
Specific Gravity	1.007
Mixing Temp. Range	325-335°F
Comp. Temp. Range	305-315°F

ANTI-STRIP ADDITIVE

Brand & Type	Morlife 5000
Minimum Required	0.25%

ATM 417
75 Blow

Related Tests
2014A-1294
2014A-1163

ASPHALT CONTENT, %

@ 4.0% Voids Total Mix	4.7
Approved Optimum	5.0
Specifications	4.6-5.4

PROPERTIES @ OPTIMUM		Specs
Max. SpG (AASHTO T209)	2.535	
Max. SpG Unit Wt., pcf	157.8	
Voids		
Filled	77	
Total Mix	3.1	2.8-4.2
In Mineral Aggregate	13.8	13.0+
In Coarse Aggregate		
Stability, lbs	3920	2150+
Flow, 0.01 inches	11	10-14
Unit Weight, pcf	152.9	
Dust/Asphalt Ratio	1.4	0.6-1.4
Rut Index		

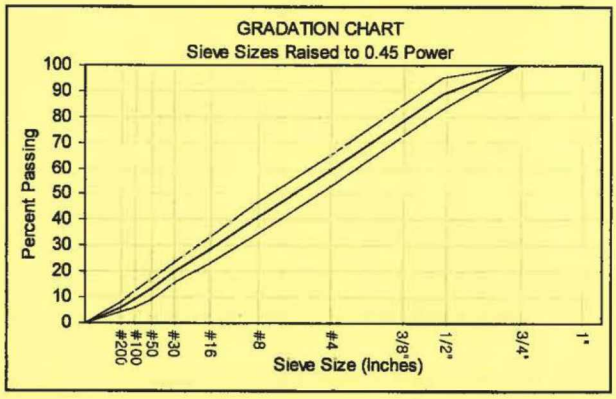

Remarks:
Not for transfer.

D9 The Material as Submitted Conforms to Specifications
Yes [X] No [ ] NA [ ]

THE TEST RESULTS ARE ONLY REPRESENTATIVE OF THE MATERIAL AS SUBMITTED

Signature: Newton Bingham
Newton J. Bingham, PE
Regional Materials Engineer

Appendix A 4. JMF for PG 58-34 Type II-A Mix with 25% RAP Central Region (#4 in Table 3.2)

STATE OF ALASKA - NORTHERN REGION
DEPARTMENT OF TRANSPORTATION AND PUBLIC FACILITIES
BITUMINOUS MIX DESIGN MARSHALL METHOD RECEIVED:
2301 PEGER ROAD
FAIRBANKS, AK 99709

PROJECT NAME:	North Pole Homestead Rd/NPHS	REGIONAL LAB # :	09-340
PROJECT NUMBER:	HPP-STP-HPRM-0002(193)/63025	FIELD # :	HMA-MD-1
GENERAL CONTRACTOR:	Exclusive	TYPE/CLASS:	II B

AGGREGATE SOURCE:	Twin Rich Pit
AGGREGATE QUALITY#:	06-142
BLEND RATIO:	16:14:70 CA:INT:FA
BLENDED BULK SPG:	2.679
EFFECTIVE SPG:	2.719

BINDER SOURCE:	Emulsion Products
BINDER GRADE:	52-28
BINDER SPG:	1.0087
ANTISTRIP:	.25% Morlife

MIX DESIGN PARAMETERS	
STABILITY	1200
FLOW	8-16
VOIDS TOTAL MIX	3-5
COMPACTION, BLOWS	50
VOIDS FILLED	65-78
VMA	12
DUST ASPHALT RATIO	.6-1.4

MIXING TEMP (DEG F)	281-290
COMPACTING TEMP (DEG F)	264-271

MARSHALL RESULTS	
% ASPHALT @ MAX UNIT WT	6
% ASPHALT @ MAX STABILITY	5.5
% ASPHALT @ 4% VOIDS	5.1
OPTIMUM OIL CONTENT = 5.2 %	
STABILITY	2200
FLOW	9
VOIDS TOTAL MIX	3.6
VOIDS FILLED	76
VMA	14.7
MTD/RICE	2.499
UNIT WEIGHT	150.3
DUST ASPHALT RATIO	1.3

APPROVED: LEO J. WOSTER C.E. 7160 8-10-07

AGGREGATE DESIGN PARAMETERS		Reg Lab	Spec
FLAT & ELONGATED		1.3	8max
LIQUID LIMIT		NV	
PLASTIC INDEX		NP	
FINENESS MODULUS			
UNCOMP. VOID -T304			
SAND EQUIVALENT			
FRACTURE:	Single Face	98	
	Double Face	94	90min

SIEVE SIZE	PROPOSED GRADATION	MIX DESIGN SPEC BAND LSL	HSL
1"		-----	-----
3/4"		100	-----
1/2"	90	84	96
3/8"	79	73	85
#4	52	46	58
#8	36	30	42
#10		-----	-----
#16	26	21	31
#20		-----	-----
#30	19	15	23
#40		-----	-----
#50	15	11	19
#60		-----	-----
#80		-----	-----
#100	9	6	12
#200	6.2	4.2	8.2

REMARKS:
Approved for 63025

Appendix A 5. JMF for PG 52-28 Mixes Central Region (#7, 9, 11 in Table 3.2)

STATE OF ALASKA - NORTHERN REGION
DEPARTMENT OF TRANSPORTATION AND PUBLIC FACILITIES
BITUMINOUS MIX DESIGN MARSHALL METHOD
2301 PEGER ROAD
FAIRBANKS, AK 99709

PROJECT NAME:	Nordale Rd Pavement Rehabilitation	REGIONAL LAB # :	10-241
PROJECT NUMBER:	STP-0653(6) / 63158	FIELD # :	NR-HMA-MD-1
GENERAL CONTRACTOR:	Exclusive	TYPE/CLASS:	II/B
		RECEIVED:	7/19/2010

AGGREGATE SOURCE:	Coarse, Fines: Van Horn Pit; Intermed.: Delta Sand & Gravel
AGGREGATE QUALITY#:	Van Horn Pit: 08-047; Delta Sand & Gravel: 10-071 = Tanana Valley alluvial agg
BLEND RATIO:	18:15:67 / Coarse:Intermed:Fines
BLENDED BULK SPG:	2.674
EFFECTIVE SPG:	2.728

BINDER SOURCE:	Emulsion Products Company
BINDER GRADE:	PG 52 -40
BINDER SPG:	0.990
ANTISTRIP:	More Life 5000 at 0.25%

MIX DESIGN PARAMETERS	
STABILITY	1200 min
FLOW	8-16
VOIDS TOTAL MIX	3-5
COMPACTION, BLOWS	50
VOIDS FILLED	65-78
VMA	12 min
DUST ASPHALT RATIO	0.6-1.4

MIX DESIGN TEMPERATURES:

MIXING TEMP (°F)	336
COMPACTING TEMP (°F)	311

MARSHALL RESULTS	
% ASPHALT @ MAX UNIT WT	5.7
% ASPHALT @ MAX STABILITY	5.5
% ASPHALT @ 4% VOIDS	5.0
OPTIMUM OIL CONTENT = 5.0 %	
STABILITY	3240
FLOW	11
VOIDS TOTAL MIX	3.9
VOIDS FILLED	73
VMA	14.4
MTD/RICE	2.508
UNIT WEIGHT	150.4
DUST ASPHALT RATIO	1.4

APPROVED: _____
Northern Region Materials Engineer 8-9-10

AGGREGATE DESIGN PARAMETERS		Reg Lab	Spec
FLAT & ELONGATED		0	0-8
LIQUID LIMIT		NV	
PLASTIC INDEX		NP	
FINENESS MODULUS			
UNCOMP. VOID -T304		0	
SAND EQUIVALENT		0	
FRACTURE:	Single Face	93	
	Double Face	89	90-100

SIEVE SIZE	PROPOSED GRADATION	MIX DESIGN SPEC BAND LSL	HSL
1"		-----	-----
3/4"	100	100	-----
1/2"	89	83	95
3/8"	79	73	85
#4	55	49	61
#8	37	31	43
#10		-----	-----
#16	24	19	29
#20		-----	-----
#30	18	14	22
#40		-----	-----
#50	12	8	16
#60		-----	-----
#80		-----	-----
#100	9	6	12
#200	6.0	4	8

REMARKS: Approved for 63159
* Approval NO LOS, Fabric ECO if Prof. Fabric is needed
.. May need to waste Bag house fines if mix too tender

Appendix A 6. JMF for PG 52-40 Mixes Northern Region (#8 and #10 in Table 3.2)

APPENDIX B AIR VOIDS OF SPECIMENS

Appendix B1. Gmm for all mixes

Mix #	Field or Lab	Sample #	Dry Weight(g)	Bucket in water(g)	Bucket & sample in water (g)	G_{mm}	Ave.	Std.
1	Field	-	-	-	-	2.504	2.504	-
2	Lab	A	1514.5	1473.2	2379.1	2.488	2.492	0.0052
		B	1511.3	1473.2	2377.3	2.489		
		C	1538.3	1473.2	2395.6	2.498		
3	Field	-	-	-	-	2.528	2.528	-
4	Field	-	-	-	-	2.535	2.535	-
5	Field	-	-	-	-	2.526	2.526	-
6	Lab	A	1506.1	1473.2	2378.9	2.508	2.504	0.0050
		B	1500.7	1473.2	2374.5	2.504		
		C	1507.6	1473.2	2377.4	2.499		
7	Lab	A	1500.3	1484.8	2370.8	2.442	2.453	0.0097
		B	1500.5	1484.8	2375.6	2.461		
		C	1511.2	1484.8	2380.6	2.456		
8	Lab	A	1502.7	1484.8	2374.2	2.450	2.450	0.0044
		B	1500.4	1484.8	2374.8	2.458		
		C	1510.6	1484.8	2377	2.443		
9	Lab	A	1500.2	1484.8	2372	2.447	2.452	0.0052
		B	1500.1	1484.8	2374	2.456		
		C	1504.2	1484.8	2376.1	2.454		
10	Lab	A	1507.1	1484.8	2374.5	2.441	2.445	0.0077
		B	1506.4	1484.8	2374.9	2.444		
		C	1509.6	1484.8	2378	2.449		
11	Lab	A	1500.9	1484.8	2377.2	2.467	2.461	0.0040
		B	1501.9	1484.8	2376	2.459		
		C	1504.8	1484.8	2377	2.456		

Appendix B2. Air voids for AMPT samples for Central region mixes

Mix #	Sample #	Dry Weight (g)	Weight in water (g)	Saturated Surface Dry (SSD) Weight (g)	G_{mb}	G_{mm}	Air Voids
1	A	2838.5	1629.6	2848	2.330	2.504	6.96%
	B	2789.7	1596.8	2793.5	2.331	2.504	6.90%
	C	2811.1	1613	2815.4	2.338	2.504	6.63%
2	A	2788.5	1592.3	2791.5	2.325	2.492	6.68%
	B	2828.9	1619	2834.2	2.328	2.492	6.57%
	C	2813.6	1610.8	2819.8	2.327	2.492	6.60%
3	A	2828.1	1633.7	2833.1	2.358	2.528	6.73%
	B	2816.9	1623.6	2819.8	2.355	2.528	6.85%
	C	2850.7	1652.8	2860.4	2.361	2.528	6.62%
4	A	2845	1645.1	2847.6	2.366	2.535	6.67%
	B	2812.1	1615.8	2814.8	2.345	2.535	7.48%
	C	2861.7	1645.3	2863.9	2.348	2.535	7.36%
5	A	2821	1617.7	2823.1	2.340	2.526	7.35%
	B	2827	1623.6	2829.2	2.345	2.526	7.17%
	C	2882.8	1662.4	2884	2.360	2.526	6.58%
6	A	2826.9	1610.7	2828.9	2.321	2.504	7.33%
	B	2769	1583.4	2772.8	2.328	2.504	7.03%
	C	2797.4	1602.3	2800.7	2.334	2.504	6.78%

Appendix B3. Air voids for AMPT samples for Northern region mixes

Mix #	Sample #	Dry Weight (g)	Weight in water (g)	Saturated Surface Dry (SSD) Weight (g)	G_{mb}	G_{mm}	Air Voids
7	A	2747.4	1554.5	2765.5	2.269	2.453	7.49%
	B	2756	1558.9	2772.1	2.272	2.453	7.37%
	C	2731.4	1542.9	2743.9	2.274	2.453	7.27%
8	A	2715.1	1534.6	2732.7	2.266	2.450	7.52%
	B	2707.5	1529.2	2722.1	2.270	2.450	7.37%
	C	2732.7	1549.1	2748.7	2.278	2.450	7.03%
9	A	2752.4	1559.6	2770.6	2.273	2.452	7.32%
	B	2751	1562.6	2770.3	2.278	2.452	7.11%
	C	2752.6	1558	2770.8	2.270	2.452	7.45%
10	A	2743.3	1552.5	2764.1	2.264	2.445	7.39%
	B	2820	1597.1	2830.5	2.286	2.445	6.48%
	C	2743.2	1557.5	2765.6	2.271	2.445	7.12%
11	A	2772.7	1582.9	2796.9	2.284	2.461	7.19%
	B	2761.3	1566.4	2777.3	2.280	2.461	7.33%
	C	2788.8	1586	2798.8	2.299	2.461	6.55%

APPENDIX C BINDER TEST RESULTS

Appendix C 1. Binder determination using A-VTS method

Binder Name: **PG 52-28**

DSR measured test data			Calculated data		
DSR Temp., °C	RTFO G* (kPa)	RTFO Phase angle (Radians)	RTFO Viscosity (cPoise)	log Temperature (Rankine)	log log Viscosity (cPoise)
46	**10.535**	**1.457**	1087	2.759	0.482
52	**4.391**	**1.491**	446	2.767	0.423
58	**1.880**	**1.514**	189	2.775	0.357

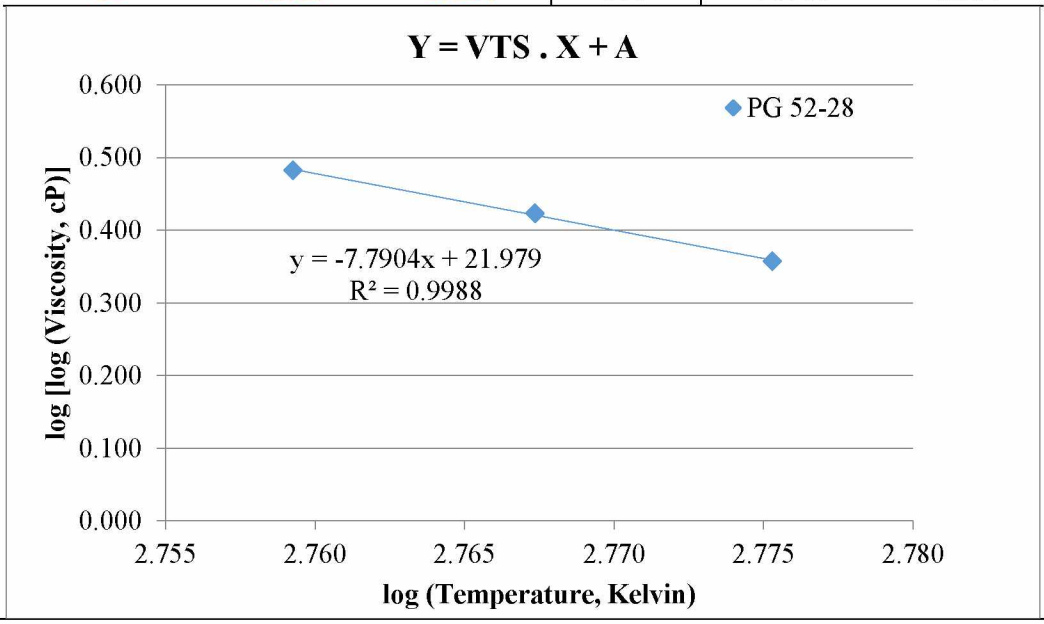

From the above plot and regression (trendline), A (intercept) and VTS (slope) are:

A	VTS
21.979	**-7.7904**

then Viscosity (cP) at other temperatures can be estimated as follows:

Temp., C	Temp., K	log (log Visc)	**Viscosity, cP**	**Viscosity, 10^6 P**
4	2.698	0.961	**1.357E+09**	1.357E+01
21	2.724	0.759	**554151**	5.542E-03
37	2.747	0.580	**6335**	6.335E-05
46	2.759	0.483	**1102**	1.102E-05
52	2.767	0.420	**428**	4.280E-06
54	2.770	0.399	**323**	3.226E-06
58	2.775	0.358	**191**	1.914E-06

Binder Name: **PG 58-34**

DSR measured test data			**Calculated data**		
DSR Temp., °C	RTFO G* (kPa)	RTFO Phase angle (Radians)	RTFO Viscosity (cPoise)	log Temperature (Rankine)	log log Viscosity (cPoise)
52	**4.504**	**1.095**	799	2.767	0.463
58	**2.586**	**1.080**	477	2.775	0.428
64	**1.545**	**1.063**	298	2.783	0.393

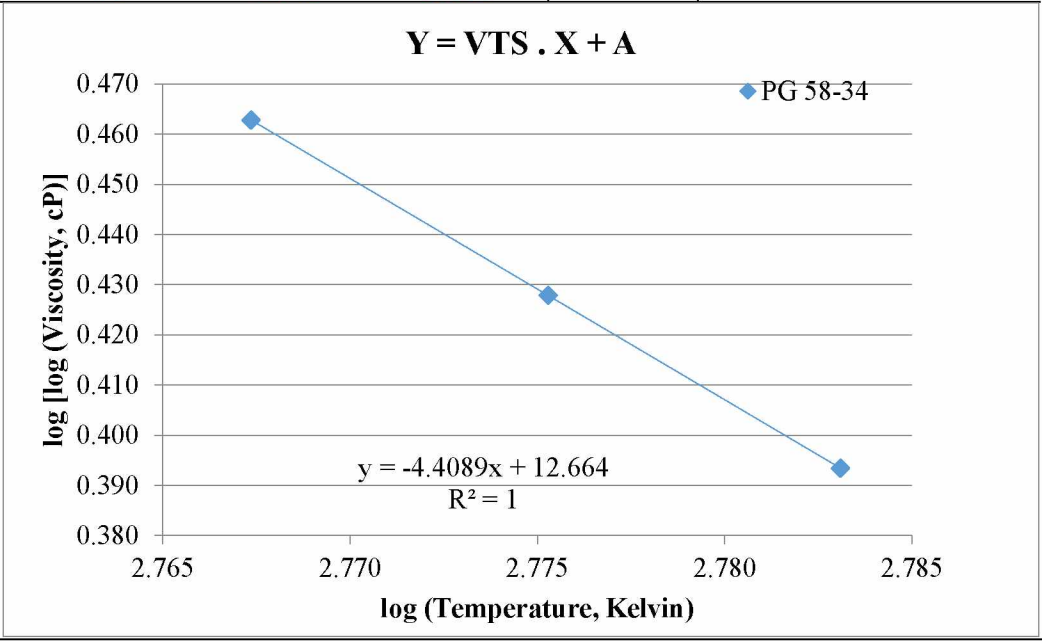

From the above plot and regression (trendline), A (intercept) and VTS (slope) are:

A	VTS
12.664	-4.4089

then Viscosity (cP) at other temperatures can be estimated as follows:

Temp., C	Temp., K	log (log Visc)	**Viscosity, cP**	**Viscosity, 10^6 P**
4	2.698	0.769	**7.461E+05**	7.461E-03
21	2.724	0.655	**32890**	3.289E-04
37	2.747	0.553	**3770**	3.770E-05
46	2.759	0.499	**1421**	1.421E-05
52	2.767	0.463	**802**	8.018E-06
54	2.770	0.451	**671**	6.708E-06
58	2.775	0.428	**478**	4.777E-06

Binder Name: PG 52-40

DSR measured test data			**Calculated data**		
DSR Temp., °C	RTFO G* (kPa)	RTFO Phase angle (Radians)	RTFO Viscosity (cPoise)	log Temperature (Rankine)	log log Viscosity (cPoise)
46	4.356	1.048	876	2.759	0.469
52	2.655	1.026	569	2.767	0.440
58	1.647	1.013	367	2.775	0.409

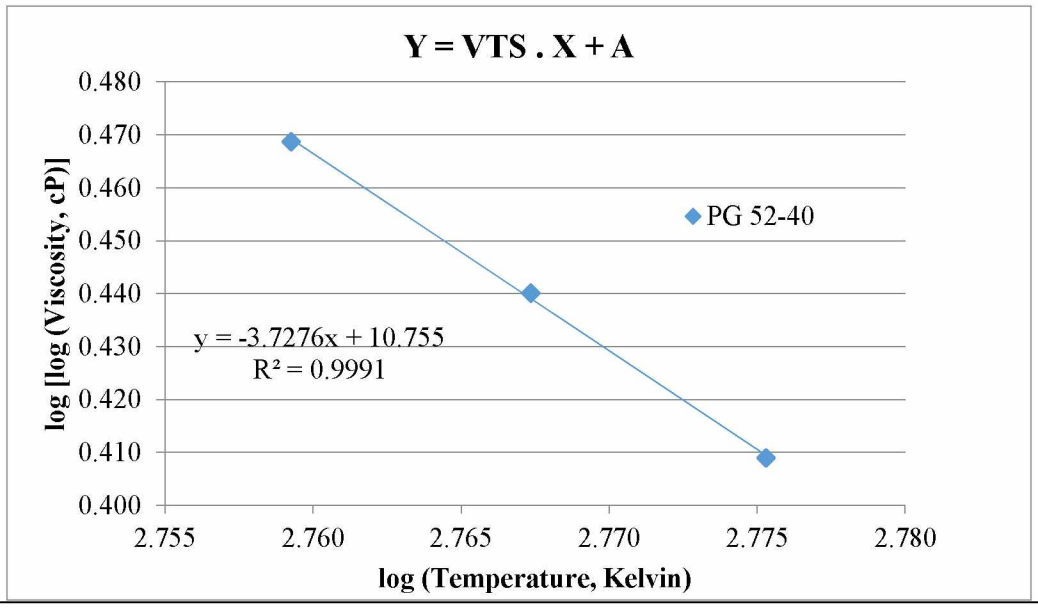

From the above plot and regression (trendline), A (intercept) and VTS (slope) are:

A	VTS
10.755	**-3.7276**

then Viscosity (cP) at other temperatures can be estimated as follows:

Temp., C	Temp., K	log (log Visc)	Viscosity, cP	Viscosity, 10^6 P
4	2.698	0.698	9.742E+04	9.74E-04
21	2.724	0.602	9905	9.90E-05
37	2.747	0.516	1905	1.91E-05
46	2.759	0.470	888	8.88E-06
52	2.767	0.439	563	5.63E-06
54	2.770	0.429	488	4.88E-06
58	2.775	0.410	371	3.71E-06

Appendix C. 2 High continuous grading temperature PG 52-28

Condition	Test Method	Specification Criteria	Test Results at T_1		Test Results at T_2		T_c (℃)	Mean (℃)
			T1(℃)	P1 (kPa)	T2(℃)	P2 (kPa)		
Original 1	D7175	|G*|/sinδ,kPa,≥1.00	52	2.003356559	58	0.81668895	56.64598978	56.57964519
Original 2				1.913027891		0.81042661	56.53161747	
Original 3				1.923246917		0.81360491	56.56132833	
RTFOT 1		|G*|/sinδ,kPa,≥2.20		4.307488084		1.84610652	56.75805402	56.89916931
RTFOT 2				4.368874654		1.90536895	56.96040105	
RTFOT 3				4.537473171		1.89651905	56.97905285	

Appendix C. 3 High continuous grading temperature PG 52-40

Condition	Test Method	Specification Criteria	Test Results at T_1		Test Results at T_2		T_c (℃)	Mean (℃)
			T1℃	P1 (kPa)	T2℃	P2 (kPa)		
Original 1	D7175	|G*|/sinδ,kPa,≥1.00	52	1.966879733	58	1.25328709	61.00573083	60.61805084
Original 2				1.814842278		1.16362113 7	60.0456673	
Original 3				1.9264517		1.23215575 1	60.80275437	
RTFOT 1		|G*|/sinδ,kPa,≥2.20		3.232827004		1.98765664 3	56.74793354	56.39171958
RTFOT 2				3.047264574		1.91961438 8	56.22990089	
RTFOT 3				3.034660633		1.91614963 5	56.19732432	

Appendix C 4. High continuous grading temperature PG 58-34

Condition	Test Method	Specification Criteria	Test Results at T_1		Test Results at T_2		T_c (℃)	Mean (℃)
			T1℃	P1 (kPa)	T2℃	P2 (kPa)		
Original 1	D7175	|G*|/sinδ,kPa,≥1.00	58	1.822189532	64	1.11864060 1	65.37867	64.29734431
Original 2				1.350028884		0.81204518 6	61.54253	
Original 3				1.795402506		1.15569463 7	65.97084	
RTFOT 1		|G*|/sinδ,kPa,≥2.20		2.855738541		1.72950288 1	61.12114	61.40405027
RTFOT 2				2.996085262		1.80258430 1	61.64721	
RTFOT 3				2.945504244		1.77153932 3	61.4438	

Appendix C 5. Dynamic shear modulus and phase angle at 10 rad/s for PG 52-28

T（℃）	Sample	|G*|(kPa)	δ(rad)
46	1	10.364	1.459606
	2	10.57064	1.455125
	3	10.66998	1.456206
	mean	10.53487	1.456979
52	1	4.293722	1.490827
	2	4.354413	1.48941
	3	4.523716	1.492905
	mean	4.390617	1.491047
58	1	1.843051	1.513251
	2	1.902683	1.517688
	3	1.893257	1.512134
	mean	1.879663	1.514358

Appendix C 6. Dynamic shear modulus and phase angle at 10 rad/s for PG 52-40

T（℃）	Sample	|G*|(kPa)	δ(rad)
46	1	4.3809131	1.0499515
	2	4.3585892	1.0496582
	3	4.3289722	1.0430544
	mean	4.3561582	1.0475547
52	1	2.7679957	1.0278985
	2	2.6067988	1.0264295
	3	2.5897104	1.02243
	mean	2.654835	1.025586
58	1	1.6859267	1.0125743
	2	1.6334822	1.0177777
	3	1.6202237	1.0076174
	mean	1.6465442	1.0126565

Appendix C 7. Dynamic shear modulus and phase angle at 10 rad/s for PG 58-34

T（℃）	Sample	|G*|(kPa)	δ(rad)
52	1	4.571312722	1.088478688
	2	4.284390272	1.101075918
	3	4.655802831	1.094854255
	mean	4.503835275	1.094802954
58	1	2.505992817	1.070684202
	2	2.648244702	1.084140227
	3	2.603536057	1.084140227
	mean	2.585924525	1.079654885
64	1	1.509863901	1.061329281
	2	1.571559735	1.058940484
	3	1.552611027	1.068375057
	mean	1.544678221	1.062881607

APPENDIX D WITCZAK |E*| PREDICTIVE MODELS

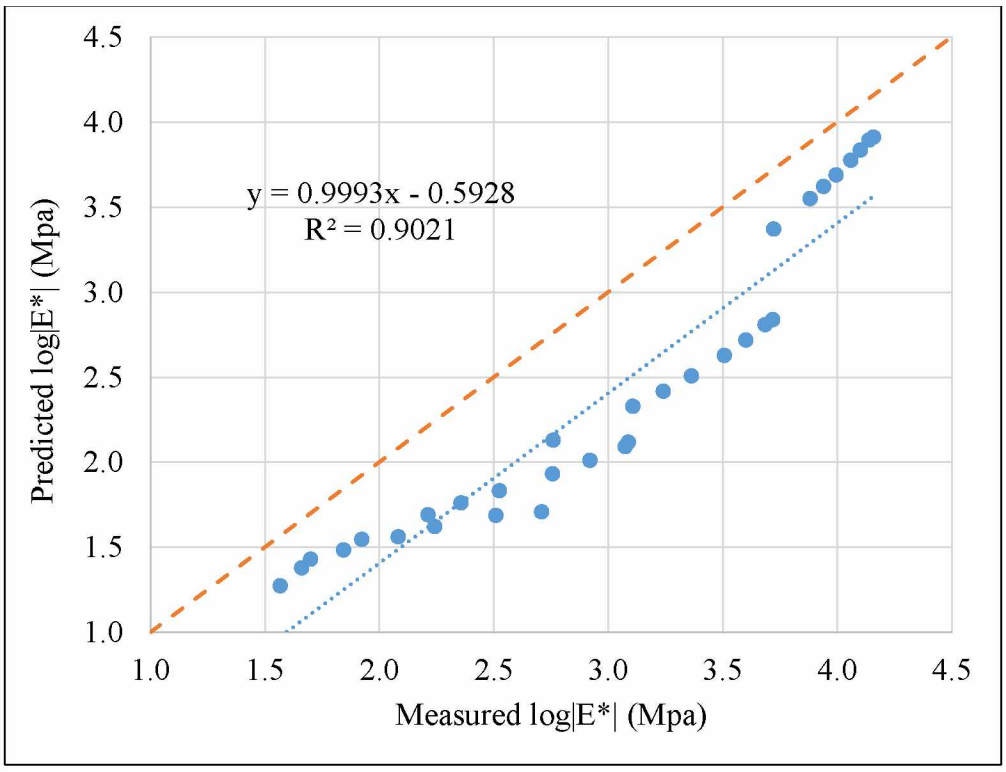

Appendix D.1 Predicted vs. Measured Mix #1 (original Witczak model, Level 2)

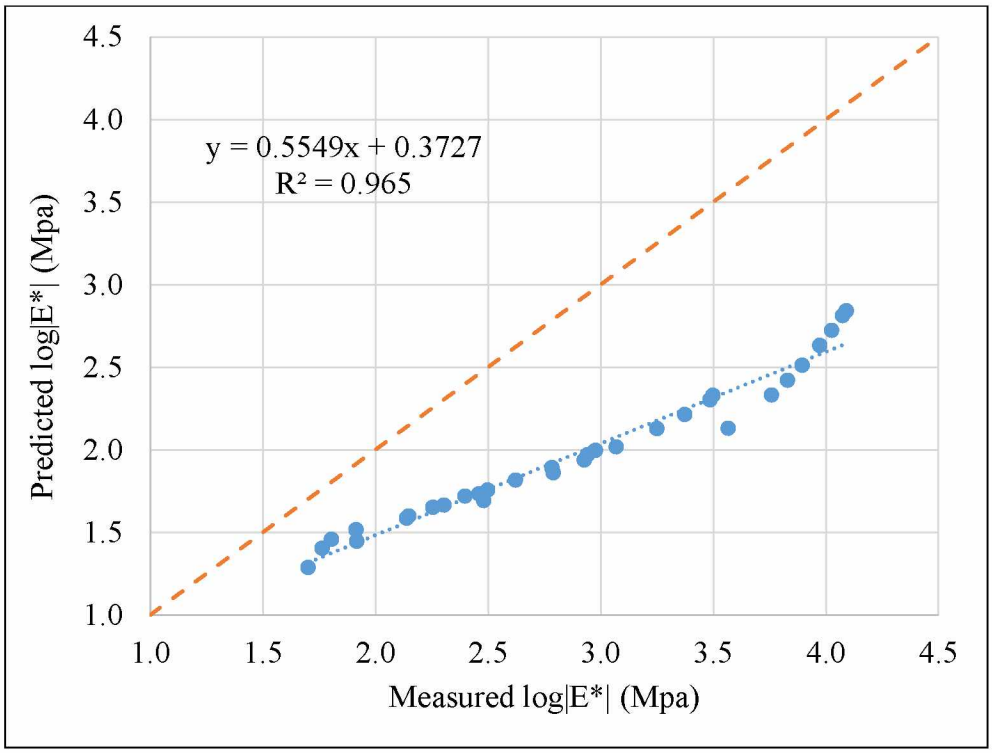

Appendix D.2 Predicted vs. Measured Mix #3 (original Witczak model, Level 2)

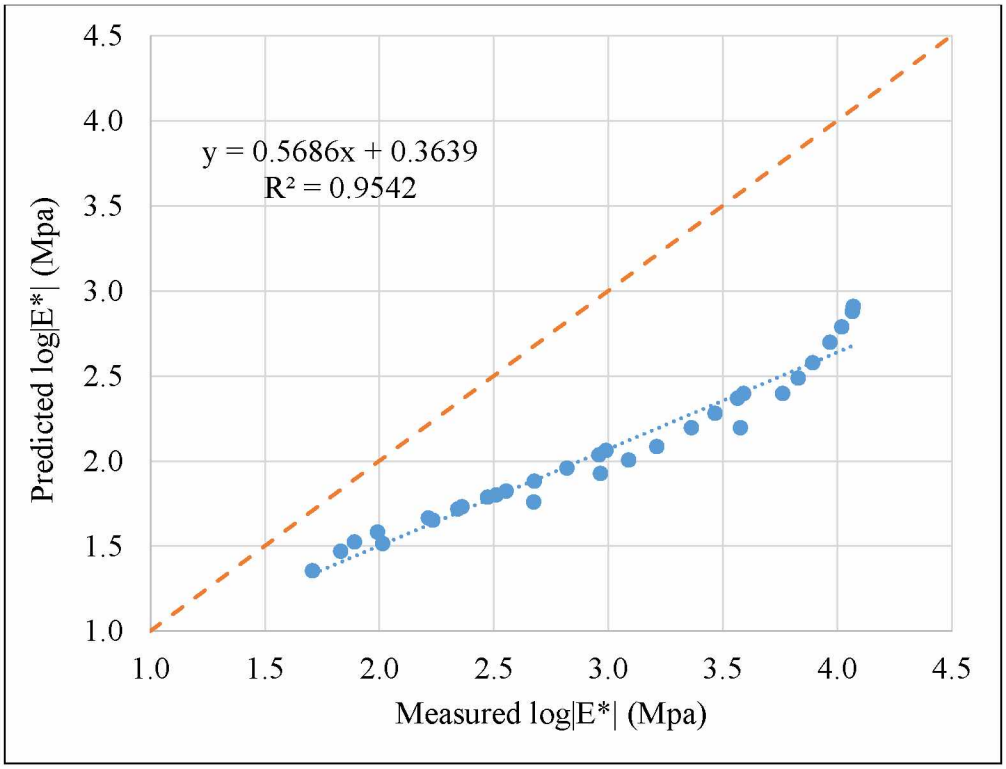

Appendix D.3 Predicted vs. Measured Mix #4 (original Witczak model, Level 2)

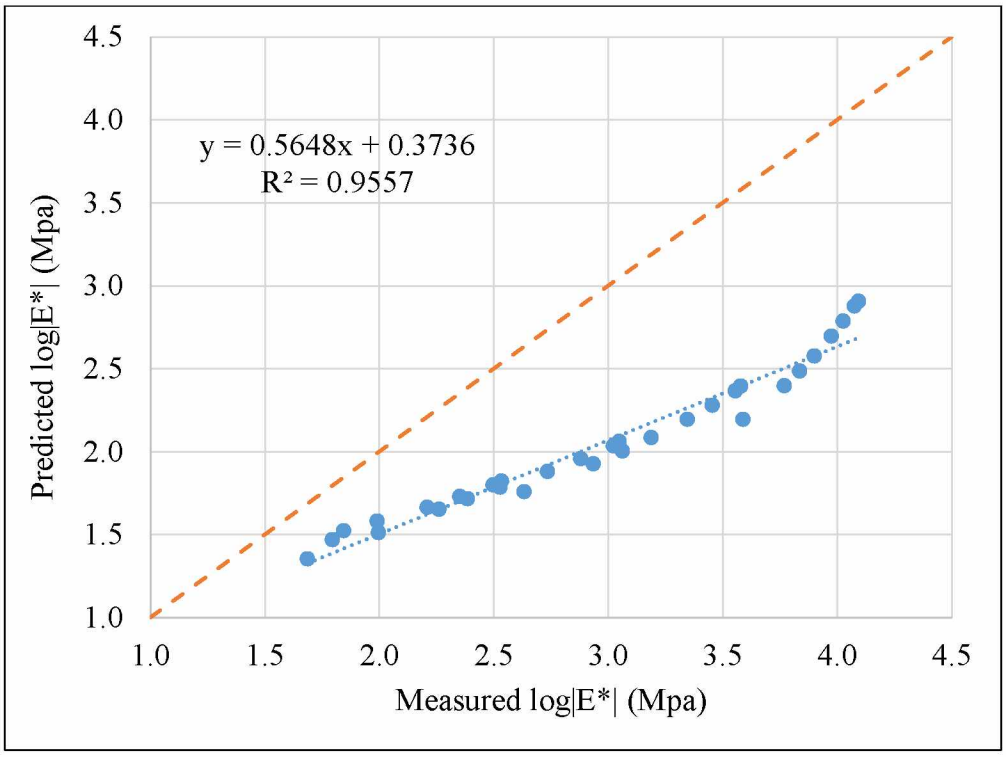

Appendix D.4 Predicted vs. Measured Mix #5 (original Witczak model, Level 2)

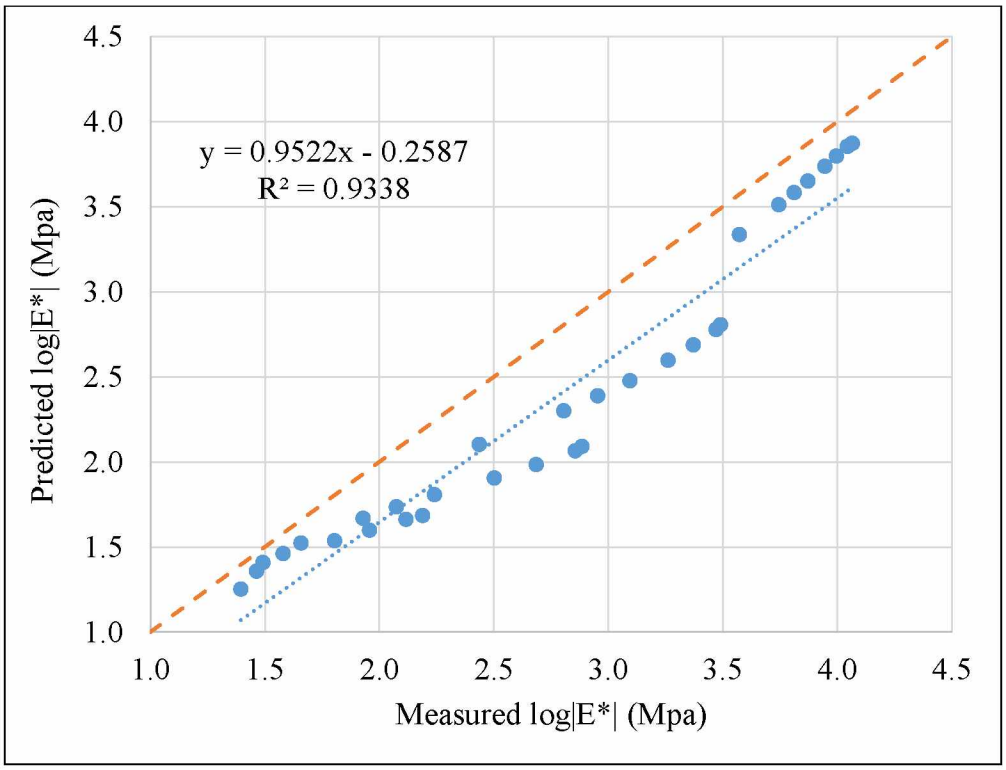

Appendix D.5 Predicted vs. Measured Mix #7 (original Witczak model, Level 2)

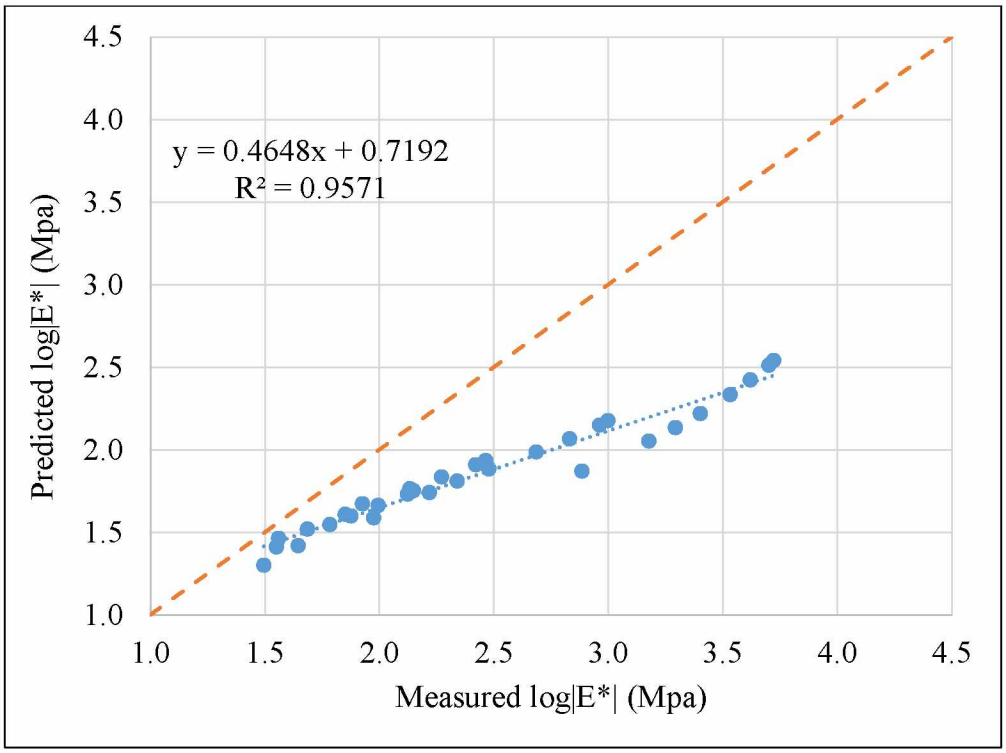

Appendix D.6 Predicted vs. Measured Mix #8 (original Witczak model, Level 2)

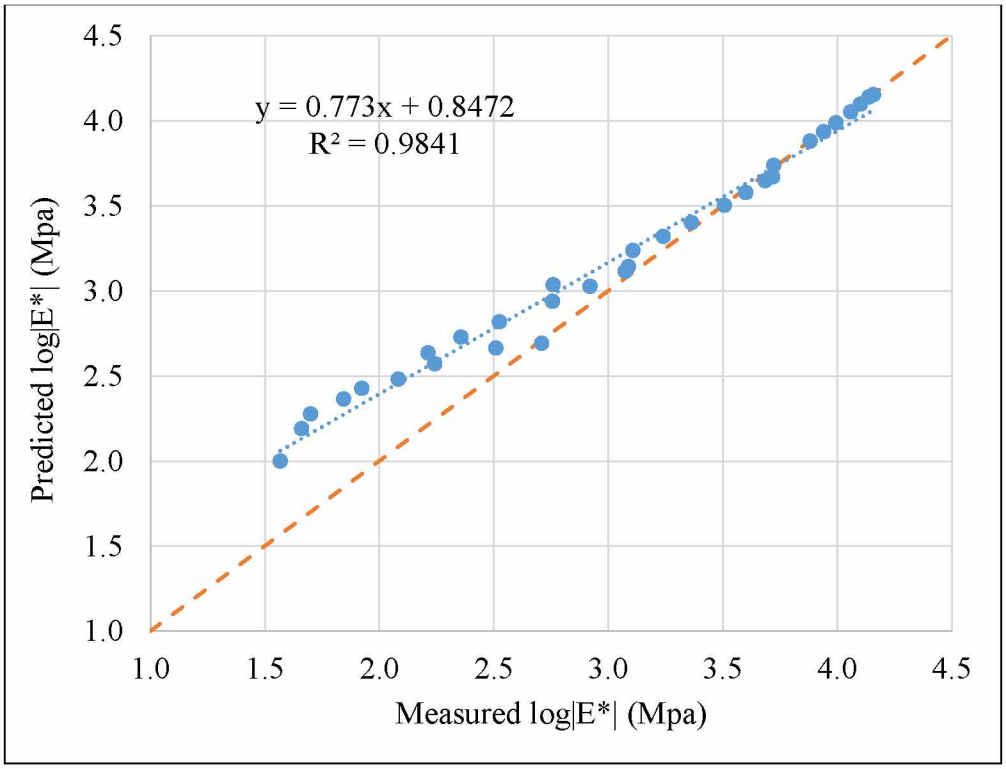

Appendix D.7 Predicted vs. Measured Mix #1 (original Witczak model, Level 3)

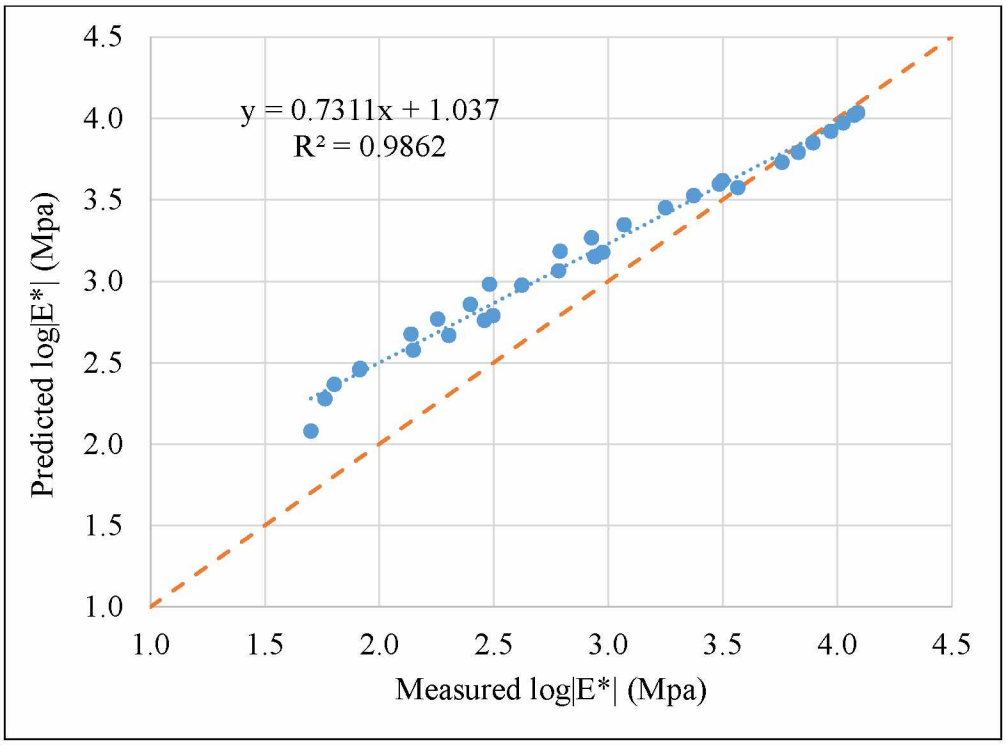

Appendix D.8 Predicted vs. Measured Mix #3 (original Witczak model, Level 3)

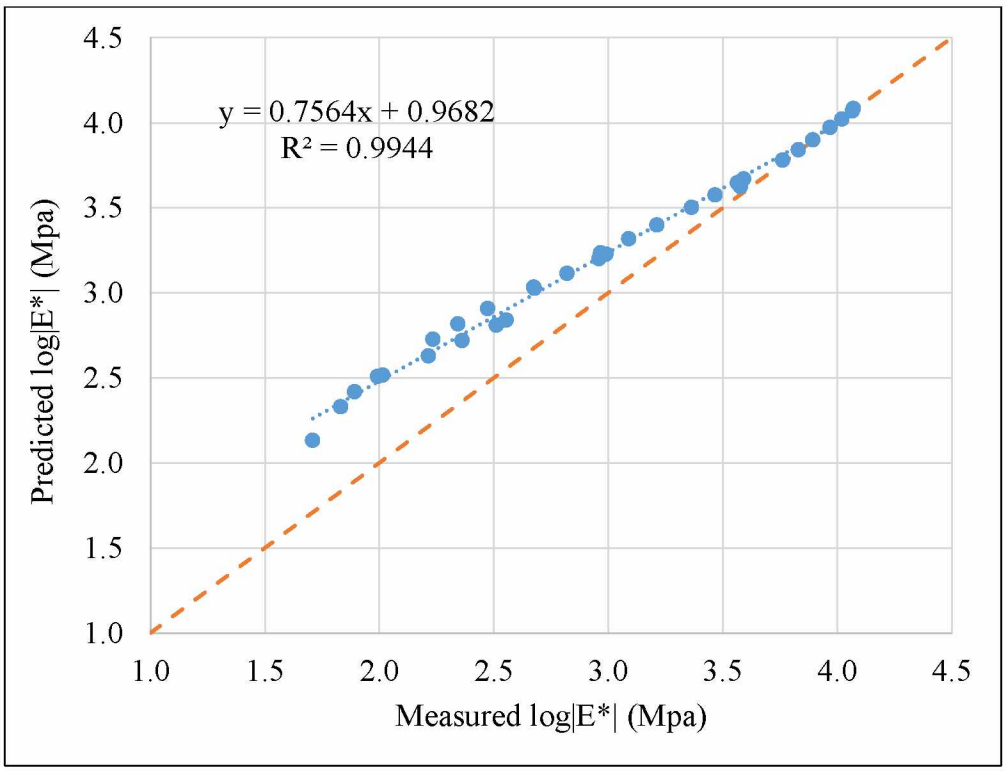

Appendix D.9 Predicted vs. Measured Mix #4 (original Witczak model, Level 3)

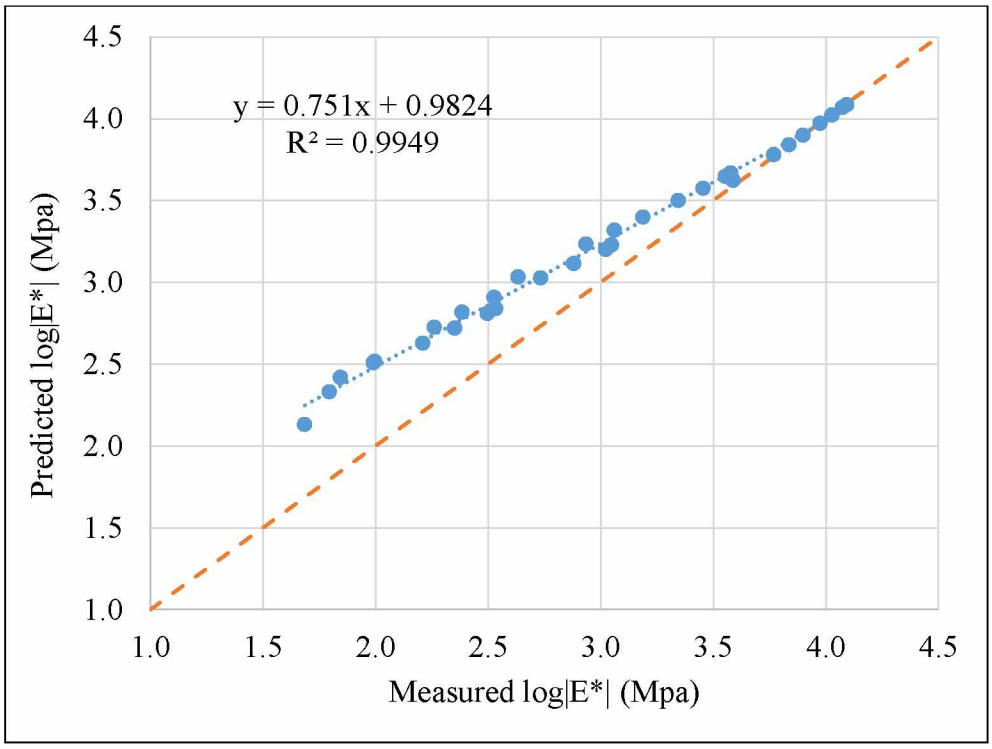

Appendix D.10 Predicted vs. Measured Mix #5 (original Witczak model, Level 3)

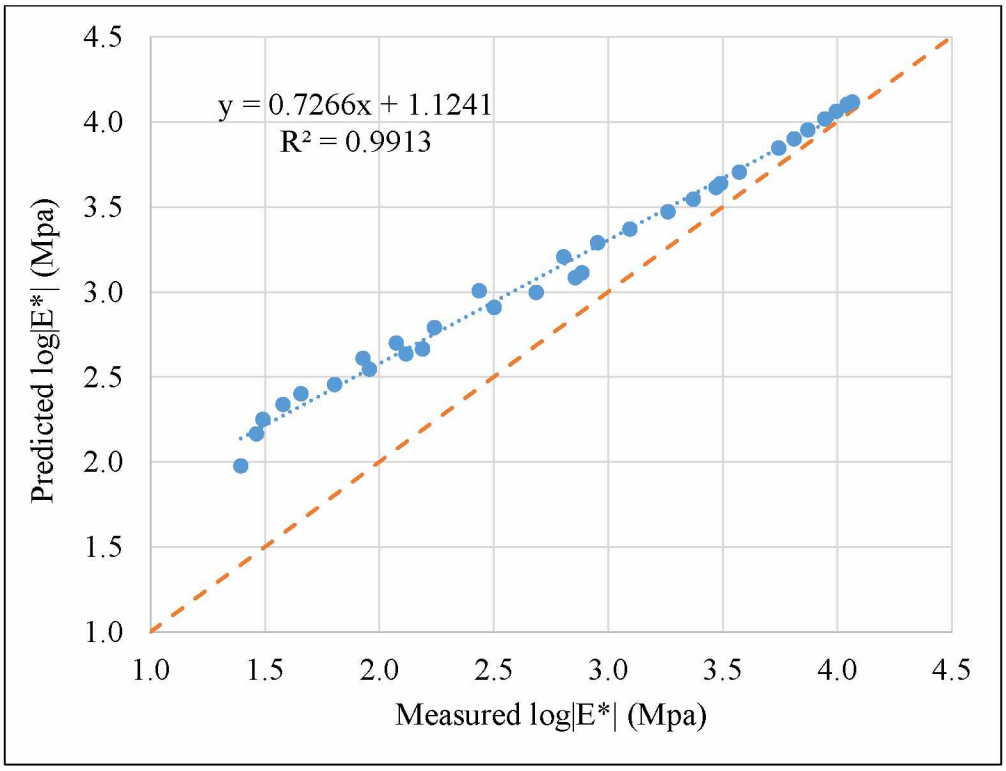

Appendix D.11 Predicted vs. Measured Mix #7 (original Witczak model, Level 3)

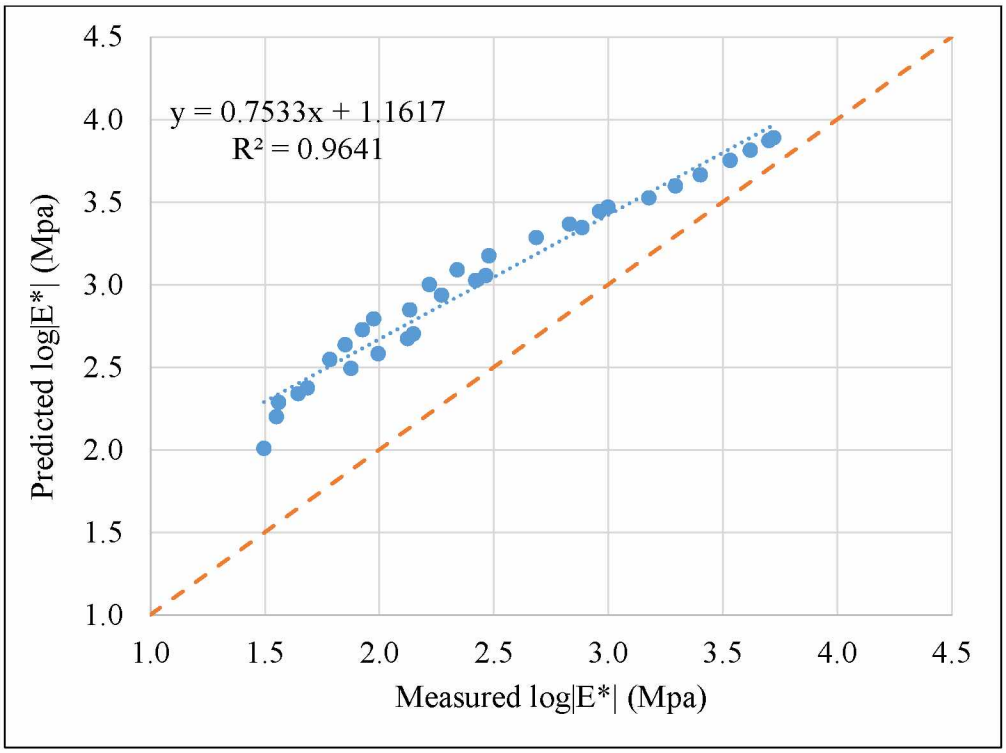

Appendix D.12 Predicted vs. Measured Mix #8 (original Witczak model, Level 3)

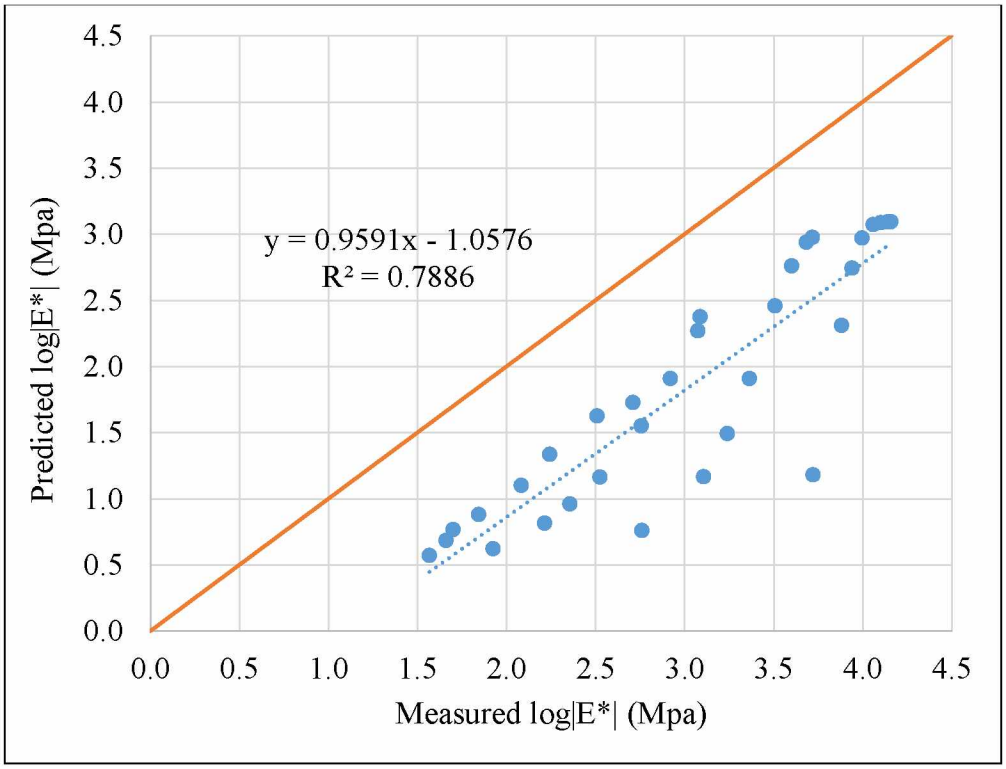

Appendix D.13 Predicted vs. Measured Mix #1 (modified Witczak model, Level 2)

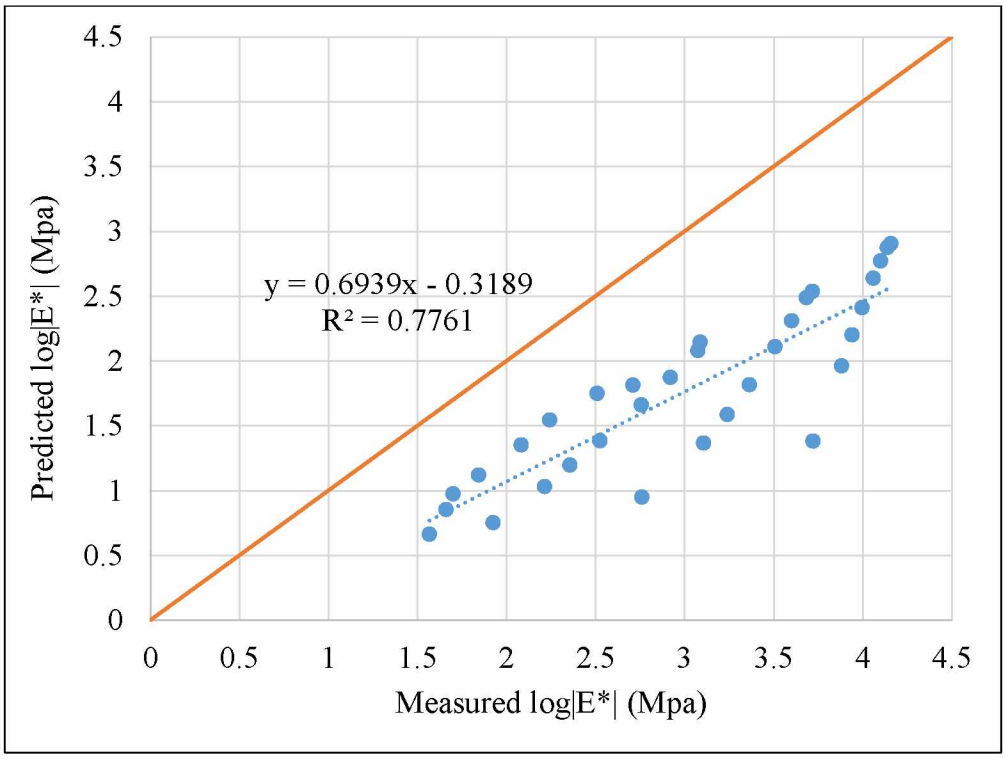

Appendix D.14 Predicted vs. Measured Mix #3 (modified Witczak model, Level 2)

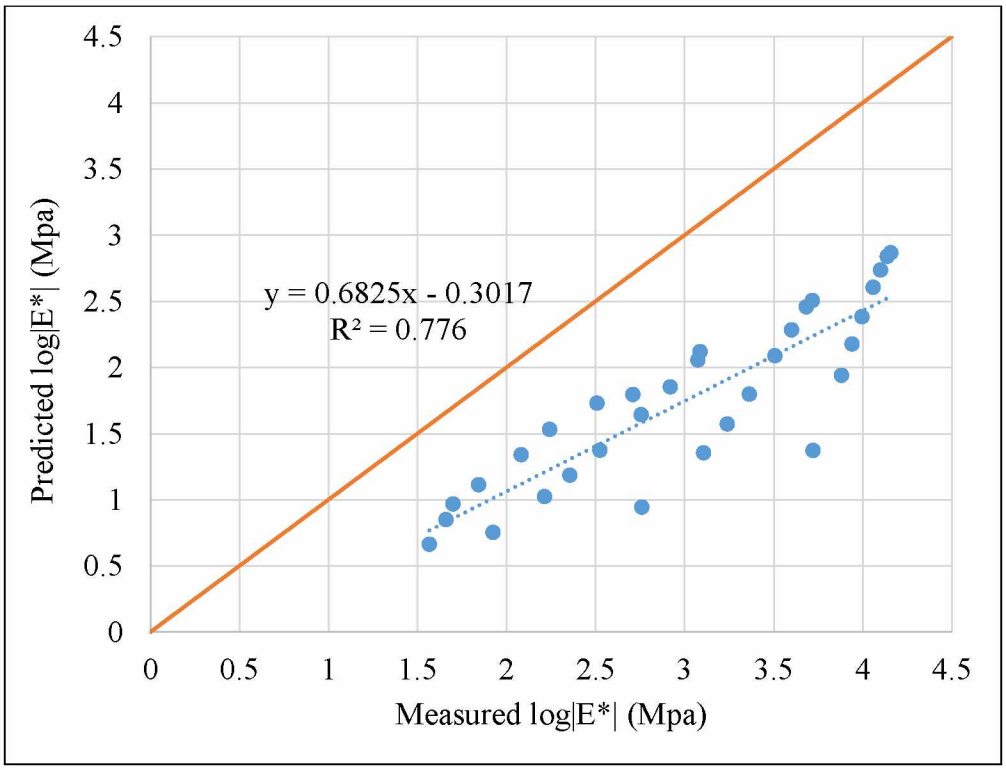

Appendix D.15 Predicted vs. Measured Mix #4 (modified Witczak model, Level 2)

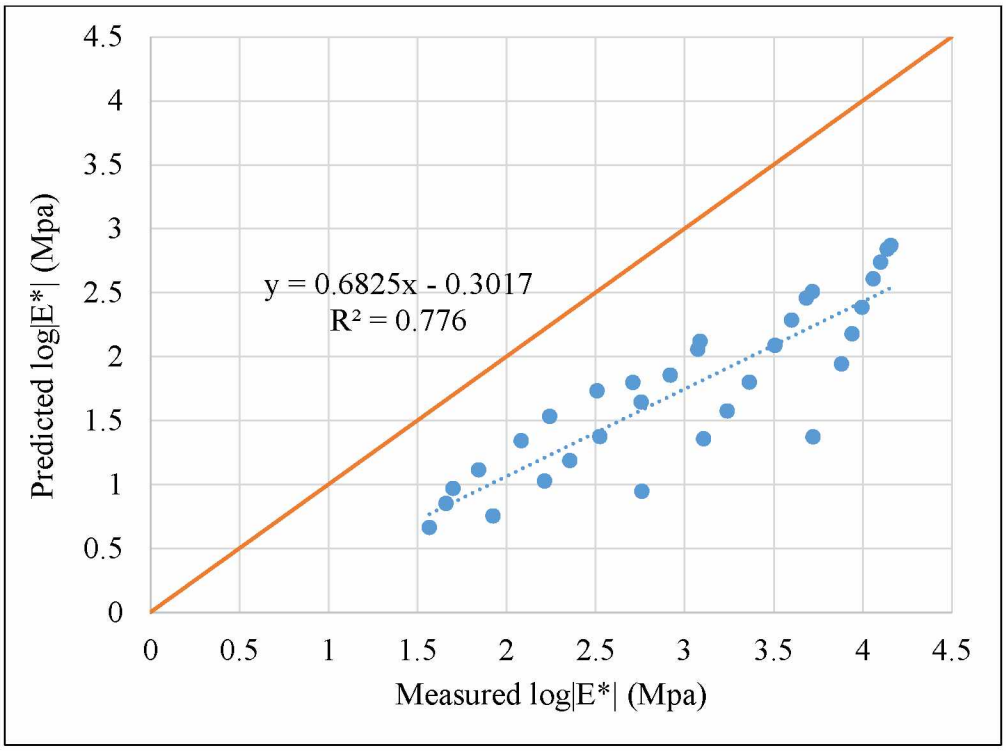

Appendix D.16 Predicted vs. Measured Mix #5 (modified Witczak model, Level 2)

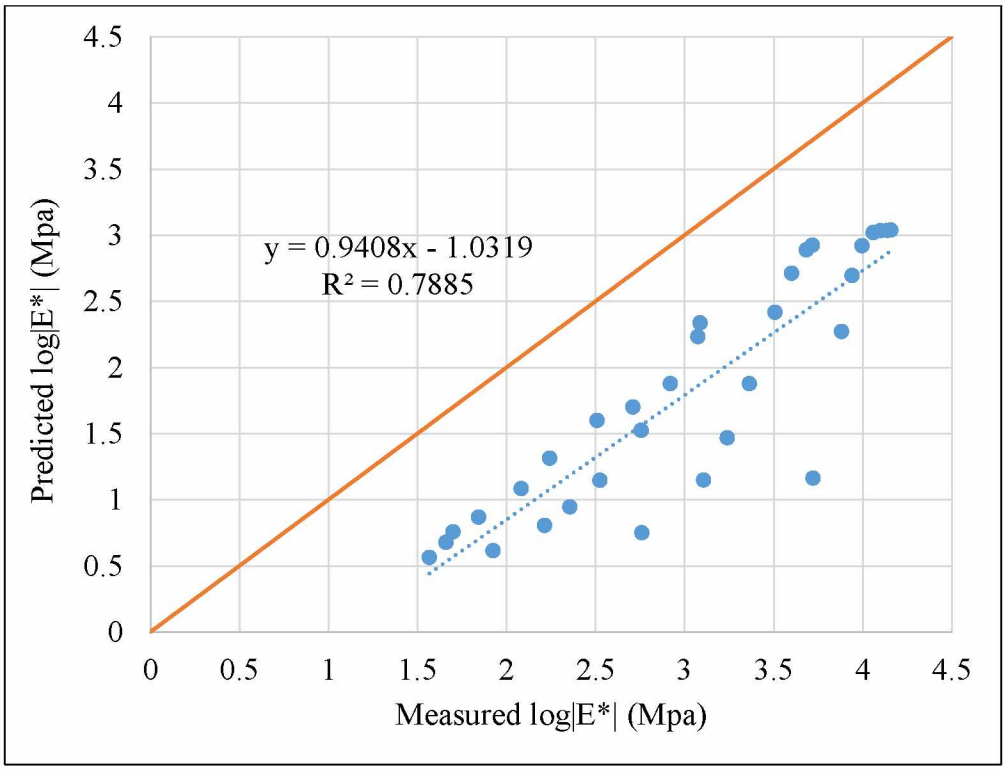

Appendix D.17 Predicted vs. Measured Mix #7 (modified Witczak model, Level 2)

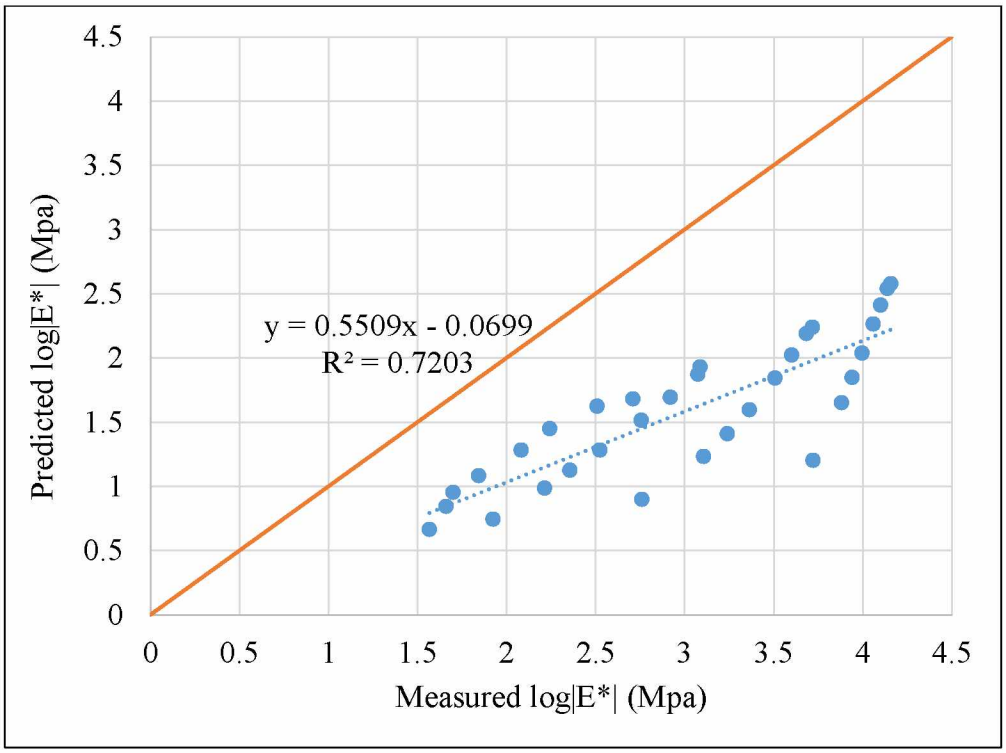

Appendix D.18 Predicted vs. Measured Mix #8 (modified Witczak model, Level 2)

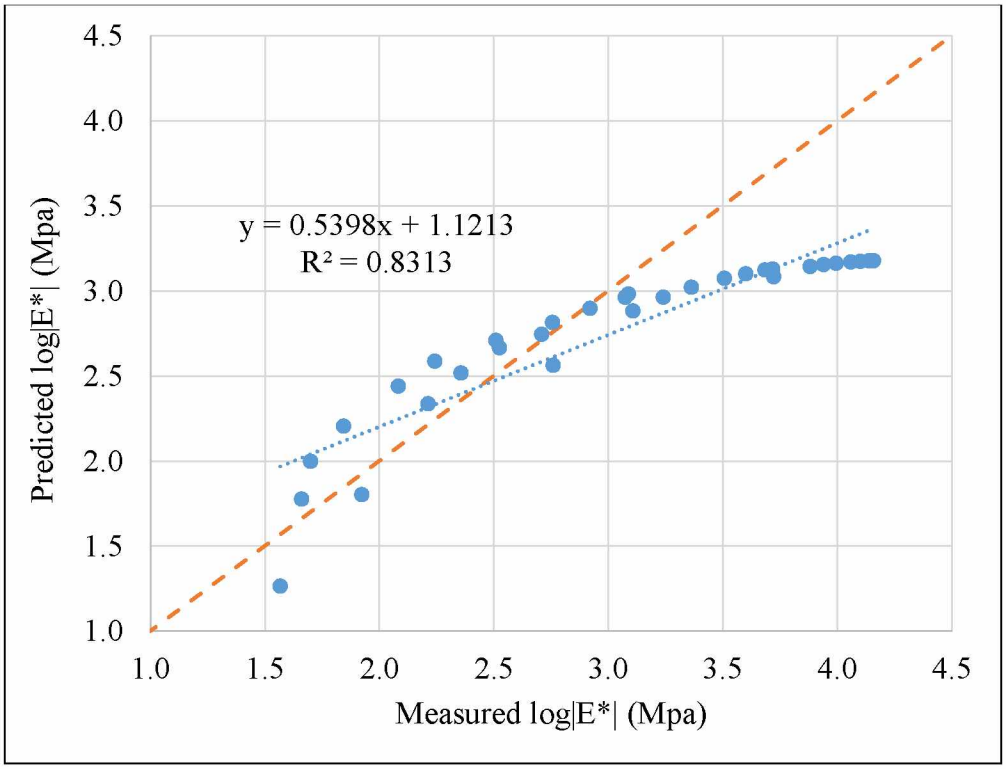

Appendix D.19 Predicted vs. Measured Mix #1 (modified Witczak model, Level 3)

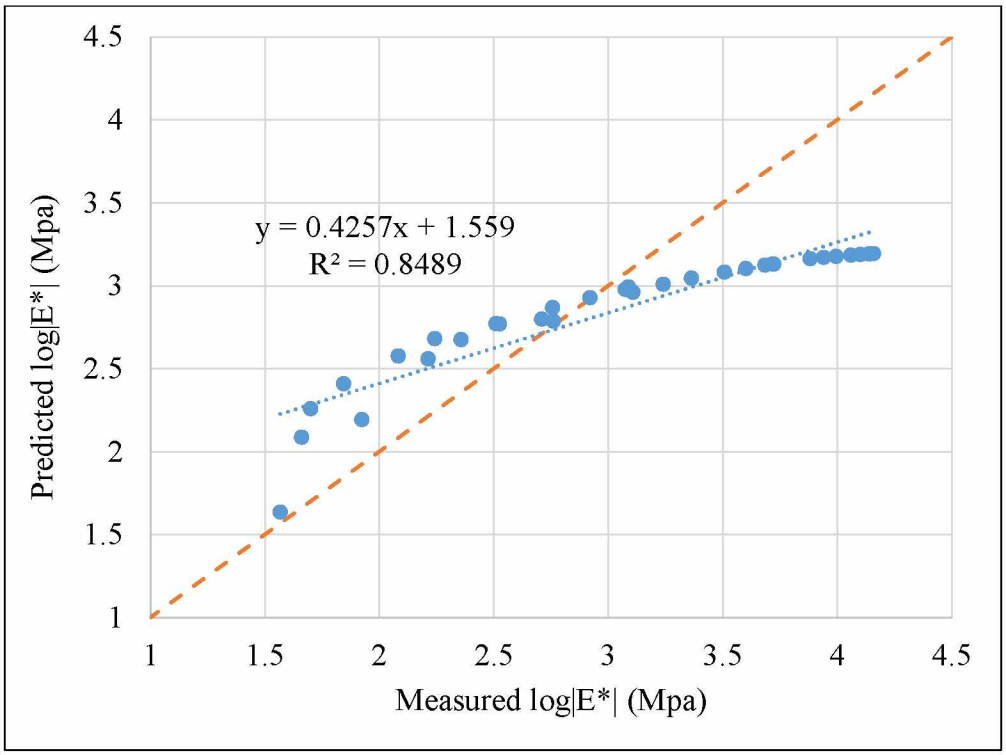

Appendix D.20 Predicted vs. Measured Mix #3 (modified Witczak model, Level 3)

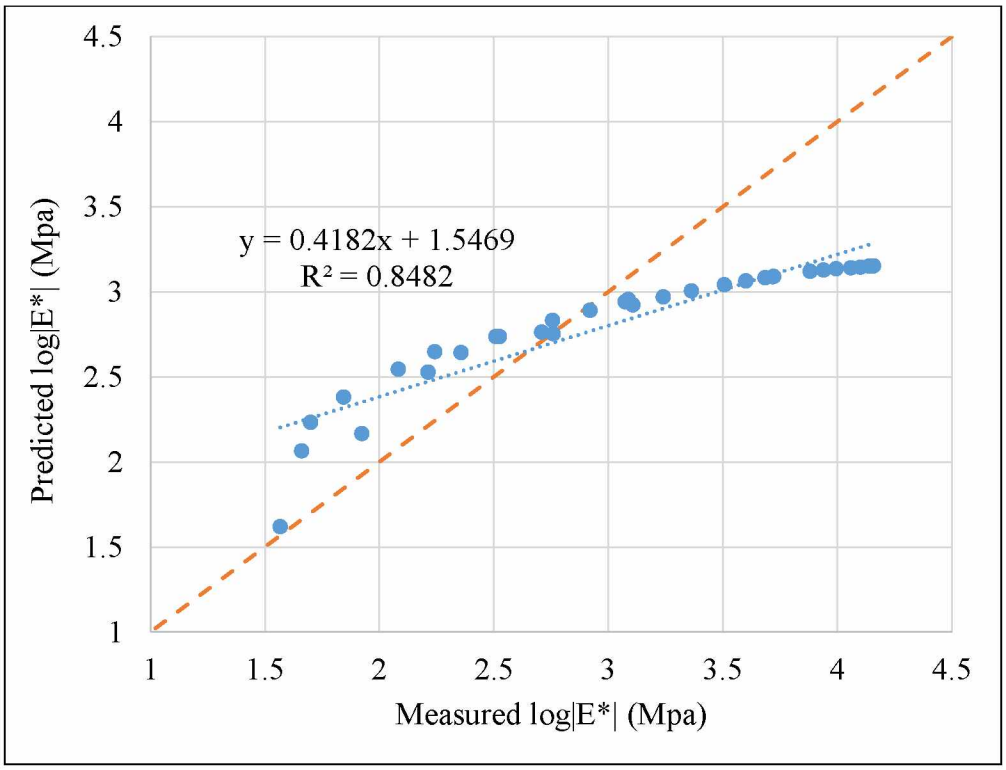

Appendix D.21 Predicted vs. Measured Mix #4 (modified Witczak model, Level 3)

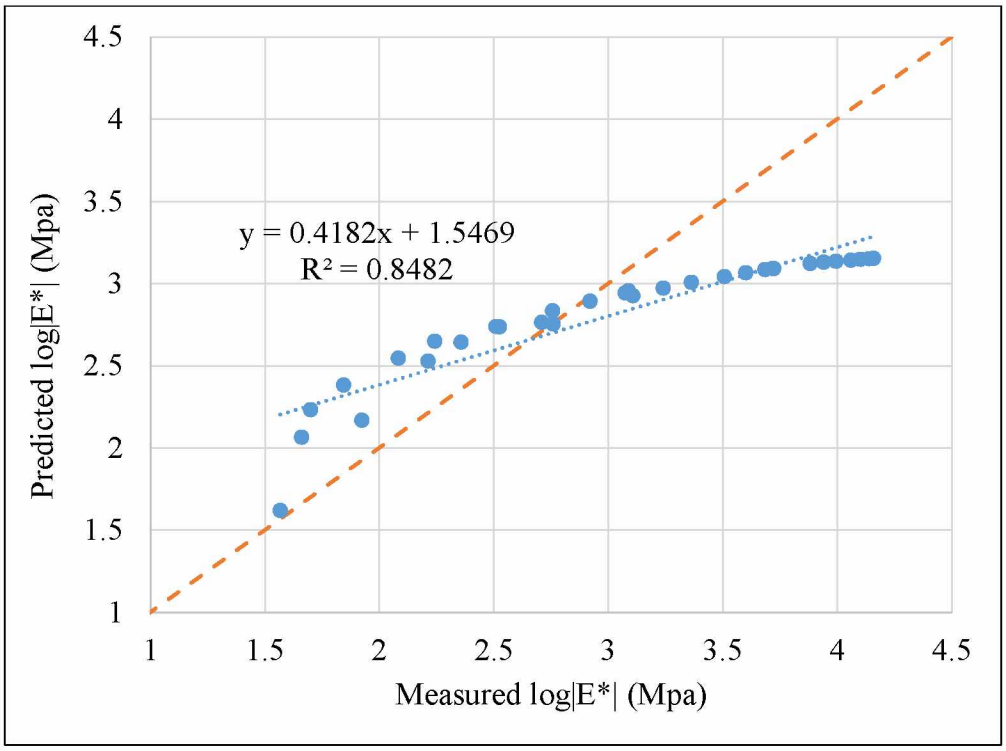

Appendix D.22 Predicted vs. Measured Mix #5 (modified Witczak model, Level 3)

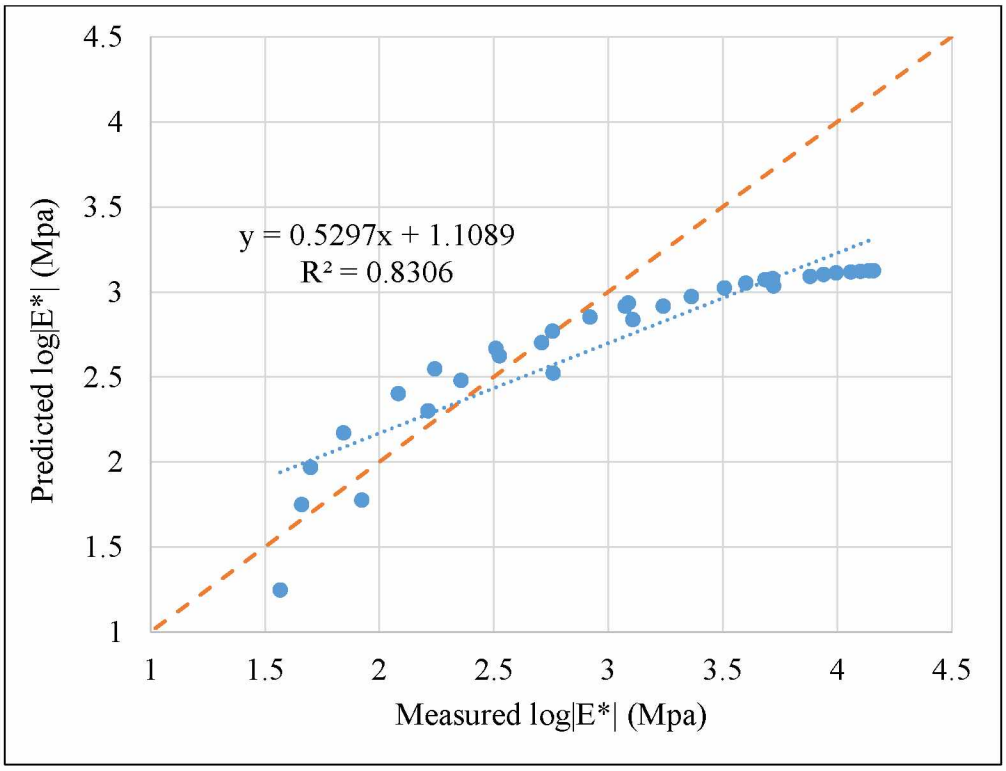

Appendix D.23 Predicted vs. Measured Mix #7 (modified Witczak model, Level 3)

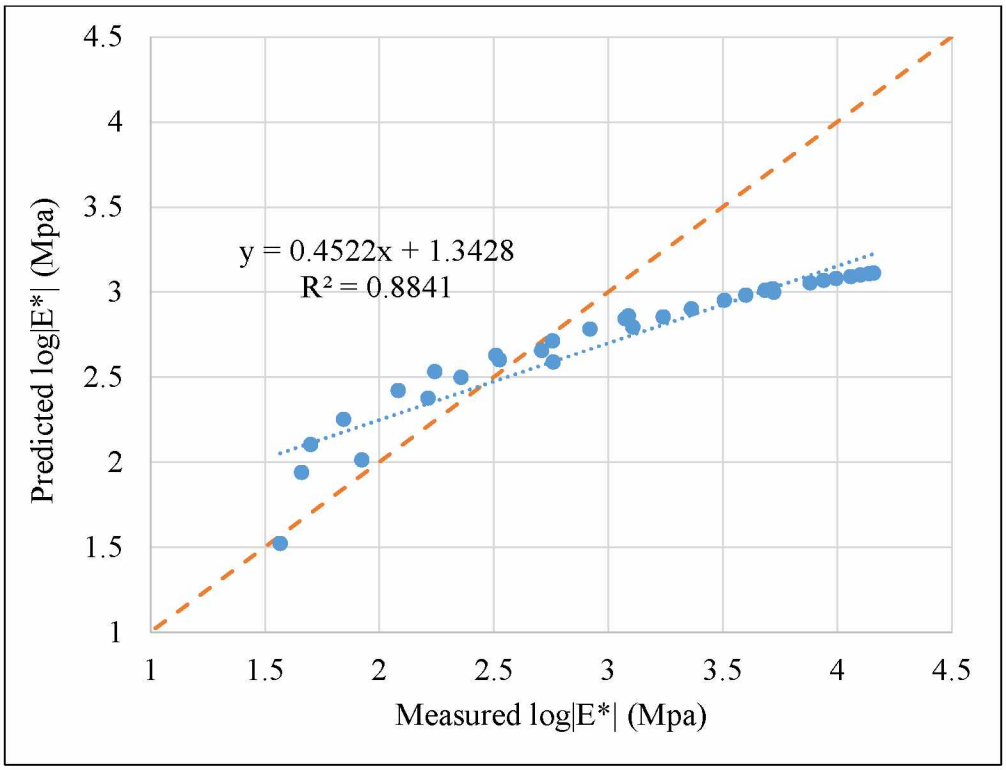

Appendix D.24 Predicted vs. Measured Mix #8 (modified Witczak model, Level 3)

APPENDIX E MIXTURE |E*| AMPT RESULTS

Appendix E.1 Dynamic modulus test results for mix #1

Dynamic Modulus, kPa							
Mix #1 Type II-B 0% RAP PG 52-28							
Temp. C	**Freq Hz**	**Sample 1**	**Sample 2**	**Sample 3**	**COV**	**sr %**	**Range %**
4	25	14969	13075	15200	8.1%	4.3%	14.7%
4	20	13830	13262	14238	3.6%	4.4%	7.1%
4	10	12590	12305	13028	2.9%	4.5%	5.7%
4	5	11369	11370	11726	1.8%	4.6%	3.1%
4	2	9812	9751	10151	2.2%	4.7%	4.0%
4	1	8660	8602	8921	1.9%	4.8%	3.7%
4	0.5	7573	7495	7779	1.9%	5.0%	3.7%
4	0.2	6208	6128	6367	2.0%	5.2%	3.8%
4	0.1	5269	5178	5378	1.9%	5.4%	3.8%
21	25	5322	5105	5250	2.1%	5.4%	4.2%
21	20	5078	4468	4966	6.7%	5.5%	12.6%
21	10	4161	3711	4100	6.1%	5.7%	11.3%
21	5	3320	3013	3313	5.5%	6.0%	9.5%
21	2	2380	2162	2394	5.6%	6.5%	10.0%
21	1	1795	1618	1807	6.1%	6.9%	10.9%
21	0.5	1328	1179	1338	6.9%	7.4%	12.4%
21	0.2	861.6	745	867.4	8.4%	8.1%	14.8%
21	0.1	605.4	512.8	609.4	9.5%	8.8%	16.8%
37	25	1247	1159	1270	4.8%	7.4%	9.1%
37	20	1210	1089	1258	7.3%	7.5%	14.3%
37	10	856.6	755.9	884.5	8.1%	8.1%	15.5%
37	5	587.6	514.3	611.1	8.8%	8.8%	17.0%
37	2	340.1	302.4	361.9	9.0%	9.9%	17.8%
37	1	227.3	209.3	245.4	7.9%	10.8%	15.9%
37	0.5	159.8	152.3	178	8.1%	11.6%	15.7%
37	0.2	104	104	120.6	8.7%	12.7%	15.2%
37	0.1	78	81.3	92.4	9.0%	13.4%	17.2%
54	25	553	413.3	570	16.8%	9.0%	30.6%
54	20	292.6	379.2	297.9	15.0%	10.0%	26.8%
54	10	170.1	151.5	203.6	15.1%	11.4%	29.8%
54	5	118.4	107.3	138	12.8%	12.4%	25.3%
54	2	66.4	64.9	78.5	10.7%	14.0%	19.4%
54	1	47.7	47.8	54.9	8.2%	15.0%	14.4%
54	0.5	42.9	44.7	49.9	7.9%	15.3%	15.3%
54	0.2	36.5	38.6	42.7	8.0%	15.9%	15.8%
54	0.1	35.1	36	39.7	6.6%	16.1%	12.5%

Appendix E.2 Dynamic modulus test results for mix #2

Dynamic Modulus, kPa							
Mix #2 Type II-B 0% RAP PG 58-34							
Temp. C	**Freq Hz**	**Sample 1**	**Sample 2**	**Sample 3**	**COV**	**sr %**	**Range %**
4	25	9596	9440	8564	6.0%	4.8%	11.2%
4	20	8522	9146	8122	6.0%	4.9%	11.9%
4	10	7410	7987	7006	6.6%	5.0%	13.1%
4	5	6377	6869	5957	7.1%	5.2%	14.2%
4	2	5131	5498	4702	7.8%	5.4%	15.6%
4	1	4277	4554	3843	8.5%	5.7%	16.8%
4	0.5	3509	3710	3092	9.2%	5.9%	18.0%
4	0.2	2627	2743	2250	10.1%	6.3%	19.4%
4	0.1	2084	2146	1742	10.9%	6.7%	20.3%
21	25	1908	2408	2061	12.1%	6.6%	23.5%
21	20	1794	2271	1940	12.2%	6.7%	23.8%
21	10	1337	1715	1445	13.0%	7.1%	25.2%
21	5	984.5	1272	1058	13.5%	7.6%	26.0%
21	2	644.7	835.3	683	14.0%	8.4%	26.4%
21	1	472.6	611.3	496.8	14.1%	9.0%	26.3%
21	0.5	360.6	459.4	372.2	13.6%	9.5%	24.9%
21	0.2	257.9	320.8	261.1	12.7%	10.3%	22.5%
21	0.1	204.9	253.2	206.3	12.4%	10.8%	21.8%
37	25	659.2	630.7	539.7	10.2%	8.7%	19.6%
37	20	606.7	600.3	497.1	10.8%	8.8%	19.3%
37	10	431.9	436.3	355.3	11.2%	9.5%	19.9%
37	5	308.5	315.6	254.8	11.3%	10.2%	20.8%
37	2	192.5	196.7	158.8	11.4%	11.3%	20.7%
37	1	148	150.1	123.6	10.5%	12.0%	18.9%
37	0.5	120.8	122.2	101.8	9.9%	12.5%	17.7%
37	0.2	93.9	94.2	80.8	8.5%	13.2%	14.9%
37	0.1	79.4	78.9	69.9	7.0%	13.7%	12.5%
54	25	303.7	276.4	230.5	13.7%	10.4%	27.1%
54	20	263.9	248.3	211.2	11.2%	10.6%	21.9%
54	10	192.1	182.1	159.9	9.3%	11.4%	18.1%
54	5	137.7	133.6	119.6	7.3%	12.2%	13.9%
54	2	84.2	82.5	76.1	5.3%	13.5%	10.0%
54	1	66.9	67.6	65.7	1.4%	14.1%	2.8%
54	0.5	60	60.1	59.5	0.5%	14.5%	1.0%
54	0.2	51	51.3	51.4	0.4%	15.0%	0.8%
54	0.1	46	46.4	46.4	0.5%	15.3%	0.9%

Appendix E.3 Dynamic modulus test results for mix #3

Dynamic Modulus, kPa							
Mix #3 Type II-A 0% RAP PG 58-34							
Temp. C	**Freq Hz**	**Sample 1**	**Sample 2**	**Sample 3**	**COV**	**sr %**	**Range %**
4	25	12837	12573	11552	5.5%	4.5%	10.4%
4	20	12954	11538	11051	8.3%	4.5%	16.1%
4	10	11720	10242	9849	9.3%	4.6%	17.6%
4	5	10477	9024	8679	10.2%	4.8%	19.1%
4	2	8842	7507	7221	11.0%	5.0%	20.6%
4	1	7665	6444	6187	11.7%	5.1%	21.8%
4	0.5	6543	5454	5225	12.3%	5.3%	23.0%
4	0.2	5169	4285	4076	12.9%	5.6%	24.2%
4	0.1	4236	3511	3318	13.1%	5.8%	24.9%
21	25	3539	2971	2951	10.6%	6.1%	18.6%
21	20	3595	2876	2698	15.5%	6.1%	29.3%
21	10	2781	2229	2075	15.7%	6.4%	29.9%
21	5	2089	1675	1567	15.5%	6.9%	29.4%
21	2	1374	1107	1043	14.9%	7.5%	28.2%
21	1	978.9	802.9	755.2	13.9%	8.1%	26.5%
21	0.5	703.8	590.3	556.2	12.5%	8.7%	23.9%
21	0.2	450.3	400.6	369.6	10.0%	9.5%	19.8%
21	0.1	321.7	308.9	277.7	7.5%	10.1%	14.5%
37	25	1078	879.3	886.9	11.9%	7.9%	21.0%
37	20	1029	752.8	837.1	16.2%	8.0%	31.6%
37	10	711.8	523	588.2	15.8%	8.7%	31.1%
37	5	485	361.7	410.4	14.8%	9.4%	29.4%
37	2	284.9	219.5	245.7	13.2%	10.6%	26.2%
37	1	199.1	160.2	180.3	10.8%	11.4%	21.6%
37	0.5	148.4	124.3	140.3	8.9%	12.0%	17.5%
37	0.2	105.6	92.3	103.9	7.2%	12.9%	13.2%
37	0.1	86	76.3	85.8	6.7%	13.5%	11.7%
54	25	371.3	295.5	276.6	15.9%	10.0%	30.1%
54	20	364.7	255.4	244.3	23.1%	10.2%	41.8%
54	10	250.3	179.7	174.9	20.9%	11.1%	37.4%
54	5	168.6	127.7	126.2	17.1%	12.0%	30.1%
54	2	94.3	75.6	76	13.0%	13.5%	22.8%
54	1	67.8	60.4	62.9	5.9%	14.3%	11.6%
54	0.5	62.2	54	57.6	7.1%	14.6%	14.2%
54	0.2	59.3	46.1	50.4	13.0%	14.9%	25.4%
54	0.1	63.7	40.7	46.3	23.9%	15.0%	45.8%

Appendix E.4 Dynamic modulus test results for mix #4

Dynamic Modulus, kPa							
Mix #4 Type II-A 25% RAP PG 58-34							
Temp. C	**Freq Hz**	**Sample 1**	**Sample 2**	**Sample 3**	**COV**	**sr %**	**Range %**
4	25	11226	12060	12041	4.0%	4.5%	7.1%
4	20	10916	12214	11859	5.8%	4.2%	11.1%
4	10	9785	11032	10592	6.0%	4.3%	11.9%
4	5	8681	9848	9362	6.3%	4.4%	12.6%
4	2	7323	8332	7825	6.4%	4.6%	12.9%
4	1	6334	7237	6742	6.7%	4.8%	13.3%
4	0.5	5422	6206	5733	6.8%	5.0%	13.5%
4	0.2	4323	4939	4525	6.8%	5.3%	13.4%
4	0.1	3585	4051	3717	6.3%	5.5%	12.3%
21	25	4182	4443	3080	18.5%	5.5%	34.9%
21	20	3813	4217	2972	17.3%	5.5%	33.9%
21	10	3071	3405	2322	18.9%	5.8%	36.9%
21	5	2434	2704	1783	20.5%	6.2%	39.9%
21	2	1733	1940	1217	22.8%	6.7%	44.4%
21	1	1312	1476	902.8	24.0%	7.2%	46.6%
21	0.5	986.5	1119	676.5	24.5%	7.7%	47.7%
21	0.2	664.6	766.6	464.6	24.3%	8.4%	47.8%
21	0.1	486.5	572	359.8	22.6%	9.0%	44.9%
37	25	1057	993.2	885.2	8.9%	7.6%	17.6%
37	20	1000	921.4	816.5	10.1%	7.7%	20.1%
37	10	729.7	675.4	577.1	11.7%	8.3%	23.1%
37	5	527.7	490.1	407.1	13.0%	9.0%	25.4%
37	2	330.6	311.7	250.3	14.1%	10.1%	27.0%
37	1	244.7	232.7	182.8	14.9%	10.8%	28.1%
37	0.5	188	181.8	144	13.9%	11.5%	25.7%
37	0.2	135.8	134.8	107.2	12.9%	12.3%	22.7%
37	0.1	109.7	112.1	88.7	12.4%	12.9%	22.6%
54	25	393.6	375.5	304.3	13.2%	9.6%	25.0%
54	20	347.4	335.8	289.5	9.4%	9.9%	17.9%
54	10	247.5	238	204.8	9.7%	10.7%	18.6%
54	5	175.1	169.1	147.3	8.9%	11.6%	17.0%
54	2	101.9	103.7	89	8.2%	13.1%	15.0%
54	1	71.5	84.8	77.2	8.6%	13.8%	17.1%
54	0.5	62.7	73.3	67.7	7.8%	14.3%	15.6%
54	0.2	51.8	61.2	57.1	8.3%	14.9%	16.6%
54	0.1	45.7	56	51.9	10.1%	15.3%	20.1%

Appendix E.5 Dynamic modulus test results for mix #5

Dynamic Modulus, kPa							
Mix #5 Type II-B 25% RAP PG 58-34							
Temp. C	**Freq Hz**	**Sample 1**	**Sample 2**	**Sample 3**	**COV**	**sr %**	**Range %**
4	25	12904	12011	12258	3.7%	4.5%	7.2%
4	20	12556	11341	11730	5.2%	4.5%	10.2%
4	10	11305	10087	10513	5.8%	4.6%	11.5%
4	5	10088	8899	9335	6.4%	4.8%	12.6%
4	2	8528	7402	7879	7.1%	4.9%	14.2%
4	1	7402	6354	6828	7.6%	5.1%	15.3%
4	0.5	6358	5376	5859	8.4%	5.3%	16.7%
4	0.2	5092	4226	4711	9.3%	5.6%	18.5%
4	0.1	4231	3461	3925	10.0%	5.8%	19.9%
21	25	4102	3891	3375	9.9%	5.8%	19.2%
21	20	3877	3626	3250	8.8%	5.9%	17.5%
21	10	3107	2863	2567	9.5%	6.2%	19.0%
21	5	2447	2221	1971	10.8%	6.5%	21.5%
21	2	1726	1536	1361	11.8%	7.1%	23.7%
21	1	1304	1140	1012	12.7%	7.6%	25.3%
21	0.5	983.2	840	754	13.5%	8.1%	26.7%
21	0.2	666.6	552.9	511	14.0%	8.8%	27.0%
21	0.1	497.2	401.4	389.1	13.8%	9.4%	25.2%
37	25	1351	962.5	1036	18.5%	7.6%	34.8%
37	20	1271	909.9	975.6	18.3%	7.7%	34.3%
37	10	926.5	647.2	702.6	19.5%	8.3%	36.8%
37	5	671.3	449.5	506.6	21.2%	8.9%	40.9%
37	2	425.6	264.5	319.7	24.3%	9.9%	47.9%
37	1	309	182.7	235.5	26.2%	10.6%	52.1%
37	0.5	232.2	133	181.5	27.2%	11.3%	54.4%
37	0.2	162.2	89.9	131.7	28.4%	12.2%	56.5%
37	0.1	123.9	68.6	105.5	28.4%	12.9%	55.7%
54	25	352.9	337.9	333.7	3.0%	9.9%	5.6%
54	20	382.7	254.4	306	20.5%	10.0%	40.8%
54	10	266.8	186.7	220.6	17.9%	10.8%	35.6%
54	5	192.2	132.2	161.6	18.5%	11.6%	37.0%
54	2	115.8	77.9	100.3	19.4%	13.0%	38.7%
54	1	73.5	50.6	85.5	25.4%	14.0%	50.0%
54	0.5	67.3	44.6	75.1	25.4%	14.3%	48.9%
54	0.2	57.9	38.3	63.8	25.0%	14.8%	47.8%
54	0.1	51.5	36	58.1	23.4%	15.1%	45.5%

Appendix E.6 Dynamic modulus test results for mix #6

Dynamic Modulus, kPa							
Mix #6 Type II-B 35% RAP PG 52-28							
Temp. C	**Freq Hz**	**Sample 1**	**Sample 2**	**Sample 3**	**COV**	**sr %**	**Range %**
4	25	15843	13272	14151	9.1%	4.3%	17.8%
4	20	14553	12998	13494	5.8%	4.4%	11.4%
4	10	13193	11770	12209	5.9%	4.5%	11.5%
4	5	11879	10625	10859	6.0%	4.6%	11.3%
4	2	10169	9148	9156	6.2%	4.8%	10.8%
4	1	8932	8062	7915	6.6%	4.9%	12.2%
4	0.5	7751	7013	6744	7.3%	5.1%	14.0%
4	0.2	6314	5731	5346	8.4%	5.3%	16.7%
4	0.1	5328	4875	4409	9.4%	5.5%	18.9%
21	25	5041	4125	3876	14.1%	5.6%	26.8%
21	20	4917	3861	3533	17.6%	5.7%	33.7%
21	10	4027	3086	2787	19.6%	6.0%	37.6%
21	5	3225	2402	2160	21.5%	6.3%	41.0%
21	2	2314	1652	1478	24.3%	6.8%	46.1%
21	1	1741	1204	1080	26.2%	7.3%	49.3%
21	0.5	1288	866.1	798.1	27.0%	7.8%	49.8%
21	0.2	836.6	554.6	531.7	26.5%	8.6%	47.6%
21	0.1	592.8	397.3	398.2	24.3%	9.2%	42.2%
37	25	1291	928.6	1289	17.8%	7.5%	31.0%
37	20	1229	870.5	1175	17.7%	7.6%	32.8%
37	10	866.7	589.7	827.9	19.7%	8.3%	36.4%
37	5	596.2	388.6	574.9	22.0%	9.0%	39.9%
37	2	348.8	214.7	347.8	25.4%	10.1%	44.1%
37	1	231	139.3	245.7	28.1%	11.0%	51.8%
37	0.5	163.8	100.2	186.1	29.7%	11.8%	57.3%
37	0.2	108.9	65.5	132.7	33.3%	12.8%	65.6%
37	0.1	82	47.3	104.4	36.9%	13.6%	73.3%
54	25	398.8	321.6	350.8	10.9%	9.8%	21.6%
54	20	349	282.3	312.4	10.6%	10.0%	21.2%
54	10	230.5	183.6	212.6	11.3%	11.0%	22.5%
54	5	152.1	120.4	147.7	12.3%	12.0%	22.6%
54	2	87.4	66.5	88.9	15.5%	13.5%	27.7%
54	1	64.9	47.6	67.2	17.9%	14.5%	32.7%
54	0.5	56.2	39.4	58.9	20.5%	14.9%	37.9%
54	0.2	45.9	30.3	49	24.0%	15.6%	44.8%
54	0.1	41.2	28.1	43.5	22.1%	16.0%	41.0%

Appendix E.7 Dynamic modulus test results for mix #7

Dynamic Modulus, kPa							
Mix #7 Type II-B 0% RAP PG 52-28							
Temp. C	**Freq Hz**	**Sample 1**	**Sample 2**	**Sample 3**	**COV**	**sr %**	**Range %**
4	25	11434	12050	11533	2.8%	4.5%	5.3%
4	20	10968	11507	10778	3.4%	4.6%	6.6%
4	10	9770	10373	9635	4.0%	4.7%	7.4%
4	5	8669	9282	8579	4.3%	4.8%	7.9%
4	2	7248	7873	7271	4.7%	5.0%	8.4%
4	1	6248	6863	6338	5.1%	5.2%	9.5%
4	0.5	5281	5932	5458	6.1%	5.3%	11.7%
4	0.2	4169	4802	4430	7.1%	5.6%	14.2%
4	0.1	3436	4047	3732	8.2%	5.8%	16.3%
21	25	2837	3357	3095	8.4%	6.1%	16.8%
21	20	2726	3228	2911	8.6%	6.1%	17.0%
21	10	2139	2599	2325	9.8%	6.5%	19.5%
21	5	1622	2035	1824	11.3%	6.8%	22.6%
21	2	1066	1398	1267	13.4%	7.4%	26.7%
21	1	749.2	1016	935.6	15.2%	8.0%	29.6%
21	0.5	519.2	724.3	674.9	16.7%	8.6%	32.1%
21	0.2	315.5	448.8	423.9	17.9%	9.5%	33.7%
21	0.1	217.4	308.9	293.5	17.9%	10.4%	33.5%
37	25	675	927.3	701	18.1%	8.3%	32.9%
37	20	629.1	872.3	653.8	18.6%	8.4%	33.9%
37	10	414.4	596.6	442.4	20.3%	9.1%	37.6%
37	5	269.6	394.2	291.5	20.9%	10.0%	39.1%
37	2	147.8	216.4	158.6	21.2%	11.4%	39.4%
37	1	104.6	143.8	107.7	18.4%	12.4%	33.0%
37	0.5	77.9	100.7	76.5	16.0%	13.4%	28.5%
37	0.2	56.4	66.2	51.4	13.0%	14.6%	25.5%
37	0.1	46.3	50.3	40.1	11.3%	15.3%	22.4%
54	25	166.6	175.9	121.6	18.8%	11.7%	35.1%
54	20	138.5	156	98.5	22.5%	12.2%	43.9%
54	10	97.4	102.2	72	17.9%	13.2%	33.4%
54	5	68.8	69.7	53	14.7%	14.3%	26.2%
54	2	39.8	41.6	32.7	12.4%	16.0%	23.4%
54	1	37	30.5	25.7	18.3%	16.7%	36.4%
54	0.5	34.5	28.2	24.7	17.0%	16.9%	33.6%
54	0.2	30.9	24.8	22.7	16.3%	17.3%	31.4%
54	0.1	29.8	22.9	21.8	17.5%	17.5%	32.2%

Appendix E.8 Dynamic modulus test results for mix #8

Dynamic Modulus, kPa							
Mix #8 Type II-B 0% RAP PG 52-40							
Temp. C	**Freq Hz**	**Sample 1**	**Sample 2**	**Sample 3**	**COV**	**sr %**	**Range %**
4	25	5064	5058	5734	7.4%	5.1%	12.8%
4	20	4962	4852	5290	4.5%	5.1%	8.7%
4	10	4112	4023	4410	4.8%	5.4%	9.3%
4	5	3330	3276	3625	5.5%	5.6%	10.2%
4	2	2429	2417	2728	7.0%	6.1%	12.3%
4	1	1858	1876	2157	8.5%	6.4%	15.2%
4	0.5	1401	1433	1684	10.3%	6.8%	18.8%
4	0.2	939.7	973.7	1181	12.7%	7.5%	23.4%
4	0.1	693.4	719.5	894.5	14.2%	8.0%	26.1%
21	25	868.3	1012	1110	12.2%	7.5%	24.2%
21	20	821.7	881.8	1049	12.8%	7.7%	24.8%
21	10	597.1	669.5	766.5	12.5%	8.3%	25.0%
21	5	427.6	470.4	556.5	13.5%	9.0%	26.6%
21	2	265.4	284.8	352.7	15.2%	10.0%	29.0%
21	1	197.4	203.1	257.2	15.1%	10.8%	27.3%
21	0.5	152.1	150.4	194.4	15.0%	11.6%	26.6%
21	0.2	111.2	104.5	138.1	15.1%	12.5%	28.5%
21	0.1	91.1	83	109.9	14.6%	13.2%	28.4%
37	25	284.4	266.6	323.7	10.0%	10.1%	19.6%
37	20	258.5	241.8	291.9	9.7%	10.3%	19.0%
37	10	185.4	167.9	207	10.5%	11.2%	20.9%
37	5	134.5	123.7	149.7	9.6%	12.1%	19.1%
37	2	82.6	76.8	94	10.4%	13.6%	20.4%
37	1	70.6	65.8	76.7	7.7%	14.1%	15.3%
37	0.5	61	56.8	64.6	6.4%	14.7%	12.8%
37	0.2	50.6	47.5	52	4.6%	15.4%	9.0%
37	0.1	44.9	42.8	45	2.8%	15.8%	5.0%
54	25	156.1	129.1	138.1	9.7%	12.0%	19.1%
54	20	153.6	120.8	125.1	13.4%	12.2%	24.6%
54	10	107.5	91.7	97.2	8.1%	13.1%	16.0%
54	5	80.2	69.6	76.1	7.1%	13.9%	14.1%
54	2	50.1	44.4	51.1	7.4%	15.5%	13.8%
54	1	37	33.8	38.4	6.5%	16.6%	12.6%
54	0.5	36.2	32.9	37.4	6.6%	16.7%	12.7%
54	0.2	34.8	30.2	34.6	7.8%	16.9%	13.9%
54	0.1	32.7	28.8	32.5	7.0%	17.2%	12.4%

Appendix E.9 Dynamic modulus test results for mix #9

Dynamic Modulus, kPa							
Mix #9 Type II-B 25% RAP PG 52-28							
Temp. C	**Freq Hz**	**Sample 1**	**Sample 2**	**Sample 3**	**COV**	**sr %**	**Range %**
4	25	13025	13288	11908	5.8%	4.5%	10.8%
4	20	12013	12272	11406	3.7%	4.5%	7.3%
4	10	10839	11124	10254	4.1%	4.6%	8.1%
4	5	9667	9987	9137	4.5%	4.7%	8.9%
4	2	8190	8522	7717	5.0%	4.9%	9.9%
4	1	7123	7460	6708	5.3%	5.1%	10.6%
4	0.5	6118	6455	5760	5.7%	5.2%	11.4%
4	0.2	4900	5223	4613	6.2%	5.5%	12.4%
4	0.1	4074	4387	3839	6.7%	5.7%	13.4%
21	25	3706	3829	3251	8.5%	5.9%	16.1%
21	20	3488	3646	3041	9.3%	6.0%	17.8%
21	10	2758	2869	2394	9.3%	6.3%	17.8%
21	5	2124	2222	1839	9.7%	6.6%	18.6%
21	2	1426	1507	1233	10.1%	7.2%	19.7%
21	1	1023	1082	881.6	10.3%	7.8%	20.1%
21	0.5	715.9	760.3	616	10.6%	8.4%	20.7%
21	0.2	433.3	462.7	372	10.9%	9.4%	21.5%
21	0.1	294	312	250.5	11.1%	10.3%	21.5%
37	25	904.3	946.8	723.4	13.8%	8.1%	26.0%
37	20	840	857.5	670.3	13.1%	8.2%	23.7%
37	10	563.6	576.1	448.9	13.2%	9.0%	24.0%
37	5	367	376	292.6	13.3%	9.8%	24.2%
37	2	201.1	203.3	156.6	14.1%	11.3%	25.0%
37	1	132.3	135.5	105.6	13.2%	12.3%	24.0%
37	0.5	93	94	76.1	11.5%	13.3%	20.4%
37	0.2	61.5	61.2	52.7	8.5%	14.5%	15.1%
37	0.1	46.8	47	42.4	5.7%	15.4%	10.1%
54	25	259.9	255.6	159.7	25.2%	10.8%	44.5%
54	20	234.5	220.3	156.7	20.3%	11.0%	38.2%
54	10	152.1	144.8	111.7	15.8%	12.1%	29.7%
54	5	97.9	94.4	79.9	10.5%	13.2%	19.8%
54	2	54.2	51.4	44.8	9.6%	15.0%	18.8%
54	1	39.1	39.4	34	8.1%	16.0%	14.4%
54	0.5	33.7	33.5	34.4	1.4%	16.4%	2.7%
54	0.2	28.3	26.5	29.7	5.7%	17.1%	11.4%
54	0.1	24.4	23.4	28.1	9.8%	17.5%	18.6%

Appendix E.10 Dynamic modulus test results for mix #10

Dynamic Modulus, kPa							
Mix #10 Type II-B 25% RAP PG 52-40							
Temp. C	**Freq Hz**	**Sample 1**	**Sample 2**	**Sample 3**	**COV**	**sr %**	**Range %**
4	25	7364	8473	7472	7.9%	5.0%	14.3%
4	20	6966	7341	7028	2.8%	5.1%	5.3%
4	10	5984	6297	5954	3.1%	5.2%	5.6%
4	5	5058	5345	4979	3.8%	5.4%	7.1%
4	2	3952	4214	3838	4.8%	5.7%	9.4%
4	1	3219	3463	3087	5.9%	6.0%	11.5%
4	0.5	2580	2805	2443	7.0%	6.3%	13.9%
4	0.2	1868	2066	1745	8.6%	6.8%	17.0%
4	0.1	1435	1612	1335	9.6%	7.2%	19.0%
21	25	1762	1928	1726	6.0%	6.8%	11.2%
21	20	1615	1826	1602	7.5%	6.9%	13.3%
21	10	1191	1357	1187	7.8%	7.4%	13.7%
21	5	874.8	1004	878.8	8.0%	7.9%	14.1%
21	2	562.2	655.4	567.1	8.8%	8.7%	15.7%
21	1	404.8	474.6	395.2	10.2%	9.4%	18.7%
21	0.5	299.3	351	309.3	8.6%	10.0%	16.2%
21	0.2	204.1	237.9	227.7	7.8%	10.8%	15.1%
21	0.1	155.5	180	186.8	9.5%	11.4%	18.0%
37	25	471.6	560.3	464.1	10.7%	9.1%	19.3%
37	20	436.7	504.1	413	10.5%	9.3%	20.2%
37	10	308.3	355.7	291.1	10.5%	10.0%	20.3%
37	5	216.1	253.5	204.9	11.3%	10.8%	21.6%
37	2	127.6	156.2	123.5	13.1%	12.1%	24.1%
37	1	101.6	119.3	96.1	11.5%	12.8%	22.0%
37	0.5	82.2	98.2	83.5	10.1%	13.3%	18.2%
37	0.2	63.1	76.5	69.3	9.6%	14.0%	19.2%
37	0.1	52.9	65	61.6	10.4%	14.5%	20.2%
54	25	211.4	262.4	226.3	11.2%	10.7%	21.9%
54	20	174.7	201.9	180.7	7.7%	11.3%	14.6%
54	10	126.8	151.5	124.4	11.2%	12.1%	20.2%
54	5	91.6	113.3	88.4	13.9%	13.0%	25.5%
54	2	56.7	71.2	50.1	18.2%	14.5%	35.6%
54	1	47.1	61.2	40.9	20.9%	15.1%	40.8%
54	0.5	45.7	58.4	37.7	22.1%	15.2%	43.8%
54	0.2	40.8	53	33.6	23.1%	15.6%	45.7%
54	0.1	36.8	50.2	30.9	25.2%	15.9%	49.1%

Appendix E.11 Dynamic modulus test results for mix #11

Dynamic Modulus, kPa							
Mix #11 Type II-B 35% RAP PG 52-28							
Temp. C	**Freq Hz**	**Sample 1**	**Sample 2**	**Sample 3**	**COV**	**sr %**	**Range %**
4	25	12673	14633	13629	7.2%	4.4%	14.4%
4	20	12101	14184	13718	8.2%	4.4%	15.6%
4	10	10958	12884	12350	8.2%	4.5%	16.0%
4	5	9834	11593	11062	8.3%	4.6%	16.2%
4	2	8387	9967	9475	8.7%	4.8%	17.0%
4	1	7349	8780	8315	9.0%	4.9%	17.6%
4	0.5	6361	7658	7254	9.4%	5.1%	18.3%
4	0.2	5149	6320	5956	10.3%	5.3%	20.2%
4	0.1	4315	5414	5086	11.4%	5.5%	22.3%
21	25	3830	4338	3439	11.7%	5.8%	23.2%
21	20	3650	3365	3242	6.1%	5.9%	11.9%
21	10	2926	2700	2598	6.1%	6.2%	12.0%
21	5	2293	2179	2047	5.7%	6.6%	11.3%
21	2	1587	1484	1421	5.6%	7.1%	11.1%
21	1	1151	1092	1045	4.8%	7.6%	9.7%
21	0.5	819.5	792.2	753.3	4.2%	8.2%	8.4%
21	0.2	510.7	504.7	473.2	4.1%	9.1%	7.6%
21	0.1	349.8	353.2	329.4	3.7%	9.8%	6.9%
37	25	1048	1378	871	23.4%	7.6%	46.1%
37	20	965.7	1030	820.1	11.5%	7.9%	22.4%
37	10	665.1	728.9	555.8	13.5%	8.6%	26.6%
37	5	443.7	493.5	364.9	14.9%	9.4%	29.6%
37	2	246.6	282.9	202.7	16.5%	10.6%	32.9%
37	1	164	194.7	133	18.8%	11.6%	37.6%
37	0.5	115.5	138.7	98.3	17.3%	12.5%	34.4%
37	0.2	77.1	93.3	68	16.1%	13.6%	31.8%
37	0.1	59.4	72.6	54.7	14.9%	14.3%	28.8%
54	25	395.3	291.6	258.9	22.6%	10.0%	43.3%
54	20	351.1	252.6	223.7	24.2%	10.3%	46.2%
54	10	241.9	176.6	152.4	24.3%	11.2%	47.0%
54	5	171.2	123.8	104.4	25.8%	12.1%	50.2%
54	2	98	71.1	61.2	24.8%	13.7%	47.9%
54	1	77.2	62.2	46.3	25.0%	14.3%	49.9%
54	0.5	67.4	55.7	42.8	22.3%	14.7%	44.5%
54	0.2	56.3	48.4	38	19.3%	15.2%	38.5%
54	0.1	50.3	45.2	36.2	16.3%	15.5%	32.1%

APPENDIX F MIXTURE PHASE ANGLE AMPT RESULTS

Appendix F.1 Phase angle test results for mix #1

Mixture Phase Angle, Degree							
Mix #1 Type II-B 0% RAP PG 52-28							
Temp. C	**Freq Hz**	**Sample 1**	**Sample 2**	**Sample 3**	**Avg.**	**Std. Dev.**	**COV**
4	25	12.6	47.4	24.5	28.2	17.7	62.7%
4	20	11.7	11.0	12.0	11.6	0.5	4.3%
4	10	12.9	13.0	13.1	13.0	0.1	0.8%
4	5	14.3	14.9	14.6	14.6	0.3	1.9%
4	2	16.4	16.4	16.6	16.5	0.1	0.5%
4	1	18.1	18.1	18.3	18.2	0.1	0.6%
4	0.5	19.9	20.0	20.1	20.0	0.1	0.4%
4	0.2	22.5	22.6	22.6	22.5	0.1	0.3%
4	0.1	24.3	24.5	24.5	24.4	0.1	0.3%
21	25	27.6	148.2	22.9	66.2	71.0	107.2%
21	20	28.1	27.6	28.6	28.1	0.5	1.7%
21	10	30.3	30.5	30.4	30.4	0.1	0.4%
21	5	32.3	32.7	32.0	32.3	0.3	1.0%
21	2	34.6	35.1	34.2	34.6	0.5	1.4%
21	1	35.8	36.3	35.2	35.8	0.5	1.5%
21	0.5	36.4	36.9	35.7	36.3	0.6	1.7%
21	0.2	36.8	37.4	36.0	36.7	0.7	1.9%
21	0.1	36.7	37.3	35.8	36.6	0.8	2.1%
37	25	43.6	42.9	41.9	42.8	0.8	2.0%
37	20	40.1	40.2	38.9	39.7	0.7	1.7%
37	10	39.6	39.6	38.1	39.1	0.9	2.2%
37	5	39.3	39.3	37.5	38.7	1.0	2.7%
37	2	39.4	38.8	36.9	38.4	1.3	3.4%
37	1	38.6	37.1	35.7	37.2	1.5	3.9%
37	0.5	36.8	34.3	33.3	34.8	1.8	5.2%
37	0.2	33.9	30.2	30.1	31.4	2.2	6.9%
37	0.1	31.3	27.3	27.8	28.8	2.2	7.6%
54	25	12.5	39.9	38.2	30.2	15.3	50.8%
54	20	32.9	28.7	33.4	31.6	2.6	8.2%
54	10	34.5	33.2	30.7	32.8	1.9	5.9%
54	5	33.0	31.6	29.1	31.2	1.9	6.2%
54	2	32.8	30.0	29.0	30.6	2.0	6.5%
54	1	32.0	28.6	28.6	29.7	1.9	6.5%
54	0.5	26.7	23.3	23.4	24.4	1.9	8.0%
54	0.2	23.5	20.7	20.3	21.5	1.8	8.2%
54	0.1	20.4	18.7	18.6	19.2	1.0	5.4%

Appendix F.2 Phase angle test results for mix #2

Mixture Phase Angle, Degree							
Mix #2 Type II-B 0% RAP PG 58-34							
Temp. C	**Freq Hz**	**Sample 1**	**Sample 2**	**Sample 3**	**Avg.**	**Std. Dev.**	**COV**
4	25	17.4	17.9	20.1	18.5	1.4	7.7%
4	20	18.8	18.7	20.5	19.3	1.0	5.2%
4	10	20.5	20.5	22.4	21.1	1.1	5.2%
4	5	22.3	22.3	24.2	22.9	1.1	4.8%
4	2	24.6	24.8	26.7	25.3	1.2	4.6%
4	1	26.2	26.6	28.4	27.1	1.2	4.3%
4	0.5	27.7	28.2	29.9	28.6	1.1	4.0%
4	0.2	29.4	30.1	31.6	30.3	1.1	3.7%
4	0.1	30.2	31.1	32.4	31.2	1.1	3.5%
21	25	38.5	36.8	37.8	37.7	0.9	2.4%
21	20	36.7	35.8	36.7	36.4	0.5	1.5%
21	10	37.2	36.2	37.1	36.8	0.6	1.5%
21	5	37.3	36.3	37.3	36.9	0.6	1.5%
21	2	37.1	36.2	37.2	36.8	0.6	1.5%
21	1	36.4	35.5	36.4	36.1	0.5	1.4%
21	0.5	34.8	34.2	35.0	34.7	0.4	1.2%
21	0.2	32.7	32.6	33.2	32.8	0.4	1.1%
21	0.1	30.8	31.2	31.4	31.1	0.3	1.0%
37	25	43.2	39.7	39.9	40.9	1.9	4.8%
37	20	39.4	36.5	36.9	37.6	1.6	4.3%
37	10	37.9	34.5	35.0	35.8	1.8	5.1%
37	5	36.5	33.3	33.7	34.5	1.7	5.0%
37	2	35.7	32.7	33.3	33.9	1.6	4.7%
37	1	33.4	30.7	30.9	31.7	1.5	4.8%
37	0.5	31.3	28.4	28.8	29.5	1.6	5.4%
37	0.2	28.9	26.0	26.1	27.0	1.6	6.1%
37	0.1	26.9	24.3	23.9	25.0	1.7	6.6%
54	25	39.4	33.3	34.0	35.6	3.3	9.3%
54	20	36.0	29.6	30.2	31.9	3.5	11.1%
54	10	33.4	27.4	27.8	29.6	3.3	11.3%
54	5	31.9	26.2	26.3	28.1	3.3	11.6%
54	2	31.7	26.4	26.5	28.2	3.0	10.7%
54	1	29.2	24.3	23.9	25.8	3.0	11.5%
54	0.5	27.6	22.2	21.7	23.8	3.3	13.7%
54	0.2	25.7	20.0	19.7	21.8	3.4	15.4%
54	0.1	24.1	18.6	18.4	20.4	3.2	15.9%

Appendix F.3 Phase angle test results for mix #3

Mixture Phase Angle, Degree							
Mix #3 Type II-A 0% RAP PG 58-34							
Temp. C	**Freq Hz**	**Sample 1**	**Sample 2**	**Sample 3**	**Avg.**	**Std. Dev.**	**COV**
4	25	13.2	13.6	15.1	14.0	1.0	7.3%
4	20	13.5	14.7	15.4	14.5	1.0	6.6%
4	10	15.1	16.2	16.9	16.1	0.9	5.6%
4	5	16.8	17.8	18.5	17.7	0.9	4.9%
4	2	19.2	20.2	20.8	20.0	0.8	4.1%
4	1	21.1	21.9	22.5	21.9	0.7	3.3%
4	0.5	23.0	23.7	24.3	23.7	0.7	2.8%
4	0.2	25.5	26.1	26.6	26.1	0.5	2.1%
4	0.1	27.3	27.6	28.2	27.7	0.4	1.6%
21	25	34.9	35.7	36.7	35.8	0.9	2.6%
21	20	32.3	33.1	35.4	33.6	1.6	4.7%
21	10	33.6	34.2	36.2	34.7	1.4	3.9%
21	5	34.8	35.2	36.9	35.6	1.1	3.1%
21	2	35.8	36.2	37.3	36.5	0.8	2.1%
21	1	36.2	36.4	37.0	36.6	0.4	1.2%
21	0.5	35.7	36.0	36.3	36.0	0.3	0.7%
21	0.2	34.9	35.0	34.9	34.9	0.1	0.2%
21	0.1	34.1	34.0	33.8	34.0	0.2	0.5%
37	25	44.2	37.3	41.2	40.9	3.4	8.4%
37	20	39.2	36.7	37.9	37.9	1.3	3.4%
37	10	37.9	36.1	36.4	36.8	1.0	2.7%
37	5	37.1	35.6	35.4	36.0	0.9	2.6%
37	2	36.5	35.2	34.9	35.5	0.9	2.4%
37	1	35.0	33.3	32.9	33.7	1.1	3.4%
37	0.5	33.1	30.8	30.4	31.4	1.4	4.5%
37	0.2	30.4	27.7	27.3	28.5	1.6	5.8%
37	0.1	28.4	25.2	25.1	26.2	1.9	7.1%
54	25	57.0	36.1	36.3	43.1	12.0	27.9%
54	20	38.8	32.2	31.0	34.0	4.2	12.4%
54	10	35.9	29.6	28.0	31.2	4.2	13.4%
54	5	34.1	28.0	26.4	29.5	4.0	13.7%
54	2	33.3	27.1	26.1	28.8	3.9	13.6%
54	1	31.3	24.6	23.6	26.5	4.2	15.9%
54	0.5	30.1	21.3	20.3	23.9	5.4	22.5%
54	0.2	13.4	18.7	17.8	16.6	2.9	17.2%
54	0.1	5.3	17.3	16.3	13.0	6.7	51.5%

Appendix F.4 Phase angle test results for mix #4

Mixture Phase Angle, Degree							
Mix #4 Type II-A 25% RAP PG 58-34							
Temp. C	**Freq Hz**	**Sample 1**	**Sample 2**	**Sample 3**	**Avg.**	**Std. Dev.**	**COV**
4	25	13.6	15.4	13.3	14.1	1.1	8.0%
4	20	14.4	15.9	13.9	14.7	1.0	6.9%
4	10	15.8	17.4	15.1	16.1	1.2	7.3%
4	5	17.3	19.0	16.5	17.6	1.3	7.4%
4	2	19.5	21.3	18.5	19.8	1.4	7.1%
4	1	21.1	23.0	20.1	21.4	1.5	6.9%
4	0.5	22.8	24.7	21.7	23.1	1.5	6.5%
4	0.2	25.0	26.9	23.9	25.3	1.5	5.9%
4	0.1	26.5	28.2	25.6	26.8	1.3	5.0%
21	25	29.3	34.8	28.6	30.9	3.4	11.0%
21	20	30.0	34.2	28.7	30.9	2.9	9.4%
21	10	31.3	35.1	29.9	32.1	2.7	8.3%
21	5	32.6	35.7	31.1	33.1	2.4	7.2%
21	2	33.9	36.4	32.2	34.2	2.1	6.1%
21	1	34.4	36.2	32.7	34.4	1.7	5.0%
21	0.5	34.4	35.4	32.8	34.2	1.3	3.8%
21	0.2	34.2	34.0	32.7	33.6	0.8	2.5%
21	0.1	33.5	32.6	32.3	32.8	0.6	1.8%
37	25	41.5	39.8	40.6	40.6	0.9	2.1%
37	20	38.2	36.8	38.3	37.7	0.9	2.3%
37	10	37.4	35.6	37.2	36.7	1.0	2.7%
37	5	36.5	34.5	36.0	35.7	1.0	2.8%
37	2	35.8	33.9	35.3	35.0	1.0	2.9%
37	1	34.3	32.3	33.7	33.4	1.0	3.1%
37	0.5	32.5	30.1	31.7	31.4	1.2	3.9%
37	0.2	30.3	27.5	29.1	29.0	1.4	4.9%
37	0.1	28.8	25.2	27.3	27.1	1.8	6.6%
54	25	36.0	32.9	35.4	34.7	1.6	4.7%
54	20	32.0	28.9	32.8	31.2	2.0	6.5%
54	10	29.8	26.6	31.5	29.3	2.5	8.5%
54	5	28.8	25.3	30.7	28.3	2.7	9.7%
54	2	29.5	25.0	30.8	28.5	3.0	10.7%
54	1	29.2	23.2	28.3	26.9	3.2	12.0%
54	0.5	25.9	20.5	26.0	24.1	3.1	12.9%
54	0.2	23.1	18.0	23.5	21.6	3.0	14.1%
54	0.1	21.1	16.6	21.6	19.8	2.8	14.1%

Appendix F.5 Phase angle test results for mix #5

Mixture Phase Angle, Degree							
Mix #5 Type II-B 25% RAP PG 58-34							
Temp. C	**Freq Hz**	**Sample 1**	**Sample 2**	**Sample 3**	**Avg.**	**Std. Dev.**	**COV**
4	25	15.3	13.9	13.2	14.1	1.1	7.7%
4	20	14.1	14.9	14.0	14.3	0.5	3.3%
4	10	15.4	16.4	15.3	15.7	0.6	3.8%
4	5	16.7	18.0	16.8	17.2	0.7	4.2%
4	2	18.7	20.2	18.8	19.2	0.8	4.2%
4	1	20.2	21.9	20.4	20.8	0.9	4.5%
4	0.5	21.8	23.7	22.0	22.5	1.0	4.6%
4	0.2	24.0	26.1	24.1	24.7	1.2	4.7%
4	0.1	25.5	27.6	25.5	26.2	1.2	4.6%
21	25	31.2	31.7	34.6	32.5	1.9	5.7%
21	20	30.9	31.6	31.7	31.4	0.4	1.4%
21	10	32.2	32.9	32.6	32.6	0.4	1.1%
21	5	33.3	34.2	33.6	33.7	0.4	1.3%
21	2	34.6	35.6	34.5	34.9	0.6	1.7%
21	1	35.0	36.0	34.8	35.2	0.6	1.8%
21	0.5	34.9	35.8	34.6	35.1	0.6	1.7%
21	0.2	34.6	35.2	34.1	34.6	0.5	1.6%
21	0.1	33.9	34.6	33.4	34.0	0.6	1.8%
37	25	40.6	39.6	40.3	40.2	0.6	1.4%
37	20	38.0	37.3	36.8	37.4	0.6	1.5%
37	10	36.9	36.8	35.6	36.4	0.7	1.9%
37	5	35.8	36.6	34.6	35.6	1.0	2.8%
37	2	34.8	36.9	33.9	35.2	1.6	4.5%
37	1	33.4	36.0	32.5	34.0	1.8	5.3%
37	0.5	31.6	34.4	30.8	32.3	1.9	5.9%
37	0.2	29.4	32.1	28.4	30.0	1.9	6.4%
37	0.1	27.8	30.5	26.7	28.3	1.9	6.9%
54	25	40.1	49.4	31.0	40.2	9.2	23.0%
54	20	31.7	32.4	28.6	30.9	2.0	6.5%
54	10	29.9	30.2	26.9	29.0	1.8	6.2%
54	5	28.7	29.3	26.0	28.0	1.7	6.2%
54	2	29.2	29.6	25.9	28.2	2.0	7.0%
54	1	30.9	29.6	23.3	27.9	4.0	14.4%
54	0.5	26.4	26.1	21.1	24.5	3.0	12.1%
54	0.2	23.1	22.4	18.8	21.5	2.3	10.8%
54	0.1	21.0	20.0	17.2	19.4	2.0	10.3%

Appendix F.6 Phase angle test results for mix #6

Mixture Phase Angle, Degree							
Mix #6 Type II-B 35% RAP PG 52-28							
Temp. C	**Freq Hz**	**Sample 1**	**Sample 2**	**Sample 3**	**Avg.**	**Std. Dev.**	**COV**
4	25	11.4	11.5	12.3	11.7	0.5	4.2%
4	20	12.3	12.2	13.7	12.7	0.8	6.6%
4	10	13.6	13.5	15.2	14.1	0.9	6.7%
4	5	15.0	14.9	16.8	15.6	1.1	6.9%
4	2	17.1	17.0	19.2	17.7	1.2	7.0%
4	1	18.7	18.6	20.9	19.4	1.3	6.8%
4	0.5	20.6	20.3	22.8	21.2	1.4	6.6%
4	0.2	23.1	22.7	25.2	23.7	1.3	5.7%
4	0.1	24.9	24.5	26.8	25.4	1.2	4.9%
21	25	29.4	31.8	143.3	68.1	65.1	95.5%
21	20	29.2	31.6	33.5	31.4	2.2	7.0%
21	10	30.8	33.2	34.5	32.8	1.9	5.7%
21	5	32.4	34.7	35.2	34.1	1.5	4.5%
21	2	34.4	36.4	36.1	35.6	1.1	3.1%
21	1	35.3	37.2	36.5	36.3	1.0	2.7%
21	0.5	35.8	37.5	36.3	36.5	0.9	2.4%
21	0.2	36.2	37.5	35.7	36.5	0.9	2.5%
21	0.1	36.2	37.2	35.1	36.2	1.0	2.9%
37	25	42.0	44.0	126.8	70.9	48.4	68.2%
37	20	39.0	40.8	39.5	39.8	1.0	2.4%
37	10	38.6	39.9	38.5	39.0	0.8	2.0%
37	5	38.2	39.5	37.6	38.4	1.0	2.6%
37	2	38.2	39.6	36.9	38.2	1.4	3.5%
37	1	38.0	38.9	35.6	37.5	1.7	4.5%
37	0.5	36.0	35.9	33.5	35.1	1.4	4.1%
37	0.2	33.0	32.1	30.7	31.9	1.1	3.6%
37	0.1	30.3	29.6	28.6	29.5	0.9	2.9%
54	25	42.3	45.1	38.3	41.9	3.4	8.2%
54	20	37.5	40.6	34.2	37.4	3.2	8.5%
54	10	35.4	39.1	32.4	35.6	3.3	9.3%
54	5	33.9	38.2	31.2	34.4	3.5	10.1%
54	2	32.6	38.0	30.4	33.7	3.9	11.7%
54	1	29.6	35.4	27.9	31.0	3.9	12.7%
54	0.5	25.5	32.2	24.4	27.4	4.2	15.4%
54	0.2	21.9	29.1	21.5	24.2	4.3	17.6%
54	0.1	19.6	30.4	19.7	23.2	6.2	26.8%

Appendix F.7 Phase angle test results for mix #7

Mixture Phase Angle, Degree							
Mix #7 Type II-B 0% RAP PG 52-28							
Temp. C	**Freq Hz**	**Sample 1**	**Sample 2**	**Sample 3**	**Avg.**	**Std. Dev.**	**COV**
4	25	14.4	13.0	12.2	13.2	1.1	8.3%
4	20	15.8	13.4	13.2	14.1	1.5	10.3%
4	10	17.4	14.8	14.6	15.6	1.6	10.0%
4	5	19.2	16.3	16.0	17.2	1.8	10.4%
4	2	21.7	18.4	18.1	19.4	2.0	10.2%
4	1	23.7	20.0	19.7	21.1	2.2	10.6%
4	0.5	25.5	21.6	21.4	22.8	2.3	10.1%
4	0.2	27.9	23.9	23.7	25.2	2.4	9.5%
4	0.1	29.7	25.5	25.3	26.9	2.5	9.3%
21	25	33.7	32.0	31.6	32.4	1.1	3.5%
21	20	33.4	31.8	31.2	32.1	1.1	3.5%
21	10	34.7	33.2	33.0	33.6	0.9	2.8%
21	5	36.1	34.6	34.5	35.1	0.9	2.5%
21	2	37.7	36.3	36.4	36.8	0.8	2.1%
21	1	38.5	37.1	37.4	37.6	0.7	1.9%
21	0.5	38.8	37.4	37.9	38.0	0.7	1.8%
21	0.2	38.5	37.4	38.3	38.1	0.6	1.5%
21	0.1	37.7	37.3	38.4	37.8	0.5	1.4%
37	25	44.5	43.6	44.9	44.3	0.7	1.5%
37	20	41.6	40.8	42.5	41.6	0.9	2.1%
37	10	40.9	40.5	42.1	41.1	0.8	2.0%
37	5	40.3	40.4	41.9	40.9	0.9	2.1%
37	2	39.8	40.7	42.2	40.9	1.2	3.0%
37	1	36.5	39.2	40.1	38.6	1.9	4.9%
37	0.5	32.5	36.6	37.3	35.5	2.6	7.2%
37	0.2	27.4	32.5	32.8	30.9	3.0	9.8%
37	0.1	23.7	29.3	29.4	27.5	3.3	11.9%
54	25	44.6	37.1	38.0	39.9	4.1	10.2%
54	20	37.2	37.7	34.7	36.5	1.6	4.4%
54	10	33.2	33.9	30.0	32.3	2.1	6.4%
54	5	29.9	31.4	26.9	29.4	2.3	7.9%
54	2	26.0	29.0	24.0	26.3	2.5	9.7%
54	1	22.2	27.3	23.2	24.2	2.7	11.1%
54	0.5	19.1	22.4	18.7	20.0	2.0	10.0%
54	0.2	16.8	20.3	16.5	17.8	2.1	11.9%
54	0.1	15.6	18.9	15.8	16.8	1.9	11.1%

Appendix F.8 Phase angle test results for mix #8

Mixture Phase Angle, Degree							
Mix #8 Type II-B 0% RAP PG 52-40							
Temp. C	**Freq Hz**	**Sample 1**	**Sample 2**	**Sample 3**	**Avg.**	**Std. Dev.**	**COV**
4	25	27.3	25.9	24.3	25.8	1.5	5.9%
4	20	26.5	26.2	24.9	25.8	0.9	3.3%
4	10	28.0	28.0	26.6	27.5	0.8	3.0%
4	5	29.6	29.7	28.1	29.1	0.9	3.0%
4	2	31.6	31.9	30.1	31.2	0.9	3.0%
4	1	32.9	33.2	31.4	32.5	1.0	3.0%
4	0.5	33.8	34.2	32.3	33.4	1.0	2.9%
4	0.2	34.6	35.2	33.3	34.4	1.0	2.8%
4	0.1	35.0	35.5	33.7	34.7	0.9	2.7%
21	25	40.6	42.3	39.2	40.7	1.6	3.8%
21	20	38.6	40.4	37.8	38.9	1.3	3.4%
21	10	37.6	38.5	37.3	37.8	0.6	1.7%
21	5	36.4	37.8	36.6	37.0	0.7	2.0%
21	2	35.3	37.2	35.8	36.1	1.0	2.7%
21	1	33.1	35.6	34.3	34.3	1.3	3.8%
21	0.5	30.7	33.7	32.3	32.3	1.5	4.7%
21	0.2	27.8	31.1	29.6	29.5	1.7	5.7%
21	0.1	25.7	29.0	27.5	27.4	1.7	6.1%
37	25	36.9	38.6	37.6	37.7	0.8	2.2%
37	20	34.0	35.6	35.1	34.9	0.8	2.3%
37	10	31.5	33.0	33.0	32.5	0.9	2.7%
37	5	29.9	31.0	31.2	30.7	0.7	2.3%
37	2	28.7	29.2	29.6	29.2	0.5	1.6%
37	1	25.5	25.8	26.5	25.9	0.5	1.9%
37	0.5	23.1	23.0	23.7	23.3	0.4	1.6%
37	0.2	20.7	20.4	20.9	20.7	0.3	1.3%
37	0.1	19.1	19.1	19.0	19.1	0.0	0.2%
54	25	32.6	37.2	32.0	33.9	2.8	8.3%
54	20	29.4	32.7	23.0	28.4	4.9	17.3%
54	10	26.0	25.8	21.1	24.3	2.8	11.4%
54	5	24.1	23.2	19.1	22.2	2.7	12.0%
54	2	23.3	21.6	18.7	21.2	2.3	11.1%
54	1	22.8	22.4	20.3	21.8	1.3	6.0%
54	0.5	19.7	18.1	15.9	17.9	1.9	10.7%
54	0.2	19.8	16.6	14.0	16.8	2.9	17.3%
54	0.1	18.0	15.7	13.2	15.6	2.4	15.6%

Appendix F.9 Phase angle test results for mix #9

Mixture Phase Angle, Degree							
Mix #9 Type II-B 25% RAP PG 52-28							
Temp. C	**Freq Hz**	**Sample 1**	**Sample 2**	**Sample 3**	**Avg.**	**Std. Dev.**	**COV**
4	25	13.8	13.4	12.6	13.3	0.6	4.6%
4	20	13.3	12.8	13.3	13.1	0.3	2.2%
4	10	14.7	14.2	14.7	14.5	0.3	2.3%
4	5	16.3	15.7	16.3	16.1	0.4	2.4%
4	2	18.6	17.9	18.6	18.4	0.4	2.4%
4	1	20.5	19.6	20.5	20.2	0.5	2.5%
4	0.5	22.4	21.4	22.4	22.1	0.6	2.7%
4	0.2	25.0	23.9	25.1	24.7	0.7	2.7%
4	0.1	26.9	25.8	27.1	26.6	0.7	2.7%
21	25	32.8	32.1	33.7	32.9	0.8	2.3%
21	20	32.8	32.1	33.6	32.9	0.8	2.3%
21	10	34.9	34.0	35.5	34.8	0.8	2.3%
21	5	36.7	35.6	37.3	36.5	0.9	2.4%
21	2	38.8	37.6	39.2	38.5	0.9	2.3%
21	1	39.7	38.6	40.1	39.5	0.8	1.9%
21	0.5	40.0	39.1	40.3	39.8	0.6	1.6%
21	0.2	40.2	39.4	40.2	39.9	0.4	1.1%
21	0.1	39.9	39.7	39.7	39.8	0.1	0.2%
37	25	46.5	44.2	46.6	45.8	1.3	2.9%
37	20	43.3	42.2	44.1	43.2	1.0	2.3%
37	10	42.9	42.2	43.4	42.8	0.6	1.4%
37	5	42.7	42.1	42.8	42.5	0.4	0.8%
37	2	42.5	42.6	42.4	42.5	0.1	0.1%
37	1	40.8	41.0	39.8	40.6	0.6	1.5%
37	0.5	37.5	38.4	36.0	37.3	1.2	3.3%
37	0.2	32.6	34.3	30.6	32.5	1.8	5.6%
37	0.1	28.9	30.8	26.5	28.7	2.1	7.4%
54	25	49.7	48.7	15.8	38.1	19.3	50.6%
54	20	46.4	44.9	43.0	44.8	1.7	3.7%
54	10	42.0	40.7	37.8	40.2	2.1	5.3%
54	5	38.7	38.0	35.2	37.3	1.9	5.0%
54	2	35.8	35.9	32.0	34.6	2.3	6.5%
54	1	32.3	31.9	29.8	31.4	1.4	4.3%
54	0.5	26.7	29.3	28.8	28.3	1.4	4.9%
54	0.2	22.4	26.0	25.0	24.5	1.8	7.5%
54	0.1	19.9	23.4	23.8	22.4	2.1	9.6%

Appendix F.10 Phase angle test results for mix #10

Mixture Phase Angle, Degree							
Mix #10 Type II-B 25% RAP PG 52-40							
Temp. C	**Freq Hz**	**Sample 1**	**Sample 2**	**Sample 3**	**Avg.**	**Std. Dev.**	**COV**
4	25	21.0	40.3	22.3	27.9	10.8	38.9%
4	20	21.7	20.9	23.0	21.8	1.1	4.9%
4	10	23.4	22.5	24.7	23.5	1.1	4.6%
4	5	25.1	24.1	26.3	25.2	1.1	4.3%
4	2	27.3	26.2	28.3	27.3	1.0	3.8%
4	1	28.7	27.7	29.6	28.7	0.9	3.3%
4	0.5	30.1	29.0	30.5	29.8	0.8	2.7%
4	0.2	31.6	30.5	31.5	31.2	0.6	2.0%
4	0.1	32.5	31.4	31.9	31.9	0.6	1.8%
21	25	37.0	36.6	38.3	37.3	0.9	2.4%
21	20	36.6	35.7	36.2	36.2	0.5	1.3%
21	10	36.9	36.1	35.9	36.3	0.5	1.5%
21	5	36.9	36.1	35.3	36.1	0.8	2.3%
21	2	36.8	36.1	34.1	35.7	1.4	3.8%
21	1	36.0	35.4	33.8	35.0	1.1	3.2%
21	0.5	34.7	34.2	31.3	33.4	1.8	5.5%
21	0.2	32.4	32.6	28.2	31.1	2.5	8.1%
21	0.1	30.6	31.1	26.0	29.2	2.8	9.6%
37	25	40.6	38.9	36.2	38.6	2.2	5.7%
37	20	37.3	36.3	32.4	35.4	2.6	7.3%
37	10	35.4	35.0	30.4	33.6	2.8	8.2%
37	5	34.0	33.7	29.2	32.3	2.7	8.3%
37	2	33.1	32.6	28.1	31.3	2.8	8.9%
37	1	29.9	30.3	26.1	28.7	2.3	8.0%
37	0.5	27.1	27.5	23.2	26.0	2.4	9.1%
37	0.2	24.4	24.9	20.3	23.2	2.5	10.9%
37	0.1	22.8	22.9	18.5	21.4	2.5	11.7%
54	25	38.5	38.9	37.3	38.3	0.8	2.1%
54	20	33.5	30.2	26.8	30.2	3.3	11.0%
54	10	29.7	26.1	24.5	26.8	2.7	9.9%
54	5	27.3	24.3	23.4	25.0	2.1	8.3%
54	2	25.7	23.4	23.0	24.0	1.5	6.0%
54	1	23.5	21.5	21.7	22.2	1.1	5.0%
54	0.5	21.2	19.5	19.1	19.9	1.1	5.4%
54	0.2	20.3	18.1	17.0	18.5	1.7	9.2%
54	0.1	19.8	17.4	15.7	17.6	2.0	11.6%

Appendix F.11 Phase angle test results for mix #11

Mixture Phase Angle, Degree							
Mix #11 Type II-B 35% RAP PG 52-28							
Temp. C	**Freq Hz**	**Sample 1**	**Sample 2**	**Sample 3**	**Avg.**	**Std. Dev.**	**COV**
4	25	12.2	12.0	11.4	11.9	0.4	3.4%
4	20	12.9	12.3	13.0	12.7	0.4	3.0%
4	10	14.3	13.5	14.1	14.0	0.4	2.8%
4	5	15.8	14.9	15.3	15.3	0.5	3.0%
4	2	18.0	16.8	17.2	17.3	0.6	3.5%
4	1	19.8	18.4	18.7	18.9	0.7	3.8%
4	0.5	21.5	20.0	20.2	20.6	0.8	4.0%
4	0.2	24.0	22.2	22.3	22.8	1.0	4.5%
4	0.1	25.8	23.8	23.7	24.4	1.2	4.9%
21	25	31.3	57.4	28.7	39.1	15.9	40.5%
21	20	31.1	28.7	27.9	29.2	1.6	5.6%
21	10	32.7	30.4	28.6	30.6	2.0	6.7%
21	5	34.3	31.8	29.7	31.9	2.3	7.1%
21	2	36.0	33.7	31.2	33.6	2.4	7.1%
21	1	37.0	34.8	32.3	34.7	2.4	6.8%
21	0.5	37.4	35.5	33.2	35.4	2.1	6.0%
21	0.2	37.4	36.0	34.5	36.0	1.5	4.1%
21	0.1	37.2	36.1	35.1	36.1	1.1	2.9%
37	25	42.6	34.4	43.0	40.0	4.9	12.2%
37	20	40.6	39.5	39.7	39.9	0.5	1.3%
37	10	40.6	39.3	39.1	39.6	0.8	2.1%
37	5	40.4	38.7	39.1	39.4	0.9	2.3%
37	2	40.3	38.6	39.2	39.4	0.9	2.2%
37	1	38.8	37.1	38.1	38.0	0.9	2.3%
37	0.5	35.9	35.0	34.7	35.2	0.6	1.7%
37	0.2	31.8	31.7	30.5	31.3	0.7	2.4%
37	0.1	28.3	29.1	26.9	28.1	1.1	3.9%
54	25	36.4	39.8	39.9	38.7	2.0	5.2%
54	20	20.6	35.1	35.6	30.4	8.5	27.9%
54	10	32.4	32.4	32.1	32.3	0.2	0.5%
54	5	25.3	31.5	30.1	29.0	3.2	11.2%
54	2	7.2	30.1	28.0	21.8	12.7	58.4%
54	1	24.7	27.5	26.6	26.3	1.5	5.6%
54	0.5	30.4	25.3	21.4	25.7	4.5	17.4%
54	0.2	28.0	22.2	18.3	22.8	4.9	21.4%
54	0.1	7.9	20.7	16.7	15.1	6.6	43.6%